AD-A069 787 GEORGIA INST OF TECH ATLANTA SCHOOL OF AEROSPACE ENG--ETC F/G 20/1
NOISE SUPPRESSION IN JET INLETS.(U)
FEB 79 B T ZINN, W I MEYER, W A BELL F49620-77-C-0066
UNCLASSIFIED AFOSR-LTR-79-0614 NL

1 OF 2
AD
A069787

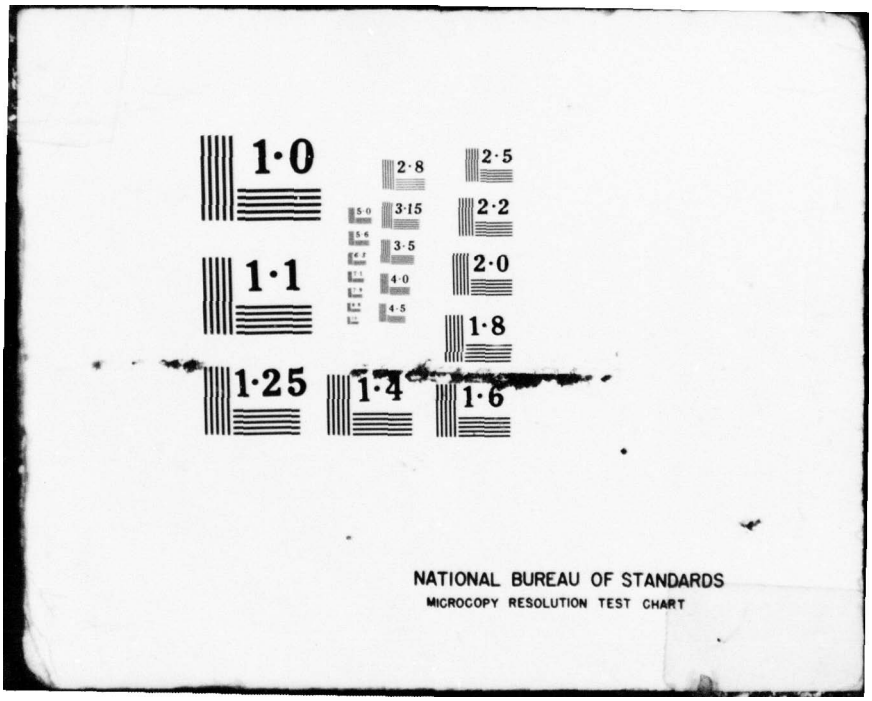
1·0
1·1
1·25
1·4
1·6
1·8
2·0
2·2
2·5
2·8
3·15
3·5
4·0
4·5
5·0
5·6
NATIONAL BUREAU OF STANDARDS
MICROCOPY RESOLUTION TEST CHART

AFOSR-TR- 79-0614

AFOSR Annual Technical Report

AFOSR-TR-

5

LEVEL II

AO54173

NOISE SUPPRESSION IN JET INLETS

Prepared for

Air Force Office of Scientific Research
Director of Aerospace Sciences

Bolling AFB, D. C.

by

Ben T. Zinn

William L. Meyer

William A. Bell

School of Aerospace Engineering
Georgia Institute of Technology
Atlanta, Georgia 30332

Approved for public release; distribution unlimited

AFOSR Contract No. F49620-77-C-0066 February 1979

UNCLASSIFIED

SECURITY CLASSIFICATION OF THIS PAGE (When Data Entered)

REPORT DOCUMENTATION PAGE

READ INSTRUCTIONS BEFORE COMPLETING FORM

1. REPORT NUMBER: AFOSR-TR-79-0614	2. GOVT ACCESSION NO.
3. RECIPIENT'S CATALOG NUMBER	
4. TITLE (and Subtitle): NOISE SUPPRESSION IN JET INLETS	5. TYPE OF REPORT & PERIOD COVERED: Annual technical INTERIM rept. 1 Feb 78 - 31 Jan 79
6. PERFORMING ORG. REPORT NUMBER	
7. AUTHOR(s): BEN T. ZINN, WILLIAM L. MEYER, WILLIAM A. BELL	8. CONTRACT OR GRANT NUMBER(s): F49620-77-C-0066
9. PERFORMING ORGANIZATION NAME AND ADDRESS: GEORGIA INSTITUTE OF TECHNOLOGY, SCHOOL OF AEROSPACE ENGINEERING, ATLANTA, GEORGIA 30332	10. PROGRAM ELEMENT, PROJECT, TASK AREA & WORK UNIT NUMBERS: 2307A2, 61102F, A2
11. CONTROLLING OFFICE NAME AND ADDRESS: AIR FORCE OFFICE OF SCIENTIFIC RESEARCH/NA, BLDG 410, BOLLING AIR FORCE BASE, D C 20332	12. REPORT DATE: Feb 79
	13. NUMBER OF PAGES: 101
14. MONITORING AGENCY NAME & ADDRESS (if different from Controlling Office): 62p.	15. SECURITY CLASS. (of this report): UNCLASSIFIED
	15a. DECLASSIFICATION/DOWNGRADING SCHEDULE

16. DISTRIBUTION STATEMENT (of this Report)

Approved for public release; distribution unlimited.

17. DISTRIBUTION STATEMENT (of the abstract entered in Block 20, if different from Report)

18. SUPPLEMENTARY NOTES

19. KEY WORDS (Continue on reverse side if necessary and identify by block number)

ACOUSTIC RADIATION
DUCT ACOUSTICS
JET PROPULSION NOISE
AIRCRAFT NOISE

20. ABSTRACT (Continue on reverse side if necessary and identify by block number)

This report summarizes the work performed during the second year of an AFOSR sponsored research program that was primarily concerned with the development of an analytical technique for determining the radiated sound field from axisymmetric jet engine inlet configurations. The analytical technique employed is based upon an integral representation of the external (radiation) solutions of the Helmholtz equation which describe the sound fields external to a given body under either no flow or constant velocity flow situations. The integral representation developed during the course of this research program is different

DD FORM 1 JAN 73 1473

403914

UNCLASSIFIED

SECURITY CLASSIFICATION OF THIS PAGE (When Data Entered)

from earlier works in the sense that it not only yields the correct (unique) solution for all radiation problems at all frequencies, but that the resulting integral equations contain no strong (i.e., nonintegrable) singularities and therefore can be solved by straight forward numerical techniques. As part of this research effort two extremely flexible computer programs were developed for the solution of these axisymmetric integral equations. These programs can be used for any closed axisymmetric body with any combination of boundary conditions on its surface, without any modification of the computer codes, to provide accurate solutions for the acoustic properties (i.e., the acoustic pressure, normal velocity, and admittance) both on the body itself and anywhere in the field surrounding the body. Also, as part of this research effort, experiments are now being conducted with various axisymmetric configurations to provide the data that will be used to check the validity of the theoretical predictions. Some preliminary experimental data are presented in this report.

AFOSR Annual Technical Report

AFOSR-TR-

NOISE SUPPRESSION IN JET INLETS

Prepared for

Air Force Office of Scientific Research
Director of Aerospace Sciences

Bolling AFB, D. C.

by

Ben T. Zinn

William L. Meyer

William A. Bell

School of Aerospace Engineering
Georgia Institute of Technology
Atlanta, Georgia 30332

Approved for public release; distribution unlimited

AFOSR Contract No. F49620-77-C-0066 February 1979

Abstract

This report summarizes the work performed during the second year of an AFOSR sponsored research program that was primarily concerned with the development of an analytical technique for determining the radiated sound field from axisymmetric jet engine inlet configurations. The analytical technique employed is based upon an integral representation of the external (radiation) solutions of the Helmholtz equation which describe the sound fields external to a given body under either no flow or constant velocity flow situations. The integral representation developed during the course of this research program is different from earlier works in the sense that it not only yields the correct (unique) solution for all radiation problems at all frequencies, but that the resulting integral equations contain no strong (i.e., non-integrable) singularities and therefore can be solved by straight forward numerical techniques. As part of this research effort two extremely flexible computer programs were developed for the solution of these axisymmetric integral equations. These programs can be used for any closed axisymmetric body with any combination of boundary conditions on its surface, without any modification of the computer codes, to provide accurate solutions for the acoustic properties (i.e., the acoustic pressure, normal velocity, and admittance) both on the body itself and anywhere in the field surrounding the body. Also, as part of this research effort, experiments are now being conducted with various axisymmetric configurations to provide the data that will be used to check the validity of the theoretical predictions. Some preliminary experimental data are presented in this report.

I. Introduction

This report summarizes the results obtained during the second year of support under AFOSR contract number F49620-77-C-0066. This contract was initiated on February 1, 1977 and the results obtained during the first year of support are contained in AFOSR Interim Scientific Report AFOSR-TR-78-0696.

The main objective of the research program conducted under this contract was to develop an analytical technique for predicting the sound field radiated from axisymmetric jet engine inlet configurations and to check the validity of these predictions with relevant experimental data. The development of this analytical solution technique was motivated by the need for a theoretical approach that could be used to predict the effects of sound source modifications and of sound suppression devices (such as acoustically lined surfaces and splitters) upon the sound field radiated from the inlet without having to resort to costly, full scale experimental testing. The experimental investigations are necessary not only for comparison with the results of the analytical technique (which has shown extremely good agreement with known exact solutions)[1,2,3*] but also to assist in the determination of the correct analytical form for describing the boundary conditions necessary to accurately model sound suppression materials in the computer programs.

---

* These references were included as appendices of the aforementioned Interim Scientific Report, AFOSR-TR-78-0696.

During the first year of this contract the integral equations and computer programs required for investigating the sound fields radiated from certain simple geometries were developed. Specifically, two different formulations of the problem were developed; that is, the full three dimensional formulation and the axisymmetric formulation. Employing both these formulations the sound radiation from both a sphere and a finite length cylinder were investigated. In these studies the effects of different boundary conditions on the accuracy of the integral solution technique was investigated by comparing the predictions of this approach for the sound fields radiated by simple sources with available exact solutions obtained using the Seperation of Variables Technique (which is only applicable to simple geometries such as those investigated). This work is described in detail in three publications[1,2,3] (See footnote on the previous page.) and it was presented at three conferences[A,B,C*]. In summary the first year of study has shown that the integral solution technique developed under this contract is both accurate and efficient from a numerical point of view.

During the second year of this contract two general computer programs were developed for the determination of the acoustic fields both on and around general axisymmetric bodies with general boundary conditions. It will be noted here that although the geometry of the bodies under consideration are constrained to be axisymmetric the allowable acoustic modes are not; that is, any cylindrically symmetric acoustic mode which may be present can be solved for using these computer programs. These programs were written in Extended Fortran IV and they are presented

---

* Letters refer to the various conference presentations conducted in connection with this program. These presentations are listed in Appendix F.

in Appendix A. They have been fully checked out on the Georgia Tech CDC Cyber 70/74 computer and have been used to theoretically predict the radiated sound fields that are associated with both lined and unlined straight ducts and an actual jet engine inlet configuration[4] shown in Fig. 1.

The details and results of these investigations are described in References 5 and 6 which are reproduced in Appendices B and C respectively. The latter of the two papers has also been accepted for presentation at the AIAA 5th Aeroacoustics Conference in March 1979 in Seattle, Washington. Probably the most significant results of this investigation is the result that the optimum theoretical admittance values found for reducing the sound radiated from a straight duct do not necessarily have the same effect in a dimensionally similar (i.e., the same length to diameter ratio) inlet. That is, the geometrical details of an axisymmetric body need to be taken into consideration when calculating optimum admittance values for acoustic liners. Another result of this investigation is that the admittance at the entrance plane of a straight duct or an inlet is not constant in the radial direction. The assumption of a constant admittance value at the entrance plane of a duct is common to many current theoretical analyses of the duct radiation problem and thus can be a large source of error in these analyses.

Since the use of a constant admittance value at the entrance plane of a duct is so common a series of computer runs were performed to determine just how accurate this assumption is. The runs were done for a straight duct configuration and various admittance values were calculated and compared with certain "classical values". The details of this analysis and the results are presented in Appendix E. In Appendix E a draft copy of a

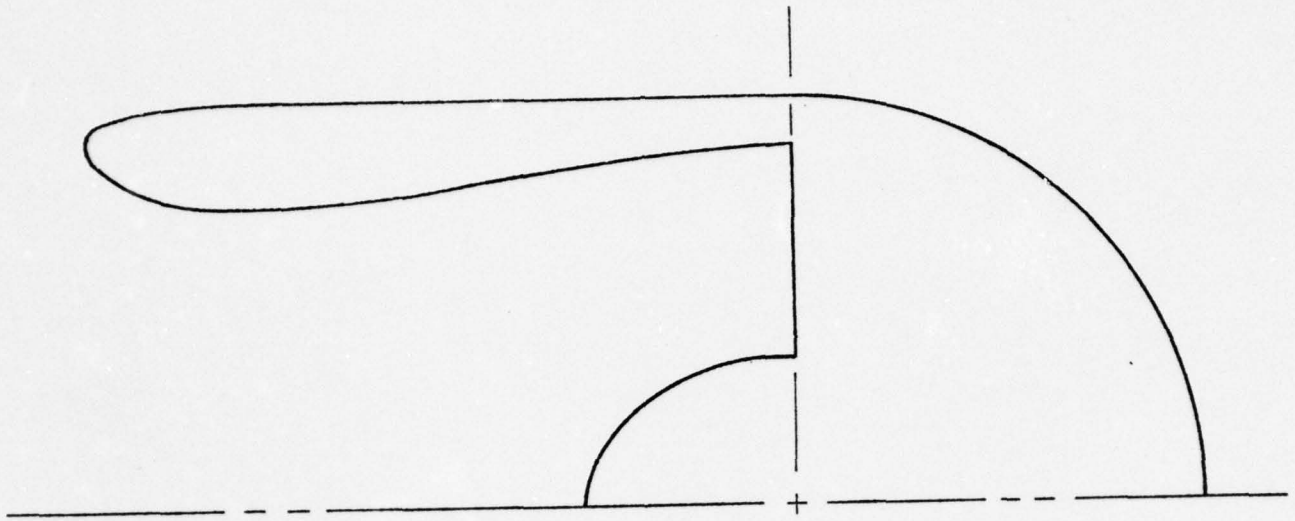

Figure 1. Axisymmetric Inlet Geometry.

technical note, to be submitted for publication in the AIAA Journal, is reproduced.

Part of the efforts expended under this contract during the second year of study were devoted to the development of experimental data that could be used to check the validity of the accompanying analytical studies. These efforts consisted of the design and development of appropriate experimental setups and the conduct of the required experiments, which are currently in progress. The experimental data acquired under this program is being compared with corresponding theoretical predictions. Some preliminary results of these comparisons are now available and they are presented in Section IV of this report. The work conducted during the second year of this contract which is not presented in the papers contained in Appendices B and C is summarized in the following sections.

II. Analytical Effort

The analytical efforts during the second year of this AFOSR contract consisted of the development of the general computer programs for handling axisymmetric geometires and their use to perform certain parametric studies of interest. The details and results of these studies are presented in Appendices B, C, and E, and the computer programs themselves are presented in Appendix A. The programs were developed so that they could not only be used for parametric analytical studies but also so that they could easily accept experimental data for any configuation without any major changes in the computer code. Another part of the analytical effort was concerned with the determination of the admittance of the liner which was used in the experimental phase of this program and with the redesign of the liner for future testing (See Appendix D.).

The initial testing under this program was conducted with an available acoustic liner which was developed in a related combustion instability program. This liner was tuned for maximum damping at a frequency, $\sim$ 740 Hertz, which is above the first tangential (i.e., 1T) mode, $\sim$695 Hz, of the duct under investigation. Since we are mainly interested in runing experiments below the 1T cut-off frequency to facilitate both the data reduction and the comparison of experimental and analytical values all of the preliminary testing was done in the frequency range 300-650 Hz which is below the 1T cut-off frequency. Thus, the liner was not expected to exert much attenuation. Since most of the planned future testing will also be conducted over a frequency range below the 1T mode of the duct, the available liner will be retuned to be more effective below the 1T cut-off frequency. The retuning of the liner is discussed in detail in Appendix D.

III. Experimental Investigations

The main objective of the experimental phase of this program was to obtain experimental data that could be readily compared with the predictions of the analytical models developed under this program. Specifically, the sound fields radiated from lined and unlined axisymmetric duct configurations were to be measured and compared with corresponding theoretical predictions. Since these studies were concerned with the measurements of the radiated sound fields, all of the required experiments were conducted in an anechoic chamber whose properties are described in Fig. 2. A typical experimental setup utilized in the course of this study is shown in Fig. 3; it consists of a lined axisymmetric duct with a sound source at one end and an open termination at the other end. The test body (i.e., the inlet) is placed on one side of the anechoic chamber and an array of microphones is used to measure the radiated sound field. The latter consisted of 5 Brüel and Kjaer condenser-type microphones. The sound source was a University driver and it was placed at the throat of a nozzle that was connected to the axisymmetric body tested as shown in Fig. 4. The available liner used for the preliminary testing was not specifically designed for maximum effectiveness in the frequency range where most of the testing was done. It was tuned for maximum damping at a frequency higher than the 1T mode of the duct under study. It consisted of 180 Helmholtz resonators (20 radial rows by 9 axial rows) which were closed off during the hard walled testing (See Appendix D for the admittance calculation). A diagram of the driver-nozzle-liner set-up and of one of the Helmholtz resonators appears in Fig. 4.

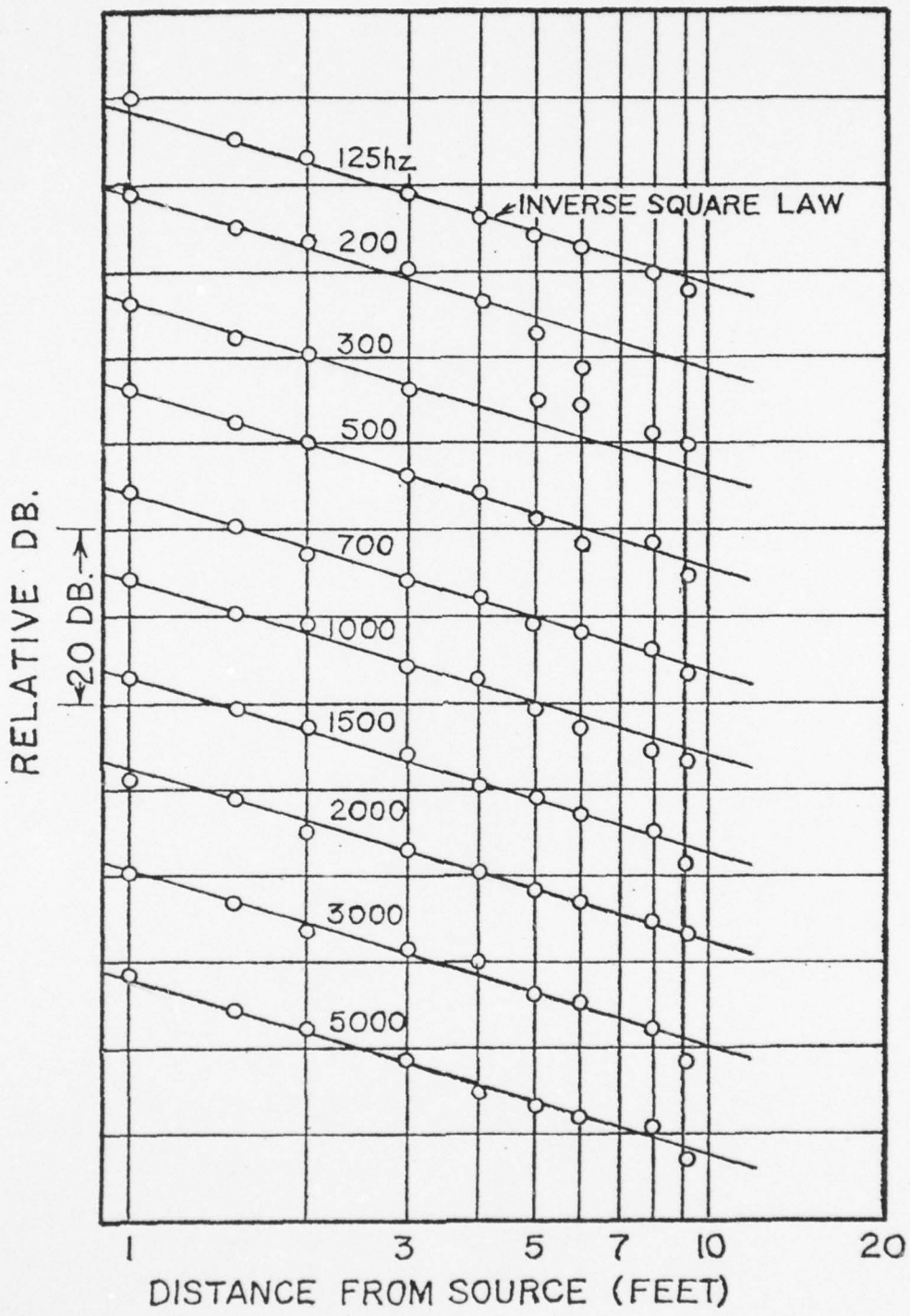

Figure 2. Anechoic Chamber Characteristics.

ANECHOIC CHAMBER

PLAN VIEW

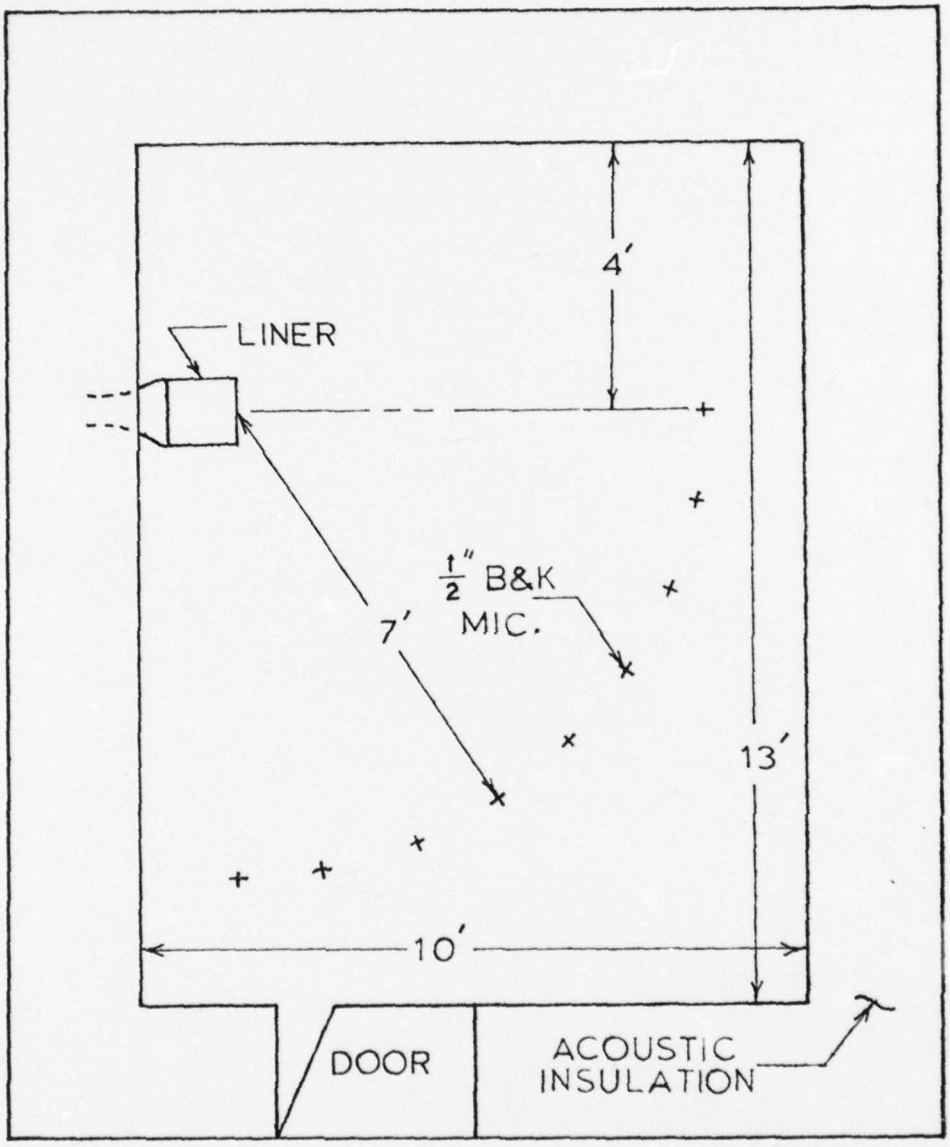

Figure 3. Experimental Set-up for Radiation Studies.

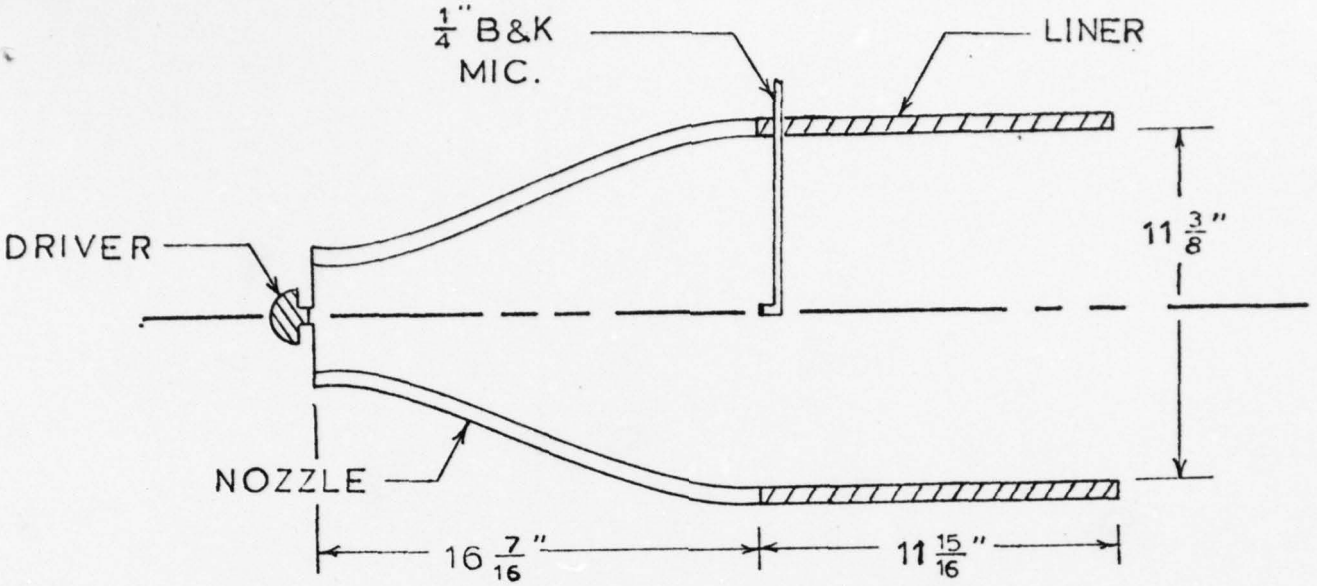

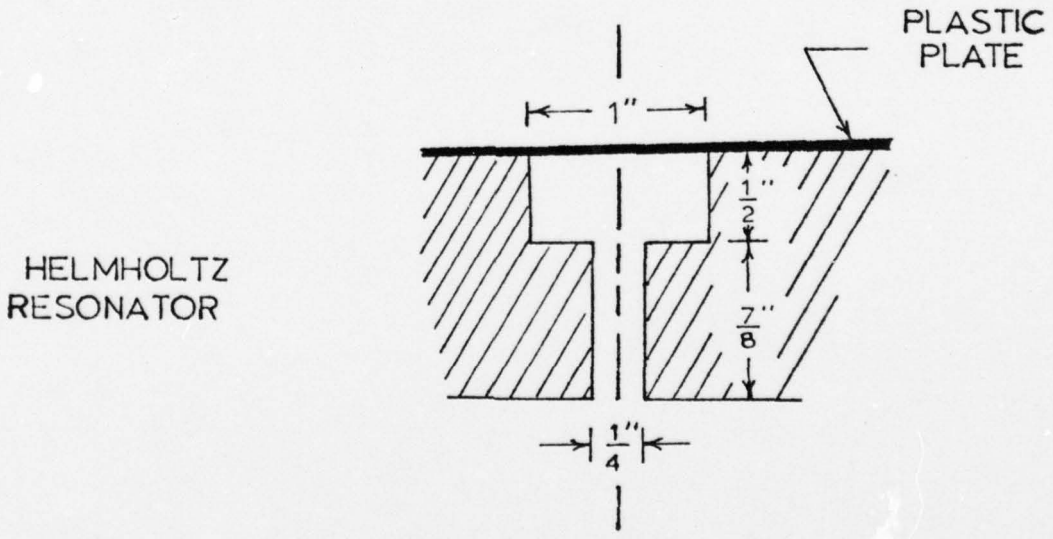

Figure 4. Testing Configuration.

This experimental set-up was found to work very well in that the acoustic waves generated by the driver remained essentially plane up to the nozzle-liner interface. This was determined by traversing a 1/4" B&K microphone radially across the nozzle-liner interface. This being the case only a single measurement of the acoustic pressure, which is needed for input to the analytical computations, was taken at this plane for each test condition.

IV. Preliminary Experimental Results and Comparisons

Some preliminary experiments have been conducted with the straight duct configuration shown in Figs. 3 ad 4. Both lined and unlined configurations were tested; however, not much difference was noted as all the tests were conducted at frequencies below the first tangential (i.e. 1T) mode of the duct and therefore in a region where the liner is only marginally effective as discussed in the previous sections (Also see Appendix D.). Tests were conducted in the frequency range 300 to 650 Hertz with 50 Hz increments. The microphones in the field were placed on a circular arc with a radius of seven feet centered at the entrance plane of the duct (See Figure 3.). The microphones were placed at increments of $11\frac{1}{4}^{\circ}$ from the centerline of the duct to 90°.

Comparisons between the experimental results and the theoretical results were made. Since an experimentally measured value of the sound pressure level at the nozzle-duct interface was used as input for the computer programs, the accuracy of the calculated far field can only be expected to be as good as this measurement. Other sources of error are the "imperfections" of the anechoic chamber at various frequencies as shown in Fig. 2, instrumentation errors, and the lack of perfect correspondence between the experimental and analytical configurations. In this connection it should be pointed out that the theoretical model employs a spherical termination at the rear end of the straight duct as shown in Fig. 5. This was done to improve the efficiency of the computer programs as it has been shown through theoretical studies that the shape of the termination of the

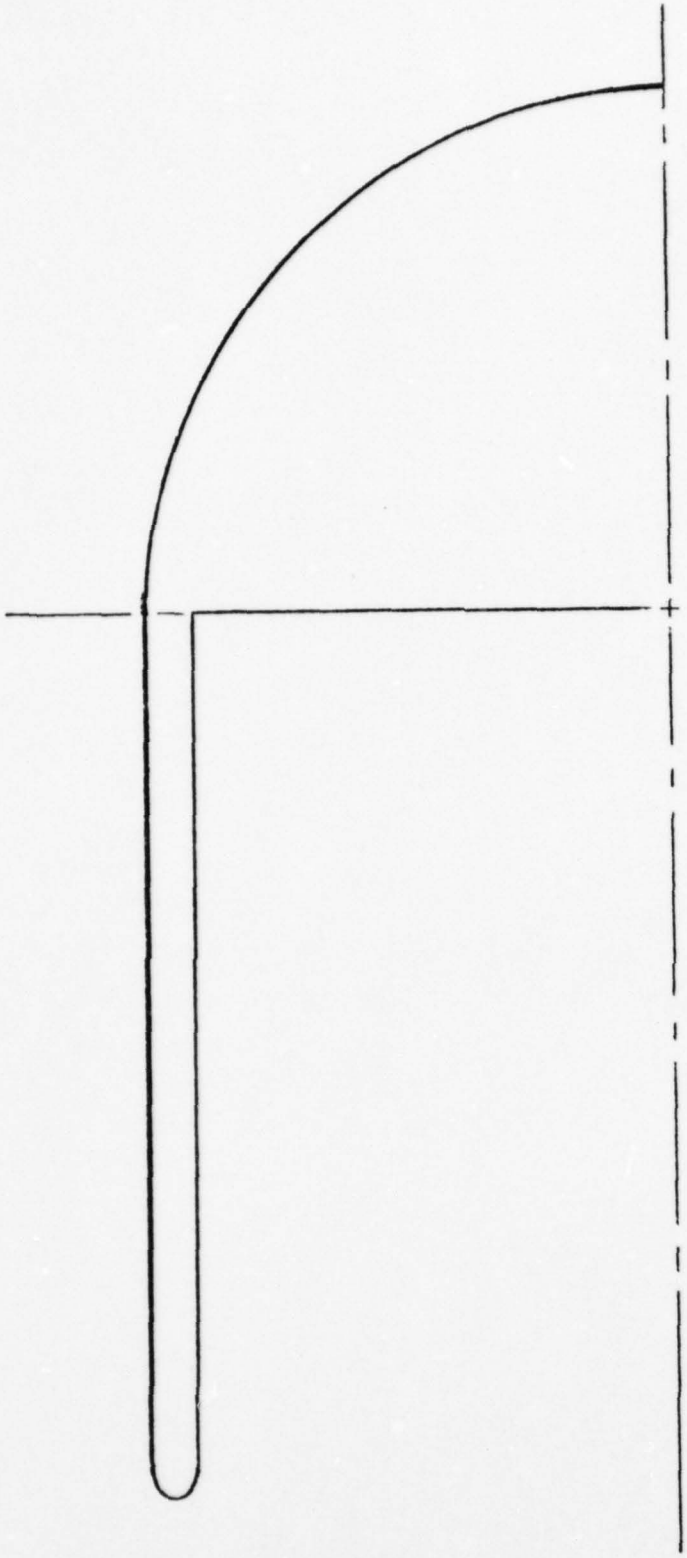

Figure 5. Straight Duct Geometry.

duct exerts little influence upon the acoustic field in the forward half plane of the duct.

Comparisons between the measured and calculated results shows good qualitative agreement for both the hard walled (i.e., See Fig. 6.) and the lined (i.e., See Fig. 7.) duct configurations. Good agreement is observed between the hard walled and lined wall cases in that the errors follow the same patterns (i.e., Compare Figs. 6 and 7.) which suggest that most of the observed errors are due to the "non-anechoicness" of the anechoic chamber. The measured data will be further analyzed in the future and they will be published together with additional data collected during the next year of study under this contract.

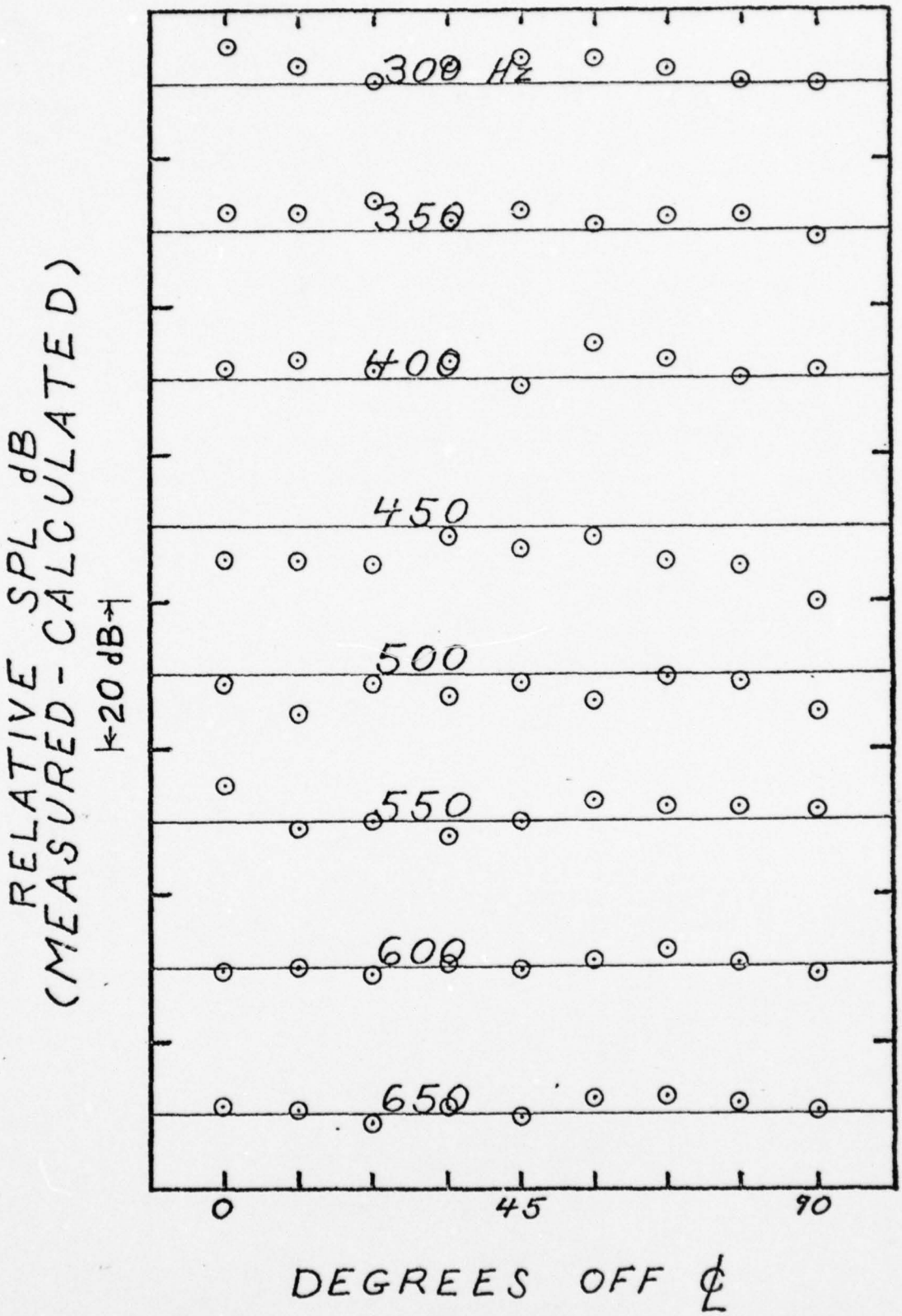

Figure 6. Results for the Hard Walled Straight Duct.

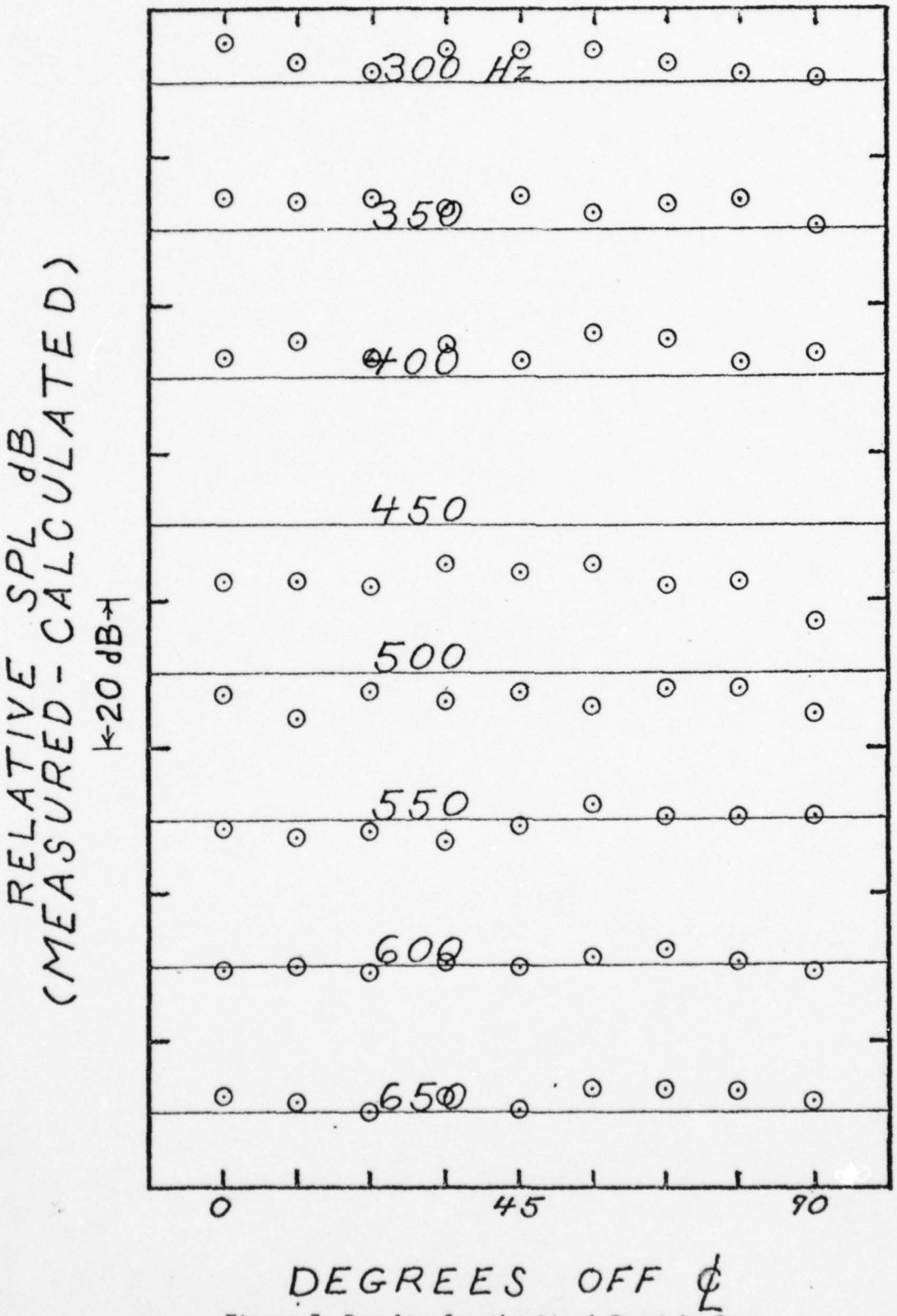

Figure 7. Results for the Lined Straight Duct.

References

1. Bell, W. A., Meyer, W. L., and Zinn, B. T., "Predicting the Acoustics of Arbitrarily Shaped Bodies Using an Integral Approach," AIAA Journal, Vol. 15, No. 6, June 1977, pp. 813-820.

2. Meyer, W. L., Bell, W. A., and Zinn, B. T., "Prediction of the Sound Field Radiated from Axisymmetric Surfaces," AIAA Paper No. 78-195, presented at the AIAA 16th Aerospace Sciences Meeting, Huntsville, Alabama, January 16-18, 1978.

3. Meyer, W. L., Bell, W. A., Stallybrass, M. P., and Zinn, B. T., "Boundary Integral Solutions of Three Dimensional Acoustic Radiation Problems," Journal of Sound and Vibration, Vol. 59, No. 2, February 1978, pp. 245-262.

4. Miller, B. A., Dastoli, B. J., and Wesoky, H. L., "Effect of Entry-Lip Design on Aerodynamics and Acoustics of High-Throat-Mach-Number Inlets for the Quiet, Clean, Short-Haul Experimental Engine," NASA TM X-3222, May 1975.

5. Meyer, W. L., Bell, W. A., Stallybrass, M. P., and Zinn, B. T., "Prediction of the Sound Field Radiated from Axisymmetric Surfaces," Journal of the Acoustical Society of America, March 1979.

6. Meyer, W. L., Bell, W. A., and Zinn, B. T., "Sound Radiation from *Finite Length Axisymmetric Ducts and Engine Inlets*," AIAA Paper No. 79-0675, presented at the 5th AIAA Aeroacoustics Conference, Seattle, Washington, March 12-14, 1979.

Appendix A

Computer Programs Developed for this Project

The computer programs described in this appendix were developed during the second year of this AFOSR research project. They are very general in that they can be used to find the acoustic properties (i.e., the acoustic potential, normal acoustic velocity, and the admittance) both on the surface and surrounding any finite (closed) axisymmetric body. Also, the boundary conditions can be specified at each point on the surface of the body; the only restriction is that the admittance may not be specified everywhere on the body as then the solution of the governing integal equation is non-unique.

The first computer program developed for this project calculates the surface distributions of the acoustic quantities for a general axisymmetric configuration. Required inputs for this program are the geometric description of the body, the boundary conditions, and the problem specification data (i.e., the mode number of the acoustic wave being solved for and the wave number). The geometric input data required includes the ρ - z coordinates of the points in the center of each integration interval, P, the two integration points on either side of the center point, Q, the normal to the body at the center point, NORMAL, and the length of each integration interval in the ρ -z plane, LENGTH. Since the body is assumed to be axisymmetric the program takes care of choosing the integration points in the θ direction through the use of a 96 point Gaussian integration formula.

The boundary conditions are specified in two vectors. The first vector, ICHECK, specifies what type of boundary condition is known at each point in the ρ-z plane.

$$\text{ICHECK} = \left.\begin{matrix} -1 \\ 0 \\ 1 \end{matrix}\right\} \longrightarrow \left\{\begin{matrix} \varphi & \text{known} \\ \partial\varphi/\partial n & \text{known} \\ y & \text{known} \end{matrix}\right. \qquad \text{(A-1)}$$

The second vector, CINDATA, contains the actual complex value of the boundary condition at each point. Finally the problem specification data consists of specifying the wave number k and the mode number m (i.e. m = 0 is the axisymmetric mode.)

This program prints out all the input data and all the acoustic quantities on the surface of the body. It also creates an output file which is read by the next program to calculate the acoustic qualtities in the field surrounding the body.

```
      PROGRAM EXPCYL ( INPUT, OUTPUT, TAPE10, TAPE11,
     .                 TAPE5 = INPUT, TAPE6 = OUTPUT)
C
C
C*****************************************************************************
C*                                                                           *
C*                                                                           *
C*     THIS PROGRAM CALCULATES EITHER THE ACOUSTIC POTENTIAL OR THE          *
C*     ACOUSTIC VELOCITY OR THE EFFECTIVE ADMITTANCE ON THE SURFACE          *
C*     OF ANY AXISYMMETRIC BODY USEING THE METHOD OF BURTON & MILLER         *
C*     WITH MY INTERPRETATION OF THE MOST SINGULAR COMPONENT.                *
C*                                                                           *
C*****************************************************************************
C*                                                                           *
C*     WILLIAM A. BELL'S OPTIMAL VALUE OF ALPHA (= I/K) IS EMPLOYED.         *
C*                                                                           *
C*****************************************************************************
C*                                                                           *
C*     A CYLINDRICAL FORMULATION OF THE PROBLEM IS EMPLOYED.                 *
C*                                                                           *
C*                                                                           *
C*****************************************************************************
C
C
      REAL K, LENGTH, NORMAL
      COMPLEX ALPHA, CEQN, CEXACT, CPHI, CVEL, CY, IK, IKSQ, TWOPIA,
     .        CINDATA
C
      COMMON /I/ M, NP, NPP1
      COMMON /R/ K, PI, TWOPI
      COMMON /C/ ALPHA, IK, IKSQ, TWOPIA
      COMMON /ID/ ICHECK (102)
      COMMON /RD/ LENGTH (102), NORMAL (102, 2), P (102, 2),
     .            Q (102, 2, 2)
      COMMON /CD/ CEQN (102, 103), CEXACT (102), CPHI (102), CVEL (102),
     .            CY (102), CINDATA (102)
      COMMON /NGAUSS/ NGAUST
      COMMON /GAUSS/ GAUSNT (48, 2)
C
      CALL INPUT
C
C     INTEGER CONSTANTS
C
      NPP1 = NP + 1
C
C     REAL CONSTANTS
C
      TWOPI = 2.0 * PI
C
C     COMPLEX CONSTANTS
C
      IK = (0.0, 1.0) * K
      IKSQ = IK * IK
      ALPHA = (0.0, 1.0) / K
      TWOPIA = ALPHA * TWOPI

      CALL EQN
C
      CALL GAUSS
C
      CALL OUTPUT
C
      STOP "NORMAL"
C
      END
```

```
      BLOCK DATA
C
      REAL K
C
      COMMON /I/ M, NP, NPP1
      COMMON /R/ K, PI, TWOPI
      COMMON /NGAUSS/ NGAUST
      COMMON /GAUSS/ GAUSNT (48, 2)
C
      DATA NP / 102 /
C
      DATA PI / 3.1415926535898 /
C
      DATA NGAUST / 48 /
C
      DATA ((GAUSNT(I, J), J = 1, 2), I = 1, 12)
     .     / 0.01627674484960, 0.03255061449236,
     .       0.04881298513605, 0.03251611871387,
     .       0.08129749546443, 0.03244716371406,
     .       0.11369535011067, 0.03234382256858,
     .       0.14597371465490, 0.03220620479403,
     .       0.17809688236762, 0.03203445623199,
     .       0.21003131046057, 0.03182875889441,
     .       0.24174315616384, 0.03158933077073,
     .       0.27319881259105, 0.03131642559686,
     .       0.30436494435450, 0.03101033258631,
     .       0.33520852289263, 0.03067137612367,
     .       0.36569686147231, 0.03029991542083 /
      DATA ((GAUSNT(I, J), J = 1, 2), I = 13, 24)
     .     / 0.39579764982891, 0.02989634413633,
     .       0.42547898840730, 0.02946108995817,
     .       0.45470942216774, 0.02899461415056,
     .       0.48345797392060, 0.02849741106509,
     .       0.51169417715467, 0.02797000761685,
     .       0.53938810832436, 0.02741296272603,
     .       0.56651041856140, 0.02682686672559,
     .       0.59303236477757, 0.02621234073567,
     .       0.61892584012547, 0.02557003600535,
     .       0.64416340373497, 0.02490063322248,
     .       0.66871831004392, 0.02420484179236,
     .       0.69256453664217, 0.02348339908593 /
      DATA ((GAUSNT(I, J), J = 1, 2), I = 25, 36)
     .     / 0.71567681234897, 0.02273706965833,
     .       0.73803064374440, 0.02196664443874,
     .       0.75960234117665, 0.02117293989219,
     .       0.78036904386743, 0.02035679715433,
     .       0.80030874413914, 0.01951908114015,
     .       0.81940031073793, 0.01866067962741,
     .       0.83762351122819, 0.01778250231605,
     .       0.85495903343460, 0.01688547986425,
     .       0.87138850590930, 0.01597056290256,
     .       0.88689451740242, 0.01503872102699,
     .       0.90146063531585, 0.01409094177231,
     .       0.91507142312090, 0.01312822956696 /
      DATA ((GAUSNT(I, J), J = 1, 2), I = 37, 48)
     .     / 0.92771245672231, 0.01215160467109,
     .       0.93937033975276, 0.01116210209984,
     .       0.95003271778444, 0.01016077053501,
     .       0.95968829144874, 0.00914867123078,
     .       0.96832682846326, 0.00812687692570,
     .       0.97593917458514, 0.00709647079115,
     .       0.98251726356301, 0.00605854550424,
     .       0.98805412632962, 0.00501420274293,
     .       0.99254390032376, 0.00396455433844,
     .       0.99598184293721, 0.00291073181793,
     .       0.99836437586318, 0.00185396078895,
     .       0.99968950388323, 0.00079679206555 /
C
      END
```

```
      SUBROUTINE INPUT
C
      REAL K, LENGTH, NORMAL
      COMPLEX CEQN, CEXACT, CPHI, CVEL, CY, CINDATA
C
      COMMON /I/ M, NP, NPP1
      COMMON /R/ K, PI, TWOPI
      COMMON /ID/ ICHECK (102)
      COMMON /RD/ LENGTH (102), NORMAL (102, 2), P (102, 2),
     .            Q (102, 2, 2)
      COMMON /CD/ CEQN (102, 103), CEXACT (102), CPHI (102), CVEL (102),
     .            CY (102), CINDATA (102)
C
      READ (5, 100) ((P(I, J), J = 1, 2), I = 1, NP)
C
      READ (5, 100) (((Q(I, J, KK), KK = 1, 2), J = 1, 2), I = 1, NP)
C
      READ (5, 100) ((NORMAL(I, J), J = 1, 2), I = 1, NP)
C
      READ (5, 100) (LENGTH(I), I = 1, NP)
C
  100 FORMAT (8G10.0)
C
      PRINT 101
C
  101 FORMAT ("1GEOMETRIC INPUT DATA:" ///
     .        " ", 25X, "-Q(RHO, Z)" /
     .        " ", 4X, "N", 21X, "P(RHO, Z)", 38X, "NORMAL(RHO, Z)",
     .                   27X, "LENGTH" /
     .        " ", 25X, "+Q(RHO, Z)" // " ")
C
      WRITE (6, 102) (Q(I, 1, 1), Q(I, 1, 2), I, P(I, 1), P(I, 2),
     .                NORMAL(I, 1), NORMAL(I, 2), LENGTH(I), Q(I, 2, 1),
     .                Q(I, 2, 2), I = 1, NP)
C
  102 FORMAT (" ", 15X, "(", F13.10, ",", F13.10, ")" /
     .        " ", 2X, I3, 10X, "(", F13.10, ",", F13.10, ")", 21X,
     .                          "(", F13.10, ",", F13.10, ")", 17X,
     .                               F13.10 /
     .        " ", 15X, "(", F13.10, ",", F13.10, ")" / " ")
C
      READ (5, 104) (ICHECK(I), I = 1, NP)
C
  104 FORMAT (16I5)
C
      READ (11, 1100) M, K
C
 1100 FORMAT (I20, G20.0)
C
      READ (11, 100) (CINDATA(I), I = 1, NP)
C
      RETURN
      END
```

```
      SUBROUTINE EQN
C
      REAL K, LENGTH, NORMAL, NP1, NP2, NRHOP, NRHOQ, NZP, NZQ
      COMPLEX ALPHA, CEQN, CEXACT, CPHI, CVEL, CY, IK, IKSQ,
     .        TWOPIA, CINDATA
C
      COMMON /I/ M, NP, NPP1
      COMMON /R/ K, PI, TWOPI
      COMMON /C/ ALPHA, IK, IKSQ, TWOPIA
      COMMON /ID/ ICHECK (102)
      COMMON /RD/ LENGTH (102), NORMAL (102, 2), P (102, 2),
     .            Q (102, 2, 2)
      COMMON /CD/ CEQN (102, 103), CEXACT (102), CPHI (102), CVEL (102),
     .            CY (102), CINDATA (102)
C
C     INITALIZE MATRIX
C
      DO 1 I = 1, NP
      DO 2 J = 1, NPP1
      CEQN(I, J) = (0.0, 0.0)
 2    CONTINUE
      P1 = P(I, 1)
      P2 = P(I, 2)
      NP1 = NORMAL(I, 1)
      NP2 = NORMAL(I, 2)
C
      IF (ICHECK(I)) 3, 4, 5
 3    CONTINUE
      CEXACT(I) = CINDATA(I)
      CVEL(I) = (0.0, 0.0)
      CY(I) = (0.0, 0.0)
      CEQN(I, NPP1) = TWOPI * CEXACT(I)
      CEQN(I, I) = -TWOPIA
      GO TO 6
 4    CONTINUE
      CEXACT(I) = (0.0, 0.0)
      CVEL(I) = CINDATA(I)
      CY(I) = (0.0, 0.0)
      CEQN(I, NPP1) = TWOPIA * CVEL(I)
      CEQN(I, I) = -TWOPI
      GO TO 6
 5    CONTINUE
      CEXACT(I) = (0.0, 0.0)
      CVEL(I) = (0.0, 0.0)
      CY(I) = CINDATA(I)
      CEQN(I, I) = -TWOPI * (1.0 + ALPHA * CY(I))
 6    CONTINUE
 1    CONTINUE
C
C     XI INTEGRATION
C
      DO 7 J = 1, NP
      NRHOQ = NORMAL(J, 1)
      NZQ = NORMAL(J, 2)
      GAUSZ = LENGTH(J) * PI
      DO 8 I = 1, NP
      RHOP = P(I, 1)
      ZP = P(I, 2)
      NRHOP = NORMAL(I, 1)
      NZP = NORMAL(I, 2)
      DO 9 L = 1, 2
      RHOQ = Q(J, L, 1)
      ZQ = Q(J, L, 2)
C
      CALL CALC (RHOP, ZP, NRHOP, NZP, RHOQ, ZQ, NRHOQ, NZQ, GAUSZ,
     .           I, J)
C
 9    CONTINUE
 8    CONTINUE
 7    CONTINUE
C
      RETURN
      END
```

```
      SUBROUTINE CALC (RHOP, ZP, NRHOP, NZP, RHOQ, ZQ, NRHOQ, NZQ,
     .                 GAUSZ, I, J)
C
      REAL K, NDOTN, NRHOP, NRHOQ, NRHOQP, NZP, NZQ, NZQP
      COMPLEX ALPHA, CEQN, CEXACT, CPHI, CVEL, CY, F1, F2, G, GP,
     .        GPP, IK, IKSQ, I1, I2, K1, K2, TWOPIA, CINDATA
C
      COMMON /I/ M, NP, NPP1
      COMMON /R/ K, PI, TWOPI
      COMMON /C/ ALPHA, IK, IKSQ, TWOPIA
      COMMON /ID/ ICHECK (102)
      COMMON /CD/ CEQN (102, 103), CEXACT (102), CPHI (102), CVEL (102),
     .            CY (102), CINDATA (102)
      COMMON /NGAUSS/ NGAUST
      COMMON /GAUSS/ GAUSNT (48, 2)
C
      ZD = ZQ - ZP
      ZSQ = ZD * ZD
      RHOSQ = (RHOQ - RHOP)**2
      RHOQP2 = 2.0 * RHOQ * RHOP
      NRHOQP = NRHOQ * NRHOP
      NZQP = NZQ * NZP
C
C     THETA INTEGRATION
C
      DO 1 IT = 1, NGAUST
      THETA = PI * GAUSNT(IT, 1)
      IF (I .EQ. J) THETA = PI * (1.0 - GAUSNT(IT, 1))
      GAUSZT = GAUSZ * GAUSNT(IT, 2)
C
      COST = COS (THETA)
      COSMT = COS (M * THETA)
C
      R = SQRT (RHOSQ + ZSQ + RHOQP2 * (1.0 - COST))
      DRDNQ = (NRHOQ * (RHOQ - RHOP * COST) + NZQ * ZD) / R
      DRDNP = (NRHOP * (RHOP - RHOQ * COST) - NZP * ZD) / R
      NDOTN = NRHOQP * COST + NZQP
C
      G = RHOQ * CEXP (IK * R) / R
      GP = G * (IK - (1.0 / R))
      GPP = G * (IKSQ - (3.0 * IK / R) + (3.0 / (R * R)))
C
      I1 = G * COSMT
      I2 = ALPHA * GP * DRDNP * COSMT
      F1 = ALPHA * G * IKSQ * NDOTN
      F2 = ALPHA * (GPP * DRDNP * DRDNQ - (GP * NDOTN / R))
      K1 = GP * DRDNQ * COSMT
      K2 = F2 * COSMT
C
      IF (ICHECK(I) .NE. -1) GO TO 3
C
      CEQN(I, NPP1) = CEQN(I, NPP1) + GAUSZT * CEXACT(I) * (F1 + F2)
C
      GO TO 4
 3    CONTINUE
C
      CEQN(I, I) = CEQN(I, I) - GAUSZT * (F1 + F2)
C
 4    CONTINUE
      IF (ICHECK(J)) 11, 12, 13
 11   CONTINUE
C
      CEQN(I, J) = CEQN(I, J) - GAUSZT * (I1 + I2)
      CEQN(I, NPP1) = CEQN(I, NPP1) - GAUSZT * (K1 + K2)
     .                              * CEXACT(J)
C
      GO TO 14
 12   CONTINUE
C
      CEQN(I, J) = CEQN(I, J) + GAUSZT * (K1 + K2)
      CEQN(I, NPP1) = CEQN(I, NPP1) + GAUSZT * (I1 + I2)
     .                              * CVEL(J)
C
      GO TO 14
 13   CONTINUE
C
      CEQN(I, J) = CEQN(I, J) + GAUSZT * ((K1 + K2) -
     .                          CY(J) * (I1 + I2))
C
 14   CONTINUE
 1    CONTINUE
C
      RETURN
```

```
      SUBROUTINE GAUSS
C
      IMPLICIT COMPLEX (C)
C
      COMMON /I/ MM, NP, NPP1
      COMMON /CD/ CEQN (102, 103), CEXACT (102), CPHI (102), CVEL (102),
     .            CY (102), CINDATA (102)
C
C     UPPER TRIANGULARIZE MATRIX
C
      DO 1 J = 1, NP
      JP1 = J + 1
      CSAVE = CEQN (J, J)
      CEQN(J, J) = (1.0, 0.0)
      DO 2 L = JP1, NPP1
      CEQN(J, L) = CEQN(J, L) / CSAVE
 2    CONTINUE
      IF (J .EQ. NP) GO TO 3
      DO 4 M = JP1, NP
      CSAVE = CEQN(M, J)
      DO 5 I = JP1, NPP1
      CEQN(M, I) = CEQN(M, I) - CEQN(J, I) * CSAVE
 5    CONTINUE
 4    CONTINUE
 1    CONTINUE
C
C     BACK SUBSTITUTION
C
 3    CONTINUE
      CSUM = (0.0, 0.0)
      DO 6 I = 1, NP
      NPMI = NP - I
      NPP1MI = NPMI + 1
      CPHI(NPP1MI) = CEQN(NPP1MI, NPP1) - CSUM
      IF (I .EQ. NP) GO TO 7
      CSUM = (0.0, 0.0)
      DO 8 J = 1, I
      NPP1MJ = NPP1 - J
      CSUM = CPHI(NPP1MJ) * CEQN(NPMI, NPP1MJ) + CSUM
 8    CONTINUE
 6    CONTINUE
 7    CONTINUE
C
      RETURN
      END
```

```
      SUBROUTINE OUTPUT
C
      REAL IEXACT, IPHI, K, LENGTH, MADMIT, MEXACT, MPHI, MVELP, MYP,
     .     NORMAL
      COMPLEX ADMIT, ALPHA, CEQN, CEXACT, CPHI, CVEL, CY, IK, IKSQ,
     .        TWOPIA, VELP, CINDATA
C
      COMMON /I/ M, NP, NPP1
      COMMON /R/ K, PI, TWOPI
      COMMON /C/ ALPHA, IK, IKSQ, TWOPIA
      COMMON /ID/ ICHECK (102)
      COMMON /RD/ LENGTH (102), NORMAL (102, 2), P (102, 2),
     .            Q (102, 2, 2)
      COMMON /CD/ CEQN (102, 103), CEXACT (102), CPHI (102), CVEL (102),
     .            CY (102), CINDATA (102)
      COMMON /NGAUSS/ NGAUST
C
      DIMENSION ADMIT (102), VELP (102), IEXACT (102), IPHI (102),
     .          MADMIT (102), MEXACT (102), MPHI (102), MVELP (102),
     .          MYP (102), PADMIT (102), PEXACT (102), PPHI (102),
     .          PPVELP (102), PVELM (102), PVELP (102), PYP (102),
     .          REXACT (102), RPHI (102)
C
      EQUIVALENCE (CEQN, ADMIT),              (CEQN(1, 2), VELP(1)),
     .            (CEQN(1, 3), IEXACT(1)),    (CEQN(1, 4), IPHI(1)),
     .            (CEQN(1, 5), MADMIT(1)),    (CEQN(1, 6), MEXACT(1)),
     .            (CEQN(1, 7), MPHI(1)),      (CEQN(1, 8), MVELP(1)),
     .            (CEQN(1, 9), MYP(1)),       (CEQN(1, 10), PADMIT(1)),
     .            (CEQN(1, 11), PEXACT(1)), (CEQN(1, 12), PPHI(1)),
     .            (CEQN(1, 13), PPVELP(1)), (CEQN(1, 14), PVELM(1)),
     .            (CEQN(1, 15), PVELP(1)),  (CEQN(1, 16), PYP(1)),
     .            (CEQN(1, 17), REXACT(1)), (CEQN(1, 18), RPHI(1))
C
      PRINT 100
C
  100 FORMAT ("1", 61X, "*********" / " ", 61X, "*       *" /
     .        " ", 61X, "* INPUT *" / " ", 61X, "*       *" /
     .        " ", 61X, "*********" //// "  N", 15X,
     .        "EFFECTIVE ADMITTANCE", 20X, "ACOUSTIC VELOCITY", 22X,
     .        "ACOUSTIC POTENTIAL" // " ")
C
      DO 1 I = 1, NP
      REXACT(I) = REAL (CEXACT(I))
      IEXACT(I) = AIMAG (CEXACT(I))
      MEXACT(I) = CABS (CEXACT(I))
      PEXACT(I) = 0.0
      IF (MEXACT(I) .NE. 0.0) PEXACT(I) = ATAN2 (IEXACT(I), REXACT(I))
      MVELP(I) = CABS (CVEL(I))
      PVELP(I) = 0.0
      IF (MVELP(I) .NE. 0.0) PVELP(I) = ATAN2 (AIMAG (CVEL(I)),
     .                        REAL (CVEL(I)))
      MYP(I) = CABS (CY(I))
      PYP(I) = 0.0
      IF (MYP(I) .NE. 0.0) PYP(I) = ATAN2 (AIMAG (CY(I)), REAL (CY(I)))
      IF (ICHECK(I)) 3, 4, 5
  3   CONTINUE
C
      WRITE (6, 101) I, CEXACT(I)
C
  101 FORMAT (" ", I3, 88X, "(", F13.10, ",", F13.10, ")")
C
      GO TO 22
  4   CONTINUE
C
      WRITE (6, 102) I, CVEL(I)
C
  102 FORMAT (" ", I3, 49X, "(", F13.10, ",", F13.10, ")")
C
      GO TO 22
  5   CONTINUE
C
      WRITE (6, 103) I, CY(I)
C
  103 FORMAT (" ", I3, 9X, "(", F13.10, ",", F13.10, ")")
C
  22  CONTINUE
  1   CONTINUE
      NGAUSZ = 2
      NGAUST = 2 * NGAUST
```

```
      WRITE (6, 104) K, M, ALPHA, NGAUSZ, NGAUST
C
 104  FORMAT ("1INPUT FOR THIS CASE IS:" ///
     .        " ", 25X, "K =", F10.6, 5X, "M =", I5, 6X, "ALPHA = (",
     .           F5.1, ",", F10.6, ")" //
     .        " ", 14X, "NUMBER OF INTEGRATION POINTS IN THE XI DIRECT",
     .        "ION =", I5, //
     .        " ", 14X, "NUMBER OF GAUSSIAN POINTS IN THE THETA DIRECT",
     .        "ION =", I5, " (GAUSS - LEGENDRE)")
C
      PRINT 105
C
 105  FORMAT ("1THE CALCULATED SURFACE DISTRIBUTIONS OF THE ACOUSTIC P",
     .        "OTENTIAL, THE ACOUSTIC VELOCITY, AND THE EFFECTIVE ADMI",
     .        "TTANCE ARE:" ////
     .        "  N", 11X, "P(RHO, Z)", 14X, "PHI/COS(M*THETA)", 20X,
     .        "VEL/COS(M*THETA)", 18X, "EFFECTIVE ADMITTNACE" // " ")
C
      DO 6 I = 1, NP
      IF (ICHECK(I)) 7, 8, 9
 7    CONTINUE
      VELP(I) = CPHI(I)
      PVELM(I) = CABS (VELP(I))
      PPVELP(I) = 0.0
      IF (PVELM(I) .NE. 0.0) PPVELP(I) = ATAN2 (AIMAG (VELP(I)),
     .                        REAL (VELP(I)))
      CPHI(I) = CEXACT(I)
      RPHI(I) = REAL (CPHI(I))
      IPHI(I) = AIMAG (CPHI(I))
      MPHI(I) = CABS (CPHI(I))
      PPHI(I) = 0.0
      IF (MPHI(I) .NE. 0.0) PPHI(I) = ATAN2 (IPHI(I), RPHI(I))
      ADMIT(I) = VELP(I) / CPHI(I)
      IF (MPHI(I) .EQ. 0.0) ADMIT(I) = (0.0, 0.0)
      MADMIT(I) = CABS (ADMIT(I))
      PADMIT(I) = 0.0
      IF (MADMIT(I) .NE. 0.0) PADMIT(I) = ATAN2 (AIMAG (ADMIT(I)),
     .                         REAL (ADMIT(I)))
C
      WRITE (6, 106) I, P(I, 1), P(I, 2), VELP(I), ADMIT(I)
C
 106  FORMAT (" ", I3, 7X, "(", F5.3, ",", F6.3, ")", 44X, 2G13.5, 10X,
     .        2G13.5)
C
      GO TO 10
 8    CONTINUE
      RPHI(I) = REAL (CPHI(I))
      IPHI(I) = AIMAG (CPHI(I))
      MPHI(I) = CABS (CPHI(I))
      PPHI(I) = 0.0
      IF (MPHI(I) .NE. 0.0) PPHI(I) = ATAN2 (IPHI(I), RPHI(I))
      VELP(I) = CVEL(I)
      PVELM(I) = CABS (VELP(I))
      PPVELP(I) = 0.0
      IF (PVELM(I) .NE. 0.0) PPVELP(I) = ATAN2 (AIMAG (VELP(I)),
     .                        REAL (VELP(I)))
      ADMIT(I) = VELP(I) / CPHI(I)
      MADMIT(I) = CABS (ADMIT(I))
      PADMIT(I) = 0.0
      IF (MADMIT(I) .NE. 0.0) PADMIT(I) = ATAN2 (AIMAG (ADMIT(I)),
     .                         REAL (ADMIT(I)))
C
      WRITE (6, 107) I, P(I, 1), P(I, 2), CPHI(I), ADMIT(I)
C
 107  FORMAT (" ", I3, 7X, "(", F5.3, ",", F6.3, ")", 8X, 2G13.5, 46X,
     .        2G13.5)
```

```
      GO TO 10
 9    CONTINUE
      RPHI(I) = REAL (CPHI(I))
      IPHI(I) = AIMAG (CPHI(I))
      MPHI(I) = CABS (CPHI(I))
      PPHI(I) = 0.0
      IF (MPHI(I) .NE. 0.0) PPHI(I) = ATAN2 (IPHI(I), RPHI(I))
      VELP(I) = CPHI(I) * CY(I)
      PVELM(I) = CABS (VELP(I))
      PPVELP(I) = 0.0
      IF (PVELM(I) .NE. 0.0) PPVELP(I) = ATAN2 (AIMAG (VELP(I)),
     .                                  REAL (VELP(I)))
      ADMIT(I) = CY(I)
      MADMIT(I) = CABS (ADMIT(I))
      PADMIT(I) = 0.0
      IF (MADMIT(I) .NE. 0.0) PADMIT(I) = ATAN2 (AIMAG (ADMIT(I)),
     .                                  REAL (ADMIT(I)))
C
      WRITE (6, 108) I, P(I, 1), P(I, 2), CPHI(I), VELP(I)
C
 108  FORMAT (" ", I3, 7X, "(", F5.3, ",", F6.3, ")", 8X, 2G13.5, 10X,
     .        2G13.5)
C
 10   CONTINUE
 6    CONTINUE
C
      PRINT 113
C
 113  FORMAT ("1THE MODULUS OF THE ACOUSTIC POTENTIAL, THE ACOUSTIC VE",
     .        "LOCITY, AND THE EFFECTIVE ADMITTANCE ARE:" ////
     .        "  N", 11X, "P(RHO, Z)", 14X, "PHI/COS(M*THETA)", 20X,
     .        "VEL/COS(M*THETA)", 18X, "EFFECTIVE ADMITTANCE" /
     .        " ", 36X, "EXACT        CALC", 20X, "EXACT        CALC",
     .           20X, "EXACT        CALC" // " ")
C
      DO 16 I = 1, NP
      IF (ICHECK(I)) 17, 18, 19
 17   CONTINUE
C
      WRITE (6, 114) I, P(I, 1), P(I, 2), MEXACT(I), MVELP(I), PVELM(I),
     .               MYP(I), MADMIT(I)
C
 114  FORMAT (" ", I3, 7X, "(", F5.3, ",", F6.3, ")", 8X, G13.5, 23X,
     .        2G13.5, 10X, 2G13.5)
C
      GO TO 20
 18   CONTINUE
C
      WRITE (6, 115) I, P(I, 1), P(I, 2), MEXACT(I), MPHI(I), MVELP(I),
     .               MYP(I), MADMIT(I)
C
 115  FORMAT (" ", I3, 7X, "(", F5.3, ",", F6.3, ")", 8X, 2G13.5, 10X,
     .        G13.5, 23X, 2G13.5)
C
      GO TO 20
 19   CONTINUE
C
      WRITE (6, 116) I, P(I, 1), P(I, 2), MEXACT(I), MPHI(I), MVELP(I),
     .               PVELM(I), MYP(I)
C
 116  FORMAT (" ", I3, 7X, "(", F5.3, ",", F6.3, ")", 8X, 2G13.5, 10X,
     .        2G13.5, 10X, G13.5)
C
 20   CONTINUE
 16   CONTINUE
```

```
C
      PRINT 120
C
  120 FORMAT ("1THE PHASE OF THE ACOUSTIC POTENTIAL, THE ACOUSTIC VELO",
     .        "CITY, AND THE EFFECTIVE ADMITTANCE ARE:" ////
     .        "   N", 11X, "P(RHO, Z)", 21X, "PHI", 33X, "VEL", 24X,
     .        "EFFECTIVE ADMITTANCE" /
     .        " ", 36X, "EXACT        CALC", 20X, "EXACT        CALC",
     .             20X, "EXACT        CALC" // " ")
C
      DO 11 I = 1, NP
      IF (ICHECK(I)) 12, 13, 14
   12 CONTINUE
C
      WRITE (6, 114) I, P(I, 1), P(I, 2), PEXACT(I), PVELP(I),
     .               PPVELP(I), PYP(I), PADMIT(I)
C
      GO TO 15
   13 CONTINUE
C
      WRITE (6, 115) I, P(I, 1), P(I, 2), PEXACT(I), PPHI(I), PVELP(I),
     .               PYP(I), PADMIT(I)
C
      GO TO 15
   14 CONTINUE
C
      WRITE (6, 116) I, P(I, 1), P(I, 2), PEXACT(I), PPHI(I), PVELP(I),
     .               PPVELP(I), PYP(I)
C
   15 CONTINUE
   11 CONTINUE
C
C     WRITE THE SURFACE DISTRIBUTIONS TO THE OUTPUT FILE.
C
      WRITE (10, 121) (CPHI(I), VELP(I), I = 1, NP)
C
  121 FORMAT (4G20.10)
C
      RETURN
      END
```

The following computer program reads the previous programs output file containing the values of the acoustic quantities on the surface of the body and calculates the values of the acoustic quantities at any given point in the field surrounding the body. The required inputs are the points where the acoustic quantities are known on the surface of the body Q, the normals to the body at these points NQ, the length of each integration interval LENGTH, the points in the field where the acoustic quantities are required P, and some arbitrary normal at these points NP as the normal acoustic velocity is calculated. The problem specification data is also required again; that is, k the wave number and m the mode number.

The program prints out all the geometric input data and the acoustic potential and normal acoustic velocity at the field points. It also calculates and prints out the SPL(dB) at each field point.

```
      PROGRAM EXPFF (INPUT, OUTPUT, TAPE10, TAPE11,
                     TAPE5 = INPUT, TAPE6 = OUTPUT)
C
C
C*****************************************************************************
C*                                                                           *
C*                                                                           *
C*      THIS PROGRAM CALCULATES THE ACOUSTIC POTENTIAL AND THE               *
C*      ACOUSTIC VELOCITY IN THE FIELD SURROUNDING ANY AXISYMMETRIC          *
C*      BODY EMPLOYING THE SURFACE DISTRIBUTIONS OF THE ACOUSTIC             *
C*      POTENTIAL AND THE NORMAL ACOUSTIC VELOCITY.                          *
C*                                                                           *
C*****************************************************************************
C*                                                                           *
C*      A CYLINDRICAL FORMULATION OF THE PROBLEM IS EMPLOYED.                *
C*                                                                           *
C*                                                                           *
C*****************************************************************************
C
C
      REAL K, LENGTH
      COMPLEX CPHIP, CPHIQ, CVELP, CVELQ, IK, IKSQ
C
      COMMON /I/ M, NP, NQ
      COMMON /R/ FOURPI, K, PI, TWOPI
      COMMON /C/ IK, IKSQ
      COMMON /RD/ LENGTH (102), P (9, 2), PNORMAL (9, 2),
     .            Q (102, 2), QNORMAL (102, 2)
      COMMON /CD/ CPHIP (9), CPHIQ (102), CVELP (9), CVELQ (102)
      COMMON /NGAUSS/ NGAUSS
      COMMON /GAUSS/ GAUSST (48, 2)
C
      CALL INPUT
C
C     REAL CONSTANTS
C
      TWOPI = 2.0 * PI
      FOURPI = 4.0 * PI
C
C     COMPLEX CONSTANTS
C
      IK = (0.0, 1.0) * K
      IKSQ = IK * IK
C
      CALL CALC
C
      CALL OUTPUT
C
      STOP "NORMAL"
C
      END
```

```
      BLOCK DATA
C
      REAL K
C
      COMMON /I/ M, NP, NQ
      COMMON /R/ FOURPI, K, PI, TWOPI
      COMMON /NGAUSS/ NGAUSS
      COMMON /CAUSS/ CAUSST (48, 2)
C
C     THE NUMBER OF POINTS IN THE FIELD WHERE THE ACOUSTIC POTENTIAL
C     AND THE ACOUSTIC VELOCITY ARE TO BE CALCULATED.
C
      DATA NP / 9 /
C
C     THE NUMBER OF POINTS ON THE SURFACE OF THE BODY WHERE THE
C     ACOUSTIC POTENTIAL AND THE NORMAL ACOUSTIC VELOCITY ARE KNOWN.
C
      DATA NQ / 102 /
C
      DATA PI / 3.1415926535898 /
C
      DATA NGAUSS / 48 /
C
      DATA ((CAUSST(I, J), J = 1, 2), I = 1, 12)
     .     / 0.01627674484960, 0.03255061449236,
     .       0.04881298513605, 0.03251611871387,
     .       0.08129749546443, 0.03244716371406,
     .       0.11369585011067, 0.03234382256858,
     .       0.14597371465490, 0.03220620479403,
     .       0.17809688236762, 0.03203445623199,
     .       0.21003131046057, 0.03182875889441,
     .       0.24174315616384, 0.03158933077073,
     .       0.27319881259105, 0.03131642559686,
     .       0.30436494435450, 0.03101033258631,
     .       0.33520852289263, 0.03067137612367,
     .       0.36569686147231, 0.03029991542083 /
      DATA ((CAUSST(I, J), J = 1, 2), I = 13, 24)
     .     / 0.39579764982891, 0.02989634413633,
     .       0.42547898840730, 0.02946108995817,
     .       0.45470942216774, 0.02899461415056,
     .       0.48345797392060, 0.02849741106509,
     .       0.51169417715467, 0.02797000761685,
     .       0.53938810832436, 0.02741296272603,
     .       0.56651041856140, 0.02682686672559,
     .       0.59303236477757, 0.02621234073567,
     .       0.61892584012547, 0.02557003600535,
     .       0.64416340378497, 0.02490063322248,
     .       0.66871831004392, 0.02420484179236,
     .       0.69256453664217, 0.02348339908593 /
      DATA ((CAUSST(I, J), J = 1, 2), I = 25, 36)
     .     / 0.71567681234897, 0.02273706965833,
     .       0.73803964374440, 0.02196664443874,
     .       0.75960234117665, 0.02117293989219,
     .       0.78036904386743, 0.02035679715433,
     .       0.80030874413914, 0.01951908114015,
     .       0.81940031073793, 0.01866067962741,
     .       0.83762351122819, 0.01778250231605,
     .       0.85495903343460, 0.01688547986425,
     .       0.87138850590930, 0.01597056290256,
     .       0.88689451740242, 0.01503872102699,
     .       0.90146063531585, 0.01409094177231,
     .       0.91507142312090, 0.01312822956696 /
      DATA ((CAUSST(I, J), J = 1, 2), I = 37, 48)
     .     / 0.92771245672231, 0.01215160467109,
     .       0.93937033975276, 0.01116210209984,
     .       0.95003271778444, 0.01016077053501,
     .       0.95968829144874, 0.00914867123078,
     .       0.96832682846326, 0.00812687692570,
     .       0.97593917458514, 0.00709647079115,
     .       0.98251726356301, 0.00605854550424,
     .       0.98805412632962, 0.00501420274293,
     .       0.99254390032376, 0.00396455433844,
     .       0.99598184298721, 0.00291073181793,
     .       0.99836437586318, 0.00185396078895,
     .       0.99968950388323, 0.00079679206555 /
C
      END
```

```
      SUBROUTINE INPUT
C
      REAL K, LENGTH
      COMPLEX CPHIP, CPHIQ, CVELP, CVELQ
C
      COMMON /I/ M, NP, NQ
      COMMON /R/ FOURPI, K, PI, TWOPI
      COMMON /RD/ LENGTH (102), P (9, 2), PNORMAL (9, 2),
     .            Q (102, 2), QNORMAL (102, 2)
      COMMON /CD/ CPHIP (9), CPHIQ (102), CVELP (9), CVELQ (102)
C
      READ (5, 100) ((P(I, J), J = 1, 2), I = 1, NP)
C
      READ (5, 100) ((PNORMAL (I, J), J = 1, 2), I = 1, NP)
C
      READ (5, 100) ((Q(I, J), J = 1, 2), I = 1, NQ)
C
      READ (5, 100) ((QNORMAL (I, J), J = 1, 2), I = 1, NQ)
C
      READ (5, 100) (LENGTH(I), I = 1, NQ)
C
  100 FORMAT (8G10.0)
C
      PRINT 101
C
  101 FORMAT ("1GEOMETRIC INPUT DATA:" ///
     .        " ", 4X, "N", 21X, "Q(RHO, Z)", 38X, "NORMAL(RHO, Z)",
     .                           29X, "LENGTH" // " ")
C
      WRITE (6, 102) (I, Q(I, 1), Q(I, 2), QNORMAL(I, 1), QNORMAL(I, 2),
     .                LENGTH(I), I = 1, NQ)
C
  102 FORMAT (" ", 2X, I3, 10X, "(", F13.10, ",", F13.10, ")", 21X,
     .                           "(", F13.10, ",", F13.10, ")", 17X,
     .                                F13.10)
C
      PRINT 103
C
  103 FORMAT ("1FIELD POINT INPUT DATA:" ///
     .        " ", 4X, "N", 21X, "P(RHO, Z)", 38X, "NORMAL(RHO, Z)" //
     .        " ")
C
      WRITE (6, 104) (I, P(I, 1), P(I, 2), PNORMAL(I, 1), PNORMAL(I, 2),
     .                I = 1, NP)
C
  104 FORMAT (" ", 2X, I3, 9X, "(", F14.10, ",", F14.10, ")", 20X,
     .                         "(", F13.10, ",", F13.10, ")")
C
      READ (10, 105) (CPHIQ(I), CVELQ(I), I = 1, NQ)
C
  105 FORMAT (4G20.10)
C
      PRINT 106
C
  106 FORMAT ("1", 61X, "********" / " ", 61X, "*      *" /
     .        " ", 61X, "* BODY *" / " ", 61X, "*      *" /
     .        " ", 61X, "********" //// "  N", 21X, "Q(RHO, Z)", 25X,
     .        "ACOUSTIC POTENTIAL", 21X, "ACOUSTIC VELOCITY" // " ")
C
      WRITE (6, 107) (I, Q(I, 1), Q(I, 2), CPHIQ(I), CVELQ(I),
     .                I = 1, NQ)
C
  107 FORMAT (" ", I3, 9X, "(", F13.10, ",", F13.10, ")",
     .                 9X, "(", F14.10, ",", F14.10, ")",
     .                 8X, "(", F14.10, ",", F14.10, ")")
C
      READ (11, 1100) M, K
C
 1100 FORMAT (I20, G20.0)
C
      RETURN
      END
```

```
      SUBROUTINE CALC
C
      REAL K, LENGTH, NDOTN, NRHOQP, NZPZD, NZQZD, NZQP
      COMPLEX CPHIP, CPHIQ, CVELP, CVELQ, G, GP, GPP, IK, IKSQ, I1, I2,
     .        I3, I4
C
      COMMON /I/ M, NP, NQ
      COMMON /R/ FOURPI, K, PI, TWOPI
      COMMON /C/ IK, IKSQ
      COMMON /RD/ LENGTH (102), P (9, 2), PNORMAL (9, 2),
     .            Q (102, 2), QNORMAL (102, 2)
      COMMON /CD/ CPHIP (9), CPHIQ (102), CVELP (9), CVELQ (102)
      COMMON /NGAUSS/ NGAUSS
      COMMON /GAUSS/ GAUSST (48, 2)
C
      DO 1 I = 1, NP
      CPHIP(I) = (0.0, 0.0)
      CVELP(I) = (0.0, 0.0)
C
C     XI INTEGRATION
C
      DO 2 J = 1, NQ
      GAUSZ = TWOPI * LENGTH(J)
      ZD = Q(J, 2) - P(I, 2)
      NZQZD = QNORMAL(J, 2) * ZD
      NZPZD = PNORMAL(I, 2) * ZD
      ZSQ = ZD * ZD
      RHOSQ = (Q(J, 1) - P(I, 1))**2
      RHOQP2 = 2.0 * Q(J, 1) * P(I, 1)
      NRHOQP = QNORMAL(J, 1) * PNORMAL(I, 1)
      NZQP = QNORMAL(J, 2) * PNORMAL(I, 2)
      RHOZSQ = RHOSQ + ZSQ
C
C     THETA INTEGRATION
C
      DO 3 IT = 1, NGAUSS
      THETA = PI * GAUSST(IT, 1)
      GAUSZT = GAUSZ * GAUSST(IT, 2)
C
      COST = COS (THETA)
      COSMT = COS (M * THETA)
C
      R = SQRT (RHOZSQ + RHOQP2 * (1.0 - COST))
      DRDNP = (PNORMAL(I, 1) * (P(I, 1) - Q(J, 1) * COST) - NZPZD) / R
      DRDNQ = (QNORMAL(J, 1) * (Q(J, 1) - P(I, 1) * COST) + NZQZD) / R
      NDOTN = NRHOQP * COST + NZQP
C
      G = Q(J, 1) * GAUSZT * COSMT * CEXP (IK * R) / R
      GP = G * (IK - (1.0 / R))
      GPP = G * (IKSQ - (3.0 * IK / R) + (3.0 / (R * R)))
C
      I1 = GP * DRDNQ
      I2 = -G
      I3 = GPP * DRDNQ * DRDNP - (GP * NDOTN / R)
      I4 = -GP * DRDNP
C
      CPHIP(I) = CPHIP(I) + I1 * CPHIQ(J) + I2 * CVELQ(J)
      CVELP(I) = CVELP(I) + I3 * CPHIQ(J) + I4 * CVELQ(J)
C
 3    CONTINUE
 2    CONTINUE
C
      CPHIP(I) = CPHIP(I) / FOURPI
      CVELP(I) = CVELP(I) / FOURPI
C
 1    CONTINUE
C
      RETURN
      END
```

```
      SUBROUTINE OUTPUT
C
      REAL IPHI, IPHIP, IVEL, IVELP, K, LENGTH, MPHI, MPHIP, MVEL,
     .     MVELP
      COMPLEX CPHIP, CPHIQ, CVELP, CVELQ, Y
C
      COMMON /I/ M, NP, NQ
      COMMON /R/ FOURPI, K, PI, TWOPI
      COMMON /RD/ LENGTH (102), P (9, 2), PNORMAL (9, 2),
     .            Q (102, 2), QNORMAL (102, 2)
      COMMON /CD/ CPHIP (9), CPHIQ (102), CVELP (9), CVELQ (102)
      COMMON /NGAUSS/ NGAUSS
C
      DIMENSION IPHI (9), IPHIP (9), MPHI (9), MPHIP (9),
     .          PPHI (9), PPHIP (9), RPHI (9), RPHIP (9),
     .          IVEL (9), IVELP (9), MVEL (9), MVELP (9),
     .          PVEL (9), PVELP (9), RVEL (9), RVELP (9)
C
C     INITIALIZE EXACT SOLUTION.
C
      DO 2 I = 1, NP
      RPHI(I) = 0.0
      IPHI(I) = 0.0
      MPHI(I) = 0.0
      PPHI(I) = 0.0
      RVEL(I) = 0.0
      IVEL(I) = 0.0
      MVEL(I) = 0.0
      PVEL(I) = 0.0
 2    CONTINUE
      NGAUSS = 2 * NGAUSS
C
      WRITE (6, 100) K, M, NGAUSS
C
 100  FORMAT ("1INPUT FOR THIS CASE IS:" ///
     .        " ", 60X, "K =", F10.6 // " ", 60X, "M =", I5 //
     .        " ", 13X, "NUMBER OF GAUSSIAN POINTS IN THE THETA DIRECT",
     .        "ION =", I5, " (GAUSS - LEGENDRE)")
C
      DO 5 I = 1, NP
      RPHIP(I) = REAL (CPHIP(I))
      RVELP(I) = REAL (CVELP(I))
      IPHIP(I) = AIMAG (CPHIP(I))
      IVELP(I) = AIMAG (CVELP(I))
      MPHIP(I) = CABS (CPHIP(I))
      MVELP(I) = CABS (CVELP(I))
      PPHIP(I) = 0.0
      PVELP(I) = 0.0
      IF (MPHIP(I) .NE. 0.0) PPHIP(I) = ATAN2 (IPHIP(I), RPHIP(I))
      IF (MVELP(I) .NE. 0.0) PVELP(I) = ATAN2 (IVELP(I), RVELP(I))
 5    CONTINUE
C
      PRINT 103
C
 103  FORMAT ("1", 58X, "**************" / " ", 58X, "*            *" /
     .        " ", 58X, "* CALCULATED *" / " ", 58X, "*            *" /
     .        " ", 58X, "**************" //// "  N", 21X, "P(RHO, Z)",
     .             25X, "ACOUSTIC POTENTIAL",
     .             21X, "ACOUSTIC VELOCITY" // " ")
C
      WRITE (6, 102) (I, P(I, 1), P(I, 2), CPHIP(I), CVELP(I),
     .                I = 1, NP)
C
 102  FORMAT (" ", I3, 8X, "(", F14.10, ",", F14.10, ")",
     .                8X, "(", F14.10, ",", F14.10, ")",
     .                8X, "(", F14.10, ",", F14.10, ")")
C
```

```
      PRINT 109
C
 109  FORMAT ("1THE MODULUS OF THE ACOUSTIC POTENTIAL AND THE ACOUSTIC",
     .        " VELOCITY ARE:" //// "  N", 11X, "P(RHO, Z)", 14X,
     .        "PHI/COS(M*THETA)", 20X, "VEL/COS(M*THETA)", 8X,
     .        "SPL (DB)", 16X, "Y" /
     .        " ", 36X, "EXACT        CALC", 20X, "EXACT        CALC" //
     .        " ")
C
      DO 7 I = 1, NP
      SPL = 20.0 * ALOG10 (K * MPHIP(I)) + 146.6
      Y = CVELP(I) / CPHIP(I)
C
      WRITE (6, 110) I, P(I, 1), P(I, 2), MPHI(I), MPHIP(I), MVEL(I),
     .               MVELP(I), SPL, Y
C
 110  FORMAT (" ", I3, 6X, "(", F6.3, ",", F7.3, ")", 7X, 2G13.5, 10X,
     .        2G13.5, 2X, F7.2, 5X, 2G13.5)
C
 7    CONTINUE
C
      PRINT 112
C
 112  FORMAT ("1THE PHASE OF THE ACOUSTIC POTENTIAL AND THE ACOUSTIC V",
     .        "ELOCITY ARE:" //// "  N", 11X, "P(RHO, Z)", 21X,
     .        "PHI", 33X, "VEL" /
     .        " ", 36X, "EXACT        CALC", 20X, "EXACT        CALC" //
     .        " ")
C
      WRITE (6, 113) (I, P(I, 1), P(I, 2), PPHI(I), PPHIP(I), PVEL(I),
     .                PVELP(I), I = 1, NP)
C
 113  FORMAT (" ", I3, 6X, "(", F6.3, ",", F7.3, ")", 7X, 2G13.5, 10X,
     .        2G13.5)
C
      RETURN
      END
```

Appendix B

Paper accepted for publication in the Journal of the Acoustical Society of America

"Prediction of the Sound Field Radiated From Axisymmetric Surfaces"

PREDICTION OF THE SOUND FIELD RADIATED FROM AXISYMMETRIC SURFACES

W. L. Meyer*, W. A. Bell*, M. P. Stallybrass** and B. T. Zinn*

*School of Aerospace Engineering
**School of Mathematics
Georgia Institute of Technology
Atlanta, Georgia 30332

Abstract

A general analytical method for determining the radiated sound fields from axisymmetric surfaces of arbitrary cross section with general boundary conditions is developed. The method is based on an integral representation for the external solutions of the Helmholtz equation. An integral equation is developed governing the surface potential distribution which gives unique solutions at all wave numbers. The axisymmetric formulation of the problem reduces its solution to the numerical evaluation of line integrals by Gaussian quadrature. The applicability of the solution approach for both a sphere and finite cylinder is demonstrated by comparing the numerical results with exact analytical solutions for both discontinuous and continuous boundary conditions. The method is then applied to a jet engine inlet configuration and the computed results are in good agreement with exact values.

I. Introduction

To reduce the noise radiated to the community from turbofan inlets, the effects of sound suppression material in the inlet and the spatial distribution of the sound source on the radiated sound levels and patterns must be determined. Analytical techniques for predicting these effects must be capable of dealing with general axisymmetric geometries and complicated boundary conditions which are encountered in multiply-lined inlets. For instance, in a typical inlet the compressor-fan combination represents a noise source

with a nonuniform spatial excitation pattern. Thus, the analytical method should be capable of taking into account sound sources of general spatial distribution. Also, inlets may contain multiple acoustic liners to reduce the radiated sound power and admittance boundary conditions are commonly used to account for the absorption characteristics of the liner. Therefore, the analytical method must be capable of dealing with spatially varying surface admittances. Finally, the method should be capable of predicting the characteristics of the radiated sound field in an infinite domain. Keeping these requirements in mind, the work presented in this paper describes the results of an investigation which has been concerned with the analytical determination of radiated sound fields from axisymmetric surfaces of arbitrary cross section and with general boundary conditions.

The method used in this investigation is based on an integral form of the solutions of the Helmholtz equation.[1-6] With this formulation the acoustic potential anywhere external to the surface can be found once the distribution on the surface is known. Thus, to determine the radiated sound field the problem reduces to the determination of the distribution of the acoustic potential on the two dimensional surface of the geometry under consideration instead of solving the Helmholtz equation in the surrounding infinite three dimensional domain.

It has been previously shown [1-5] that when applied to exterior sound radiation problems the classical techniques fail to produce unique solutions at frequencies corresponding to certain interior eigenvalues of the geometries under consideration. Unless special precautions are taken, straight-forward numerical solution of the integral equation produces large errors at frequencies close to these eigenvalues. For the general geometries of interest in this study, these eigenfrequencies are not known a priori. Therefore,

the frequencies about which large numerical errors can occur cannot be easily avoided. A critical review of available analytical techniques for avoiding these errors is provided by Burton in Ref. 1. In a search for an appropriate technique for use in the present study of inlets, the authors programmed each of these methods for a sphere and obtained numerical results for the surface and radiated sound field. This study showed that the method of Burton and Miller[4] was the most straightforward to implement. However, an interpretation of a strongly singular integral, given in the analysis in Ref. 5 by Meyer, et.al. was necessary for the equations to be amenable to numerical solution. Basically the method proposed by Burton and Miller involves a reformulation of the integral equation for the acoustic potential and the solutions obtained are valid at all frequencies. It also yields the most consistently accurate results for a given number of points at which the acoustic potential is numerically evaluated on the surface. Therefore, the method based on the analysis in Ref. 5 has been chosen for this investigation.

The resulting integral equation for the surface acoustic potential is solved numerically and, for axisymmetric geometries, the equation reduces to the evaluation of line integrals. Thus, the axisymmetric case can be reduced to an equivalent one-dimensional problem. Having discretized the integral equation, the resulting system of algebraic equations is solved using complex Gauss-Jordan elimination. Since the coefficient matrix involves the free space Green's function, which becomes singular as two points on the surface approach one another, numerical techniques are presented which can deal with these singularities and yield accurate results. Gaussian integration is used to increase the accuracy of the solution without significant penalties in computer storage and time requirements. The applicability of the integral formulation and the accuracy of the numerical techniques are demonstrated by

computing the surface and far field distributions of the acoustic potential on both a sphere and a finite cylinder. The numerical results are compared with known exact solutions generated by the separation of variables technique. Surfaces with spatially varying forcing functions and admittances are considered, for different tangential modes, to evaluate the capability of the integral approach to handle boundary conditions of a general nature. With the sphere, agreement between computed and exact results is to three significant figures. For the cylinder agreement is to two significant figures. The effect on the accuracy of discontinuous boundary conditions involving nonzero admittances over the surface and of the corners encountered in the cylindrical configuration are also presented. Finally, the numerical results for an inlet configuration are compared with exact solutions and agreement is to within ten per cent.

II. Theoretical Considerations

In this section the general three dimensional integral representation of the solutions of the Helmholtz equation is developed for application to radiation problems. This particular formulation yields unique solutions at all frequencies and does not have strong singularities which are difficult to handle numerically. The general integral equation is then specialized for axisymmetric geometries. A more detailed development is presented in Ref. 5.

General Formulation

Beginning with the three dimensional Helmholtz equation which governs the spatial dependence of the acoustic field for harmonic oscillations

$$\nabla^2 \varphi + k^2 \varphi = 0 \tag{1}$$

where φ is the acoustic potential and k is the wave number; the standard integral representation of the exterior potential is found to be[1,6]

$$\iint_S \left(\varphi(Q) \frac{\partial G(P,Q)}{\partial n_q} - G(P,Q) \frac{\partial \varphi(Q)}{\partial n_q}\right) dS_q = 4\pi\varphi(P) \tag{2}$$

where the term $\frac{\partial}{\partial n_q}$ represents an outward normal derivative with respect to the body S as shown in Fig. 1; that is,

$$\frac{\partial \varphi(Q)}{\partial n_q} = \vec{\nabla}_q \varphi(Q) \cdot \vec{n}_q \tag{3}$$

Also, G(P,Q) is a fundamental three dimensional solution of the Helmholtz equation and is taken to be the free space Green's Function for a point source[6] defined as

$$G(P,Q) = \frac{e^{ikr(P,Q)}}{r(P,Q)} \tag{4}$$

From Eq. (2), if the acoustic potential and the normal acoustic velocity $\frac{\partial \varphi(Q)}{\partial n_q}$ are known at each point on the surface of the body then the acoustic potential may be calculated anywhere in the exterior domain.

To solve for the surface potential, the point P is moved to the surface of the body, and Eq. (2) then becomes

$$\iint_S \left(\varphi(Q) \frac{\partial G(P,Q)}{\partial n_q} - G(P,Q) \frac{\partial \varphi(Q)}{\partial n_q}\right) dS_q = 2\pi\varphi(P) \tag{5}$$

For the inhomogeneous Robin boundary condition employed in this study, a relation between $\partial\varphi(Q)/\partial n_q$ and $\varphi(Q)$ exists which is given by

$$\frac{\partial \varphi(Q)}{\partial n_q} - Y(Q)\varphi(Q) = A(Q), \tag{6}$$

so that Eq. (5) can be written in terms of the potential only; that is,

$$\iint_S \varphi(Q) \frac{\partial G(P,Q)}{\partial n_q} dS_q - \iint_S \varphi(Q)G(P,Q)Y(Q)dS_q \tag{7}$$

$$= 2\pi\varphi(P) + \int\int_S A(Q)\ G(P,Q)\ dS_q$$

If the acoustic velocity A(Q) and the admittance Y(Q) are specified at each point on the surface of the body, then the acoustic potential may be calculated at each point using Eq.(7).

As mentioned earlier this equation does not yield unique solutions when the wave number k is an internal eigenvalue associated with the problem under consideration. Since these eigenvalues are not known a priori for general bodies, the formulation cannot be relied upon to give consistently good results. There are a number of papers in the literature [2,3,4] dealing with this problem, and the relative merits and shortcomings of the methods employed are discussed in detail in Ref. 1.

An attractive approach from an analytical point of view is provided by Burton and Miller[4] who have suggested the use of the following identity to derive an alternative integral equation for the acoustic potential at the surface.

$$2\pi\ \frac{\partial\varphi(P)}{\partial n_p} = \int_S\int\left[\varphi(Q)\ \frac{\partial^2 G(P,Q)}{\partial n_p \partial n_q} - \frac{\partial G(P,Q)}{\partial n_p}\ \frac{\partial\varphi(Q)}{\partial n_q}\right]dS_q \qquad (8)$$

This equation can now be solved for $\varphi(P)$ by using Eq. (6) to relate the normal acoustic velocity and the potential at the surface. However this integral equation has its own set of associated eigenvalues at which unique solutions cannot be obtained. To circumvent the problem associated with the solution of the integral equations derived from Eqs.(5) and (8), Burton and Miller suggested the solution of the following linear combination of these equations:

$$\int\int_S \left(\varphi(Q)\ \frac{\partial G(P,Q)}{\partial n_q} - G(P,Q)\ \frac{\partial\varphi(Q)}{\partial n_q}\right) dS_q$$

$$+ \alpha \int\int_S \left(\varphi(Q) \frac{\partial^2 G(P,Q)}{\partial n_p \partial n_q} - \frac{\partial G(P,Q)}{\partial n_p} \frac{\partial \varphi(Q)}{\partial n_q} \right) dS_q$$

$$= 2\pi \left(\varphi(P) + \alpha \frac{\partial \varphi(P)}{\partial n_p} \right) \tag{9}$$

where $\partial \varphi / \partial n$ and φ are related by Eq. (6). Equation (9) will yield unique solutions if the complex coupling constant is properly chosen. It is shown that α must meet the following restrictions to guarantee that Eq. (9) yields unique solutions:*

$$\begin{aligned} &\text{Im } (\alpha) \neq 0 \quad && k \text{ real or imaginary} \\ &\text{Im } (\alpha) = 0 \quad && k \text{ complex} \end{aligned} \tag{10}$$

A problem arises in the numerical solution of Eq. (9) as the third term on the left hand side is strongly singular in its present form as the point Q approaches the point P on the surface of the body. The authors of this paper have shown that this difficulty can be overcome by a proper interpretation of this singular term.[5] Employing a vector transformation[8] and taking the Cauchy Principle Value, Eq. (9) is shown to be equivalent to

$$\int\int_S \left[\varphi(Q) \frac{\partial G(P,Q)}{\partial n_q} - G(P,Q) \frac{\partial \varphi(Q)}{\partial n_q} \right] dS_q$$

$$+ \alpha \int\int_S \left[\varphi(Q) - \varphi(P) \right] \frac{\partial^2 G(P,Q)}{\partial n_p \partial n_q} \, dS_q \tag{11}$$

$$- \alpha \varphi(P) \int\int_S (n_p \cdot n_q)(ik)^2 \, G(P,Q) \, dS_q$$

---

* It has been pointed out to us by a reviewer that an equation of the same general form as Eq. (9) has been given by Chertock[7]. However, for an arbitrary, smooth surface, Chertock did not interpret this integral equation correctly. Specifically, the limit indicated in the final term of (A17), Ref. (7), does not exist as may be verified for the simple case of a sphere.

$$- \alpha \iint_S \frac{\partial G(P,Q)}{\partial n_p} \frac{\partial \varphi(Q)}{\partial n_q} \, dS_q = 2\pi \left[\varphi(P) + \alpha \frac{\partial \varphi(P)}{\partial n_p} \right]$$

All of the terms in Eq. (11) are now well defined; however, all the integrands are oscillatory and singular so that care must be taken in their numerical approximation.

Axisymmetric Formulation

When dealing with a body of revolution as shown in Fig. 2 an axisymmetric formulation of the problem is advantageous.[9] This being the case an element of area dS_q becomes $\rho ds d\theta$ where s is the distance along the perimeter of the surface in the ρ-z plane. Assuming an acoustic velocity distribution of the form

$$\frac{\partial \varphi}{\partial n} = v(s) \cos m \theta \tag{12}$$

and describing the s dependence of the potential function by

$$\Phi(s) \equiv \frac{\varphi}{\cos m \theta} \tag{13}$$

and letting $\theta_p = 0$ (so that $\cos \theta_p = 1$) Eq. (11) becomes:

$$\begin{aligned} &\iint_S \Phi(s_q) \frac{\partial G(P,Q)}{\partial n_q} \cos m \theta_q \, dS_q \\ &- \alpha \Phi(s_p) \iint_S G(P,Q)(ik)^2 (n_p \cdot n_q) \, dS_q \\ &+ \alpha \iint_S \left[\Phi(s_q) \cos m \theta_q - \Phi(s_p) \right] \frac{\partial^2 G(P,Q)}{\partial n_p \partial n_q} \, dS_q \\ &- \iint_S v(s_q) \, G(P,Q) \cos m \theta_q \, dS_q \end{aligned} \tag{14}$$

$$- \alpha \int_S \int v(s_q) \frac{\partial G(P,Q)}{\partial n_p} \cos m \theta_q \, dS_q$$

$$= 2\pi \left[\Phi(s_p) + \alpha \, v(s_p) \right]$$

Now, three sets of functions are defined:

Influence Functions

$$I_1 (r_{pq}) = 2 \int_0^{\pi} G(P,Q) \cos m \theta_q \, d\theta_q$$

$$I_2 (r_{pq}) = 2\alpha \int_0^{\pi} \frac{\partial G(P,Q)}{\partial n_p} \cos m \theta_q \, d\theta_q \qquad (15)$$

Kernel Functions

$$K_1 (r_{pq}) = 2 \int_0^{\pi} \frac{\partial G(P,Q)}{\partial n_q} \cos m \theta_q \, d\theta_q$$

$$K_2 (r_{pq}) = 2\alpha \int_0^{\pi} \frac{\partial^2 G(P,Q)}{\partial n_p \partial n_q} \cos m \theta_q \, d\theta_q, \quad \theta_q \neq \theta_p \qquad (16)$$

Forcing Functions

$$F_1 (r_{pq}) = 2\alpha \int_0^{\pi} G(P,Q) (ik)^2 (n_p \cdot n_q) \, d\theta_q$$

$$F_2 (r_{pq}) = 2\alpha \int_0^{\pi} \frac{\partial^2 G(P,Q)}{\partial n_p \partial n_q} \, d\theta_q , \quad \theta_q \neq \theta_p \qquad (17)$$

where r_{pq} is the distance between points P and Q and n_p and n_q are the outward normals to the surface at points P and Q, respectively. In evaluating K_2 and F_2, the point at which $\theta_p = \theta_q$ is excluded from the integration. Substituting Eqs. (15)-(17) into Eq. (14) gives

$$\int_0^{\ell} \Phi(s_q) \left\{ K_1 (r_{pq}) + K_2 (r_{pq}) \right\} ds_q$$

$$
\begin{aligned}
&- \Phi(s_p) \int_0^{\ell} \left\{ F_1(r_{pq}) + F_2(r_{pq}) \right\} ds_q \\
&- \int_0^{\ell} v(s_q) \left\{ I_1(r_{pq}) + I_2\ (r_{pq}) \right\} ds_q \\
&= 2\pi \left[\Phi(s_p) + \alpha v(s_p) \right]
\end{aligned}
\tag{18}
$$

where ℓ is the length of the generating line of the surface of revolution. The s-θ coordinate directions have now been essentially uncoupled so that the problem has been reduced to the evaluation of the line integrals in the coordinate directions on the surface of the body. This formulation does not restrict the form or type of boundary conditions on the body; it merely assumes that the boundary conditions can be represented by a sum (expanded in a set) of tangential modes.

III. Results

The acoustic fields for a sphere, cylinder, and inlet configuration have been computed by numerical solution of Eq. (18) using the techniques described in Ref. 10. Basically, this method consists of first specifying the ρ-z coordinates and the normal vector at each point on the surface. From these quantities the distances and the normal derivatives can be obtained. The integral in Eq. (18) is then separated into n integrals taken over subintervals of length ℓ/n. The acoustic potential is assumed constant over each subinterval and the integrations are performed numerically using *Gauss-Legendre* quadrature in the ρ-z plane. Over the subinterval containing the point P, the integrand in Eq. (18) becomes infinite since r_{pq} approaches zero. Thus, only an even number of points is used in the quadrature algorithim, since an odd number would necessitate inclusion of the point where $r_{pq} = 0$.

A Gauss-Legendre quadrature formula is used in the circumferential direction to evaluate Eqs. (15) - (17). All calculations were performed on the Georgia Tech CDC Cyber 70/74 with sixteen significant figures.

In all geometries investigated, exact solutions were obtained for m = 0 by assuming a monopole source located at point (ρ ,z) = (0,0) inside the surface. The normal velocities and/or admittance values are then computed at each point on the surface using Eq. (6) and taken as the boundary conditions in Eq. (18). The surface potential Φ (s_p) is then computed from Eq. (18) and the far field potential is obtained by numerically solving Eq. (2) with Eq. (6). The computed surface and far field potentials are then compared with the known potential distribution of the monopole source

$$\varphi(p) = \frac{-e^{ika}}{a} \tag{19}$$

where a is the distance from the source to the observation point. For m = 1 a dipole source was used to generate exact solutions, and for m = 2 a quadrapole source was used.

To investigate the effect of the coupling constant α in Eqs. (15) - (17), the surface potential distributions for a sphere of unit radius with a uniformly vibrating surface (i.e. m = 0) were computed for α =0,i, and i/k. Twenty subintervals were taken in the ρ -z plane, a four-point Gauss-Legendre quadrature formula was used over each subinterval and a twenty-point Gauss-Legendre formula was used in the θ direction. The magnitude of the potential should be unity at all points on the surface. The results presented in Fig. 3 show the computed magnitudes of the surface acoustic potential to be in error by 12 per cent for α = 0 at nondimensional wave numbers ka close to π , 2 π , and 3π. These results are those that would be obtained from Eq. (7). The relatively large errors are expected from the analysis of Burton and Miller[4] and from previous investigations using Eq. (7).[2,5] Burton proves that setting the imaginary

part of α nonzero guarantees unique solutions to Eq. (18), For α = i the maximum error is reduced to less than four per cent except when k is close to 8.0. However, when α = i, and for sufficiently high values of ka, Eq. (9) is dominated by terms arising from Eq. (8). As a result, the solution equations become ill-conditioned when ka is sufficiently high and close to one of the eigenfrequencies associated with the integral equation based on Eq. (8). In Table I computed values close to these eigenfrequencies and the eigenfrequencies of Eq. (7) are compared with exact results for α = 0, i, and i/k. In all cases, the value of i/k gives the most accurate results. In Table II, the effect of introducing an admittance condition is presented for α = i/k. The admittance Y(Q) and forcing function A(Q) in Eq. (6) are chosen so that the relations

$$\frac{\partial \varphi}{\partial n_q} - Y(Q)\varphi = A(Q) \quad ; \quad \varphi = \frac{-e^{ikr}}{r} \tag{20}$$

are satisfied on the surface and the exact solutions can be readily computed. The loss in accuracy when an admittance condition is used is minimal and restricted to the third significant figure. However, for discontinuous boundary conditions, where the forcing function is specified over one part of the surface (i.e., the admittance is zero there) and the admittance is specified over the remaining surface, errors of over ten per cent in the real and imaginary parts of the computed surface potential result. For comparison, the case of a constant forcing function and admittance over the sphere for α = 0 is also presented and in all cases yields results of less accuracy than those obtained with α = i/k.

In this study consistently good results were obtained with α = i/k. In Fig. 3 the computed and exact values for α = i/k agree to three significant figures over the range of nondimensional wave numbers from one to ten. In

fact, for this value of α , the accuracy is significantly better at all wave numbers investigated. While Burton and Miller[4] provide no recommendations for choosing one value of α over any other value with an imaginary component, the choice $\alpha = i/k$ used in the present study can be explained as follows. The terms in Eqs. (15) - (17) which involve α are of order k^2 whereas the remaining terms are of order k. Therefore, at higher wave numbers the terms of order k^2 dominate. By choosing α to vary inversely with the wave number, all terms in Eqs. (15) - (17) remain of the same order with respect to wave number.*

A problem of more practical importance is the finite axisymmetric duct since this surface approximates an engine configuration. The surface potential distributions are presented in Fig. 4 at different nondimensional wave numbers for m = 0. The normal acoustic velocity distribution A(Q) is chosen so that the solution for the acoustic potential satisfies Eq. (19). The parameter α is taken to be i/k. Twenty subintervals are taken in the ρ -z plane and a twenty-point Gauss-Legendre quadrature is used in the θ direction. In Fig. 4 the variations of the magnitude and phase with distance along the perimeter s are presented. The largest errors in the computed magnitude of the potential of about ten per cent occur on the ends of the cylinder and at the corners. The results at the ends can be improved without increasing the number of points by area weighting rather than taking equidistant points along the perimeter. The errors in the phase are less than four per cent in all cases. The errors in the magnitude of the computed surface potential increase with increasing nondimensional wave number;

---

* It is interesting to note that in the report by Chertock[7] he suggests the use of 1/k on the grounds that it has the correct physical dimensions (i.e. length) that will maintain the dimensional homogeneity of Eq. (18).

but, even when ka = 10, the numerical results are within ten per cent of the exact solutions. For $\alpha = 0$ or i the errors are significantly larger above ka = 2.

In most inlet problems the boundary conditions are discontinuous with the acoustic velocity or potential (which is directly proportional to the acoustic pressure) specified over part of the surface and the admittance (representing liners) over the rest. To determine the effect of the discontinuities and the use of an admittance function on the numerical results for m = 0, a cylinder was investigated. The velocity was specified on the ends and the admittance was specified in the center so that the solution for Φ was given by Eq. (19) and Eq. (6) is satisfied. Again, twenty points are used in the ρ-z and θ directions. The results are shown in Fig. 5. Although the errors in the numerical results for this case are higher than those observed in Fig. 4, the errors still remain within 10 per cent for values of ka less than 5. However, when ka = 10 errors of up to 40 per cent in the magnitude of the potential are encountered close to the discontinuity in the boundary condition. This error can be reduced by increasing the number of subintervals in the ρ-z plane. Doubling the number of subintervals halves the error. When both the normal acoustic velocity and the admittance are continuous on the surface, the errors are of the same order of magnitude as those of Fig. 4. For tangential modes, the variation in the circumferential direction behaves as cos m θ where m = 0,1,2..... To check the numerical integration scheme in the circumferential direction, the surface acoustic potential was computed for m = 1 and m = 2 for the cylinder shown in Fig. 4. The results are presented in Fig. 6 for ka = 2 with the normal acoustic velocity specified everywhere on the surface. The computed and exact results (i.e. from a dipole and qudrapole) are in agreement to within two per cent for both m = 1

and $m = 2$.

It has been shown[5] that once the surface potential has been accurately computed, the far field can be determined to at least the same accuracy as the surface potential. This result is confirmed by the data presented in Fig. 7 for the cylinder of Fig. 4 with the velocity specified everywhere on the surface with $ka = 2$ and $m = 0$. The results at 20 radii from the surface are in agreement with exact results obtained from Eq. (19) to within one per cent even though the surface errors at some points are above two per cent. Data in Fig. 8 show that accurate results are obtained at distances greater than one integration stepsize from the surface. At closer distances errors from the numerical evaluation of the singularity in the Green's function defined by Eq. (4) leads to large errors.

The studies of the acoustic fields of the sphere and cylinder served to check out and refine the numerical procedures and programming techniques. The next configuration investigated was an inlet used in a study by NASA.[11] This inlet is shown in Fig. 9 and was chosen because:

(1) unlike most inlets used in research studies, it does not have a bell-mouth shape but is shaped like a typical inlet used in existing aircraft; and

(2) complete details on generating the inlet boundary are given in Ref. 11.

For this inlet, all cases were investigated with $\alpha = i/k$.

As seen in Fig. 10, the normal velocity distribution, which represents a forcing function, is highly discontinuous and provides a severe test of the numerical techniques employed. The numerical and exact solutions for the surface acoustic potential are compared in Fig. 10 for 32 and 54 subintervals taken along the perimeter of the inlet in the ρ-z plane. Because of the errors in approximating the lengths of each subinterval, the exact solutions differ

slightly as the distance along the perimeter s increases. The centerbody in Fig. 9 extends from $0 \leq s \leq 0.8$, the fan inlet covers $0.8 \leq s \leq 1.4$, the interior contour extends from $1.4 \leq s \leq 3.5$, the exterior from $3.5 \leq s \leq 5.5$, and the circular arc lies within the interval $5.5 \leq s \leq 7.45$. Increasing the number of points decreases the error proportionately as indicated by the data in Fig. 10 at a nondimensional wave number ka of unity where a is the radius of the inlet at the fan entrance section. The absolute average error in the results decreases from 10.2 per cent for 32 subintervals to 4.16 per cent for 53 subintervals. The computation time increased from 53 seconds to 143 seconds, respectively.

As shown in Fig. 11, the errors increase with increasing frequency. Like the cylinder, the maximum error in the acousitc potential for the inlet configuration occurs at the points of discontinuity. The average error increases from 4.16 per cent at ka = 1 to 15 per cent at ka = 10.

For the data in Figs. 10 and 11, the acoustic potential is assumed constant in the tangential plane. The results for a $\cos(m\,\theta)$ distribution are presented in Fig. 12 at ka = 2. These results show the insensitivity of the accuracy of the computed results to the tangential distribution for m = 1,2. The exact soltuions were again generated by assuming dipole and quadrapole sources located at $(\rho, z) = (0,0)$.

Based on the above results our numerical and programming techniques are capable of yielding reliable results for arbitrary geometries and boundary conditions. At higher frequencies, (ka > 5) it appears that more points must be taken to increase the accuracy of the computed results.

IV. Summary and Conclusions

An integral solution of the Helmholtz equation is developed for use in acoustic radiation problems. Unlike the classical formulation which can lead to integral equations that do not have unique solutions at frequencies corresponding to certain internal eigenfrequencies of the region enclosed by the surface under consideration, the formulation used in this study is valid at all frequencies. Also, unlike most current methods and formulations it is straight forward to implement regardless of how complicated the surface or the boundary conditions may be. The surface potentials computed numerically for a sphere and cylinder using 20 subintervals along the perimeter and for an inlet configuration with 53 subintervals are accurate to within ten per cent for nondimensional wave numbers ka of from one to ten where k is the wave number and a is the characteristic length. For discontinuous boundary conditions, the numerical and exact values are in agreement to within 10 per cent for $ka < 5$. At higher frequencies the results are as much as 40 per cent in error at points of discontinuity which suggests taking more points in evaluating the integral equation to increase the accuracy when discontinuous boundary conditions are specified. Increasing the number of subintervals decreases the error proportionately. At distances greater than the numerical integration stepsize, the far field results are at least as accurate as the corresponding surface potential solutions.

Acknowledgement

This work was supported by the AFOSR under Contract Number F49620-77-C-0066, Lt. Col. Lowell Ormand project monitor.

References

1. Burton, A. J., "The Solution of Helmholtz' Equation in Exterior Domains using Integral Equations," NPL Report NAC 30, National Physical Laboratory,

Teddington, Middlesex, Jan. 1973.

2. Schenck, H. A., "Improved Integral Formulation for Radiation Problems," Journal of the Acoustical Society of America. Vol. 44, No. 1, Jan. 1968, pp. 41-58.

3. Ursell, F., "On the Exterior Problems of Acoustics," Proceedings of the Cambridge Philosophical Society, Vol. 74, 1973, pp. 117-125.

4. Burton, A. J. and Miller, G. F., "The Application of Integral Equation Methods to the Numerical Solutions of Some Exterior Boundary Value Problems," Proceedings of the Royal Society of London, A. 323, June, 1971, pp. 201-210.

5. W. L. Meyer, W. A. Bell, M. P. Stallybrass and B. T. Zinn, "Boundary Integral Solutions of Three Dimensional Acoustic Radiation Problems," Journal of Sound and Vibration, Vol. 59, No. 2, July, 1978, pp. 245-262.

6. Morse, P. M. and Ingard, K. U., Theoretical Acoustics, McGraw-Hill, New York, 1969, Chapter 7.

7. Chertock, "Intergral Equation Methods in Sound Radiation and Scattering from Arbitrary Surfaces," David W. Taylor, Naval Ship Research and Development Center Report 3538, June, 1971.

8. Stallybrass, M. P., "On a Pointwise Variational Principle for the Approximate Solution of Linear Boundary Value Problems," Journal of Mathematics and Mechanics, Vol. 16, No. 11, May 1967, pp. 1247-1286.

9. Chertock, G., "Sound Radiation from Vibrating Surfaces," Journal of the Acoustical Society of America, Vol. 36, No. 7, July 1964, pp. 1305-1313.

10. Bell, W. A., Meyer, W. L., and Zinn, B. T., "Predicting the Acoustics of Arbitrarily Shaped Bodies Using an Integral Approach," AIAA Journal, Vol. 15, No. 6, June 1977, pp. 813-820.

11. Miller, B. A., Dastoli, B. J., and Worosky, H. L., "Effect of Entry-Lip Design on Aerodynamics and Acoustics of High-Throat-Mach-Number Inlets for the Quick, Clean, Short-Haul Experimental Engine," NASA TM X-3222, 1975.

Table I

Effect of the coupling parameter α on the computed values of the surface potential for a sphere. On the surface $A(Q) = (1-ik)e^{ik}$, $Y(Q) = 0$, $\varphi^{(Q)}_{exact} = -e^{ik} =$ constant, $m = 0$. All values of ka correspond to internal eigenfrequencies. Twenty subintervals were taken in the ρ-z plane.

ka \ α		0	i/k	i	EXACT
π	φ_r	2.0	1.000	0.998	1
	φ_i	-6.3	0.001	-0.012	0
4.493409	φ_r	0.190	0.217	0.308	0.217
	φ_i	0.979	0.976	0.955	0.976
2π	φ_r	-2.0	-1.000	-0.996	-1
	φ_i	12.6	0.000	0.031	0
7.725252	φ_r	-0.081	-0.128	-0.400	-0.128
	φ_i	-0.994	-0.992	-0.872	-0.992
3π	φ_r	2.0	1.000	0.995	1
	φ_i	-19.0	0.000	-0.050	0

Table II

Effect of specifying an admittance on the computed surface potential for a sphere. In all cases m = 0, twenty subintervals are taken in the $\rho - z$ plane, and $\varphi_{exact} = -e^{ik}$ everywhere on the surface. For Case I, $A(Q) = e^{ik}$ and $Y(Q) = ik$ everywhere on the surface. For case III, $A(Q) = e^{ik}(1-ik)$ and $Y(Q) = 0$ over 1/5 of the surface and $A(Q) = 0$, $Y = -(1-ik)$ over the remainder. Case II is considered in Table I.

ka	CASE I $\alpha = i/k$		CASE I $\alpha = 0$	CASE II $\alpha = i/k$	CASE III $\alpha = i/k$	EXACT VALUES
1	φ_r	-0.539	-0.537	-0.538	-0.52	-0.540
	φ_i	-0.845	0.849	-0.843	-0.87	-0.842
2	φ_r	0.418	0.422	0.417	0.43	0.416
	φ_i	-0.911	-0.937	-0.909	-0.92	-0.909
3	φ_r	0.993	0.916	0.990	1.00	0.990
	φ_i	-0.142	-0.496	-0.140	-0.16	-0.141
5	φ_r	-0.285	-0.288	-0.284	-0.25	-0.284
	φ_i	0.961	1.145	0.959	1.00	0.959
10	φ_r	0.841	-0.3	0.839	0.90	0.839
	φ_i	0.546	0.9	0.544	0.49	0.544

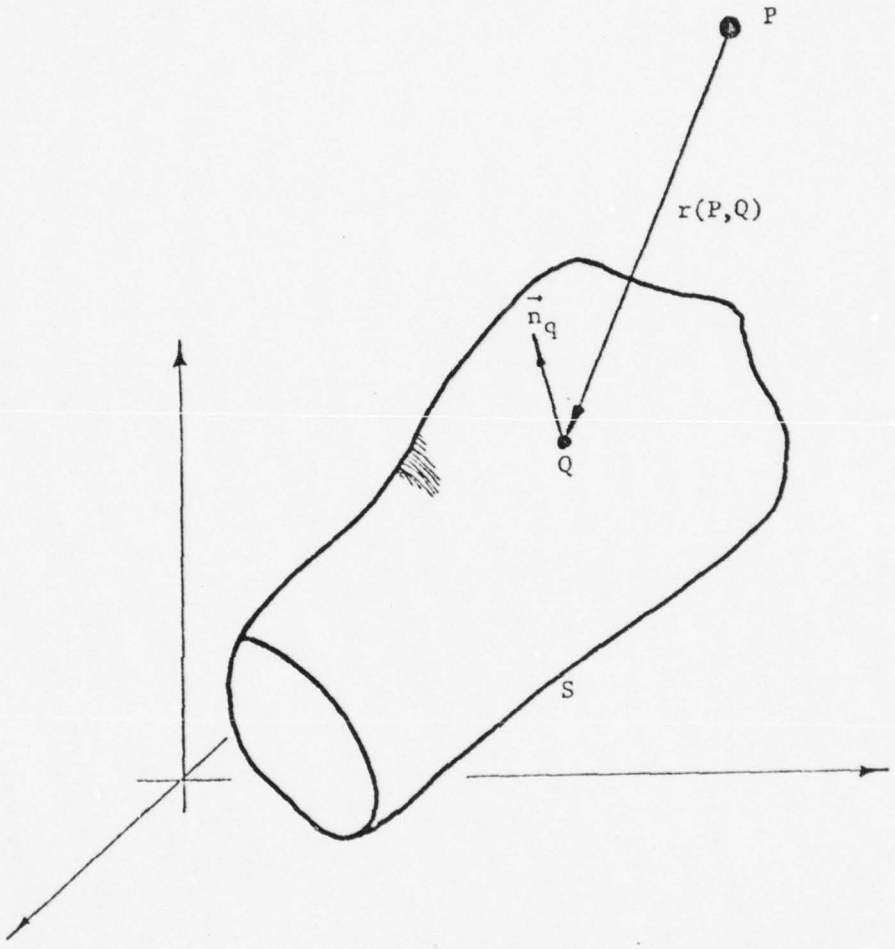

Figure 1. Geometrical Properties of the General Acoustic Radiation Problem.

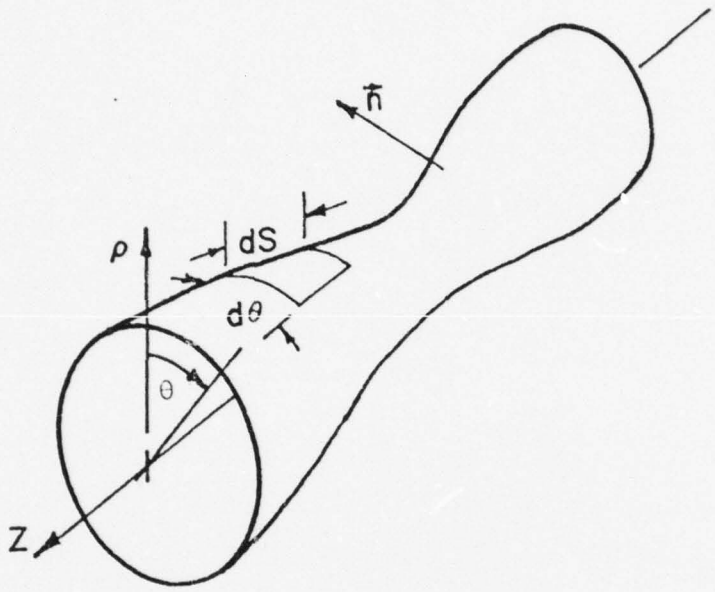

Figure 2. Cylindrical Surface Geometry

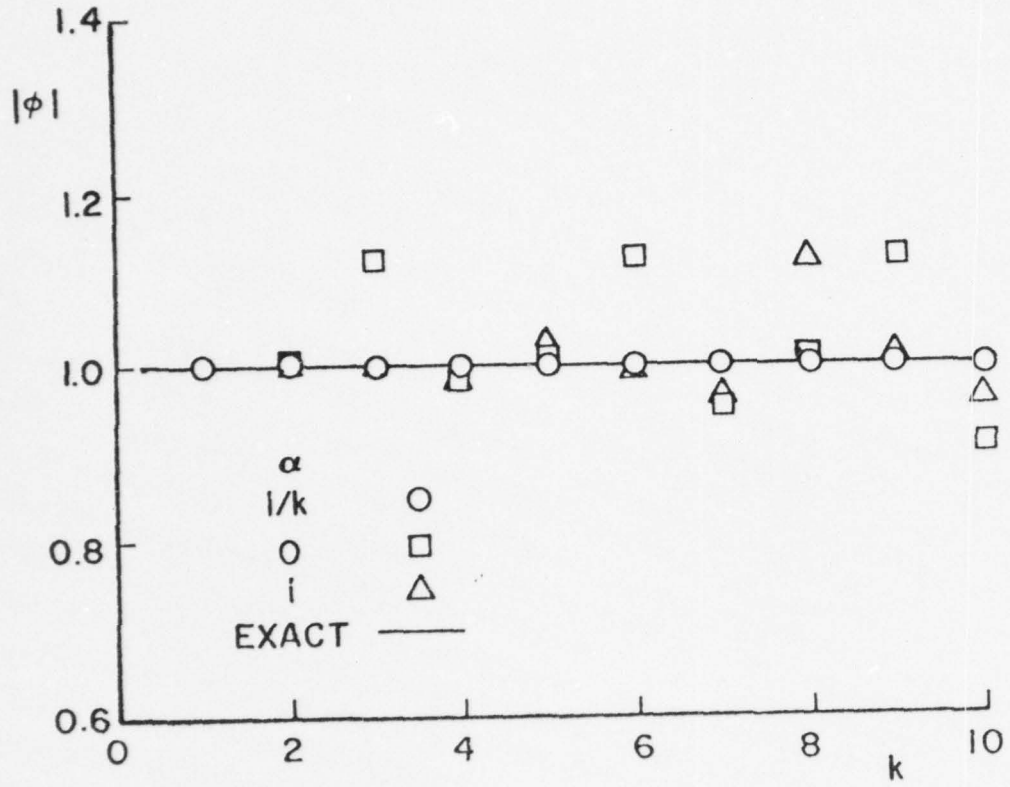

Figure 3. Effect of the Coupling Constant on the Computed Surface Potential for a Sphere of Unit Radius with 20 Subintervals.

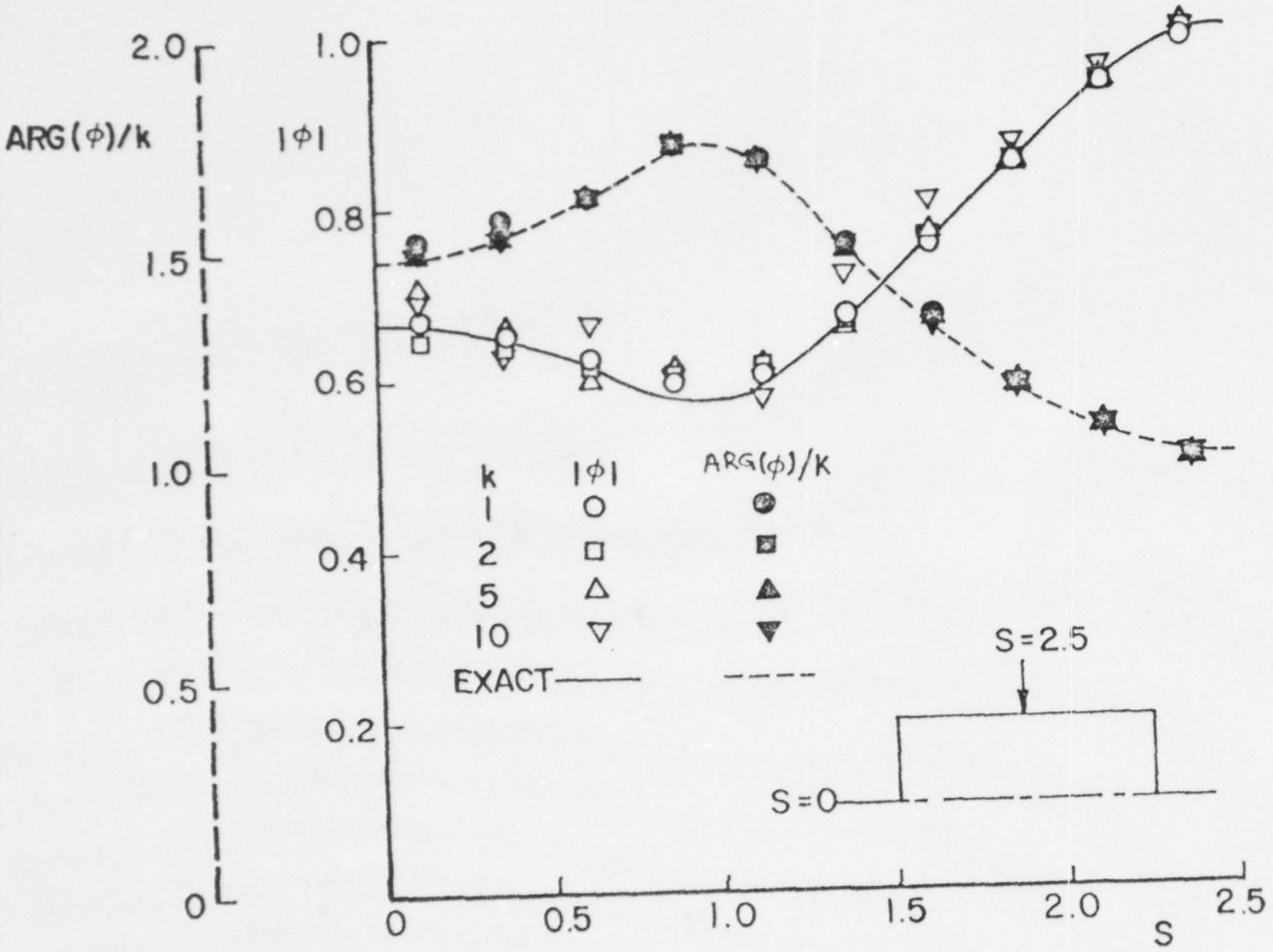

Figure 4. Dependence of the Computed Surface Potential for a Finite Cylinder with a Zero Admittance and Nonzero Normal Velocity Everywhere on the Surface for 20 Subintervals, $\alpha = i/k$.

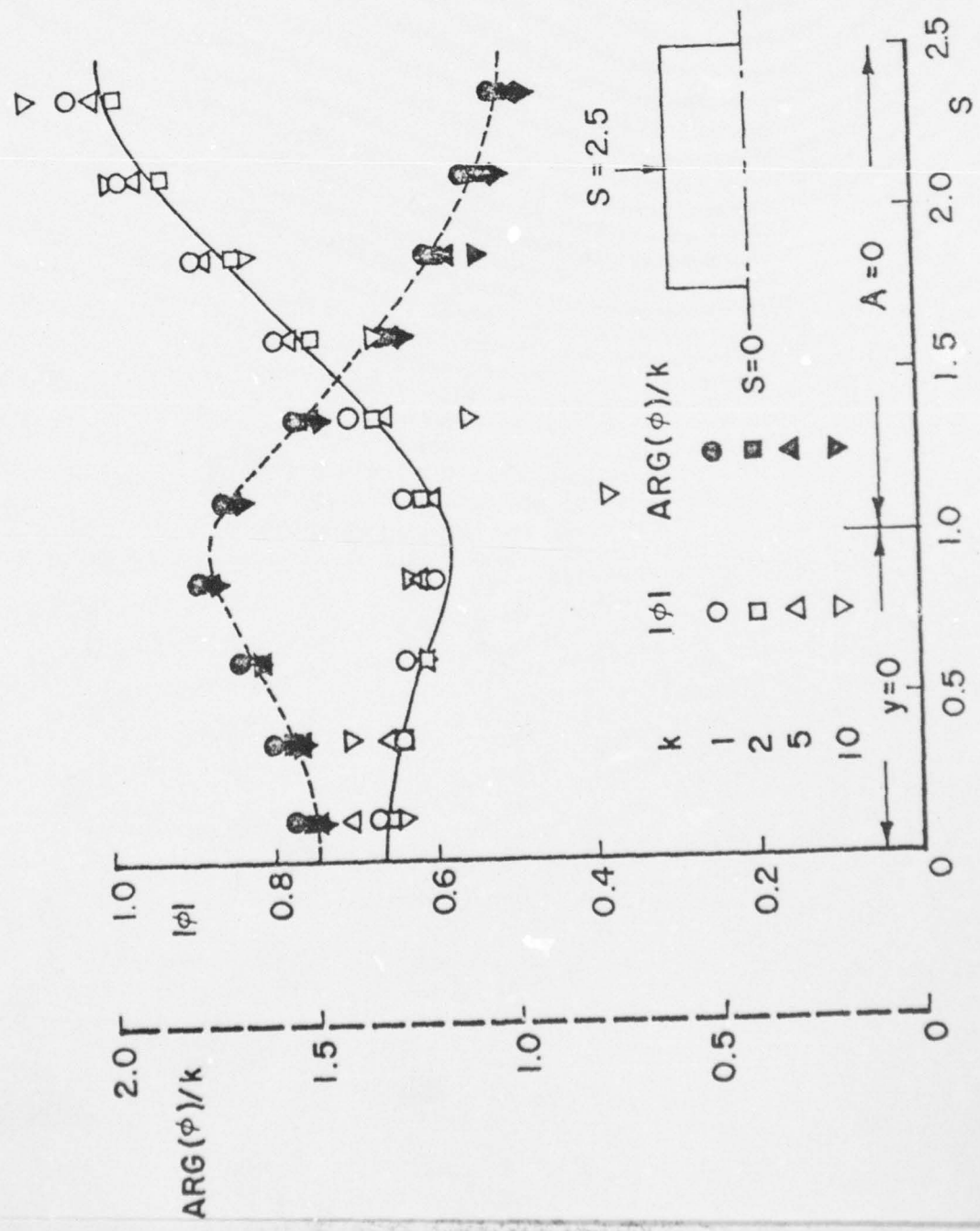

Figure 5. Effect of Discontinuous Boundary Conditions on the Accuracy of the Computed Surface Potential for a Cylinder, $\alpha = i/k$.

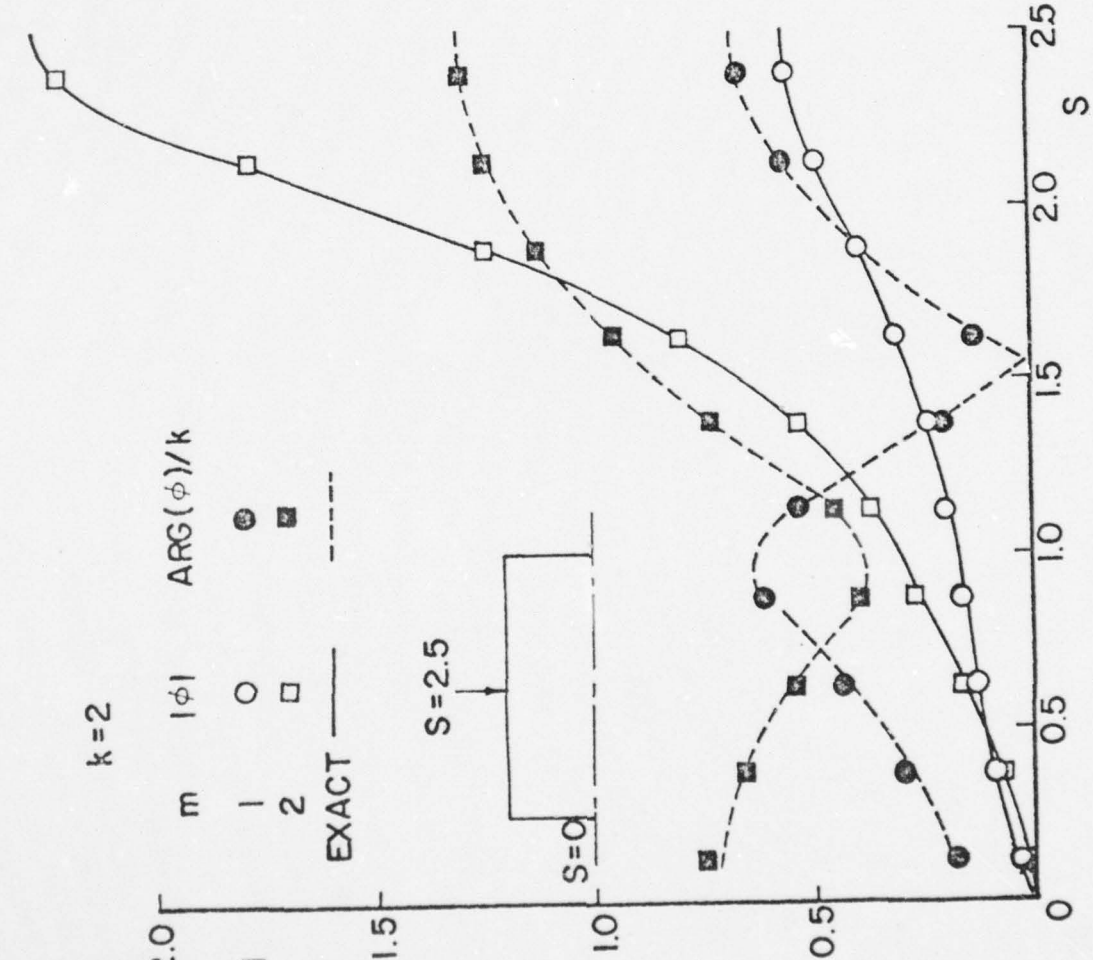

Figure 6. Computed Surface Potential for a Cylinder at the First and Second Tangential Modes for ka = 2.

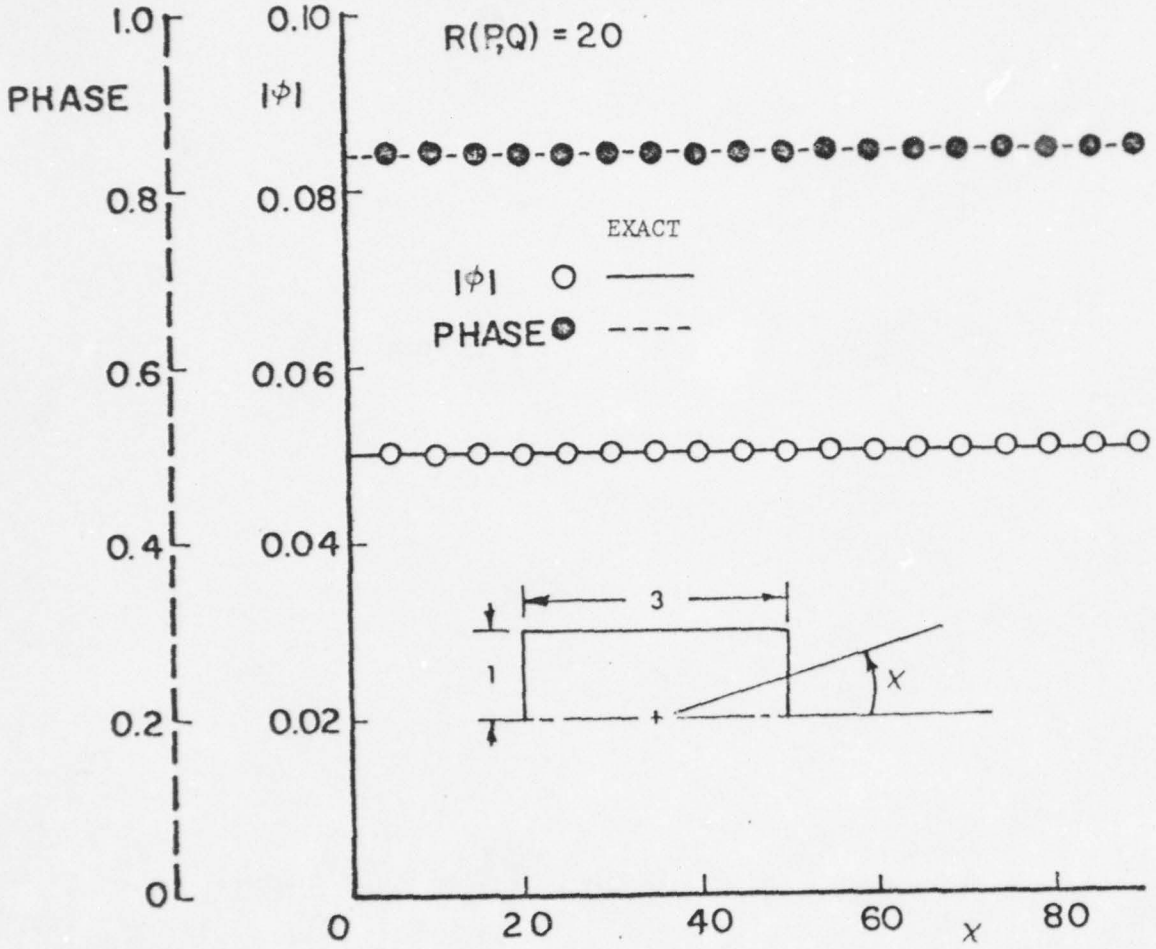

Figure 7. Computed Far Field Potential Distribution for a Cylinder at k = 2, m = 0, and 20 Radii from the Center.

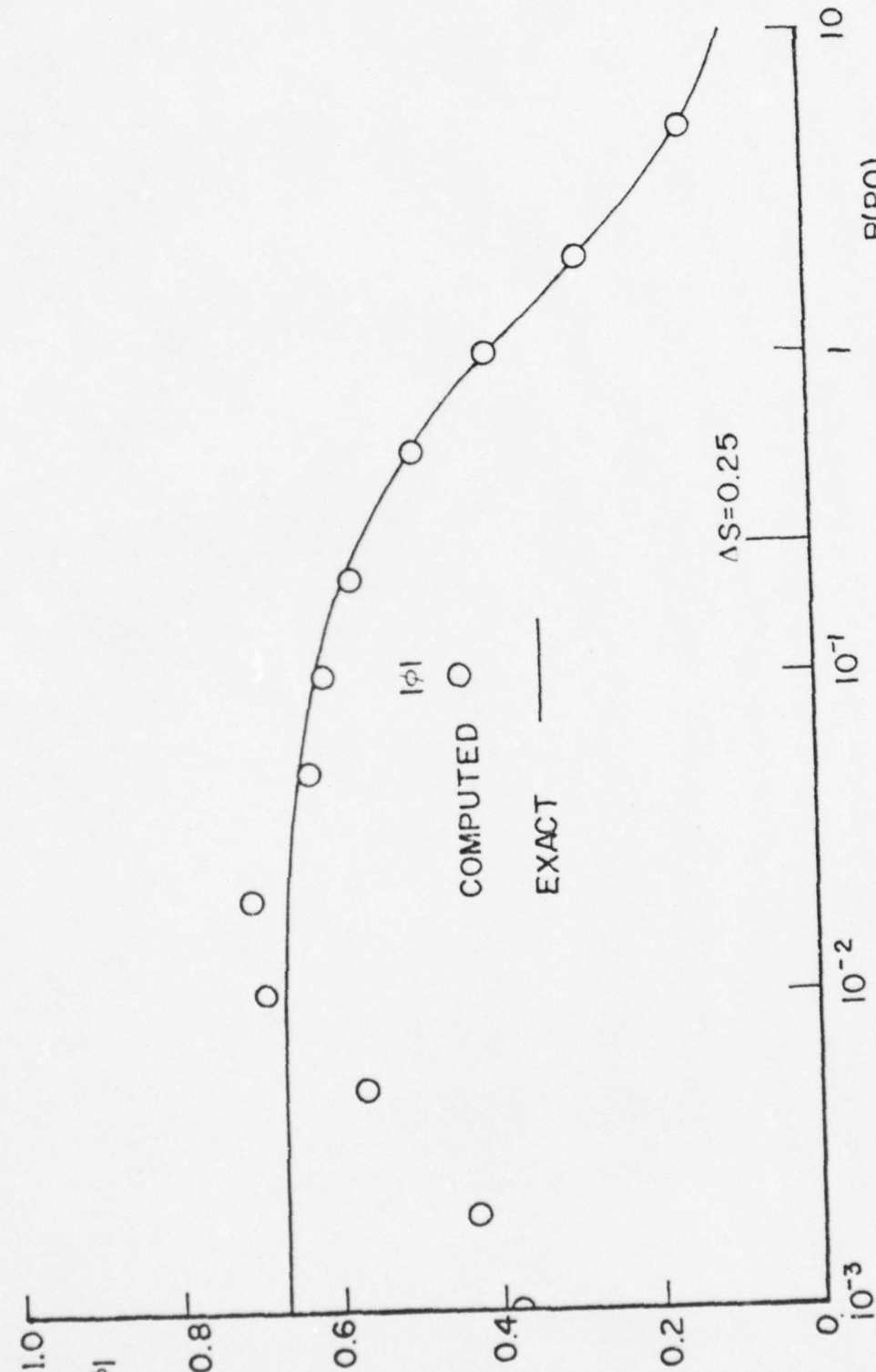

Figure 8. Dependence of the Accuracy of the Computed Far Field Solution of a Cylinder upon the Distance from the Surface for k = 2 and m = 0.

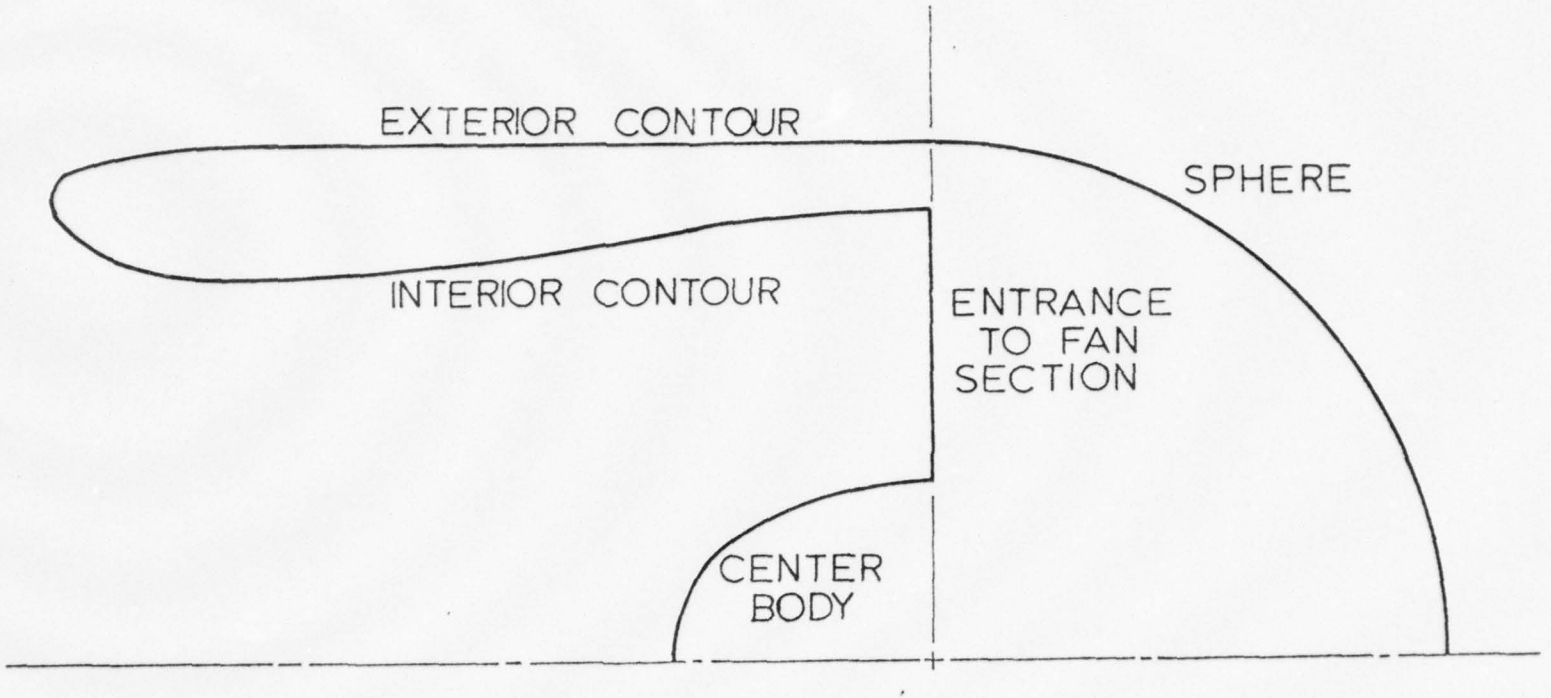

Figure 9. Inlet Geometry.

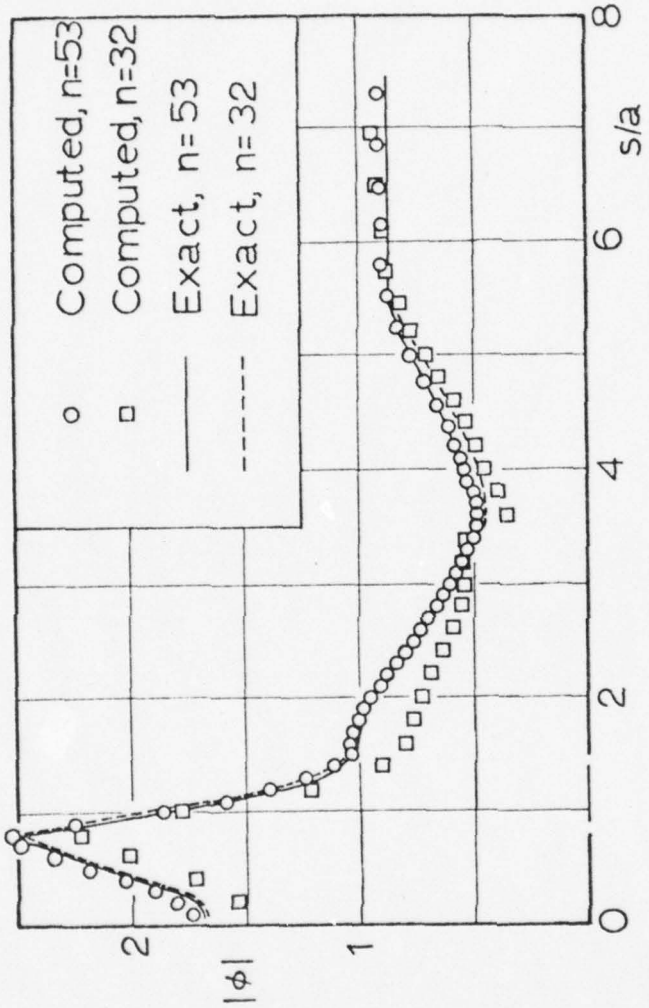

Figure 10. Effect of Increasing the Number of Subintervals in Computing the Surface Potential for the Inlet Configuration at ka = 1, m = 0.

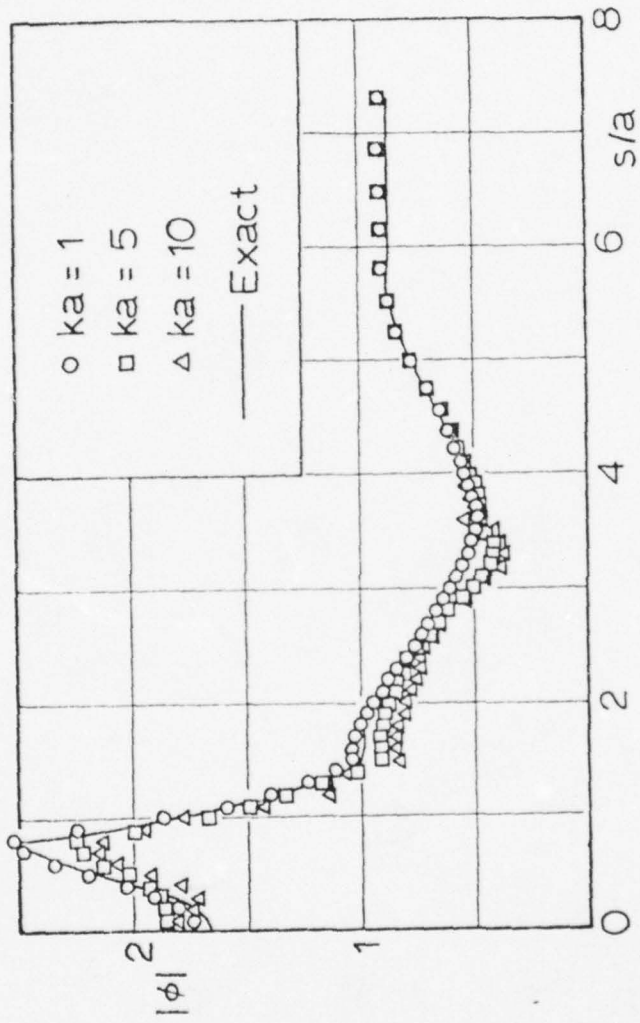

Figure 11. Effect of Increasing Frequency for the Inlet Configuration at m = 0, n = 53 on the Computed Surface Potential.

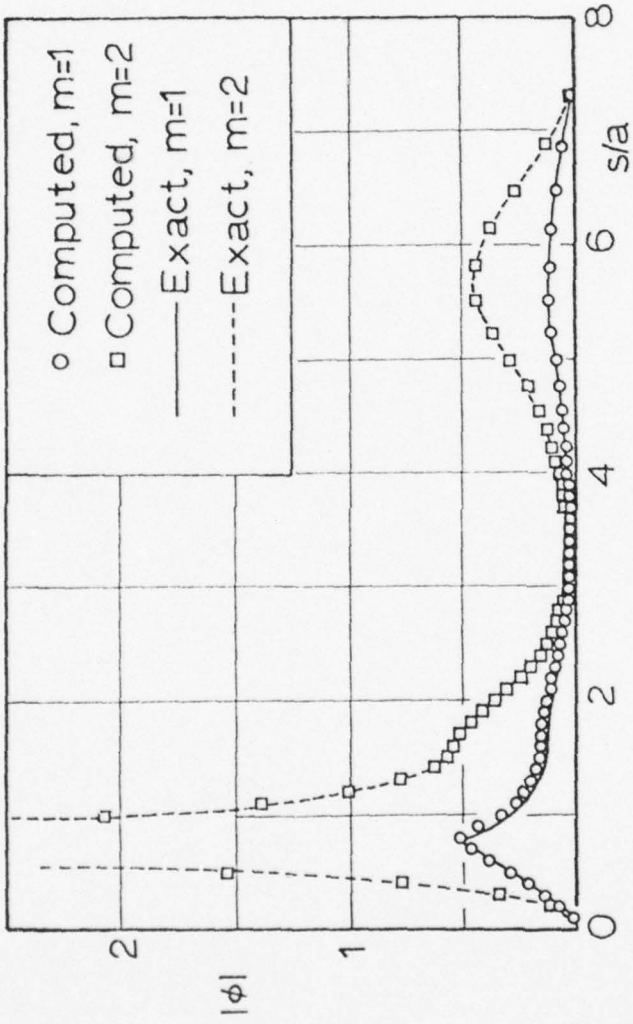

Figure 12. Effect of Mode Number m on the Computed Surface Potential of the Inlet Configuration for ka = 2 and n = 53.

Appendix C

Paper presented at the AIAA 5th Aeroacoustics Conference in Seattle, Washington, March 12-14, 1979, AIAA Paper No. 79-0675

"Sound Radiation From Finite Length Axisymmetric Ducts and Engine Inlets"

79-0675

Sound Radiation from Finite Length Axisymmetric Ducts and Engine Inlets

W.L. Meyer, W.A. Bell and B.T. Zinn, Georgia Institute of Technology, Atlanta, Ga.

AIAA 5th AEROACOUSTICS CONFERENCE

Seattle, Washington—March 12-14, 1979

American Institute of Aeronautics and Astronautics
1290 Avenue of the Americas New York, N.Y. 10019

SOUND RADIATION FROM FINITE LENGTH AXISYMMETRIC DUCTS AND ENGINE INLETS*

W. L. Meyer**, W. A. Bell†, and B. T. Zinn‡

School of Aerospace Engineering
Georgia Institute of Technology
Atlanta, Georgia 30332

Abstract

Results are obtained by numerical integration of a cylindrically symmetric integral representation of the exterior solutions of the Helmholtz equation which is valid (yields unique solutions) at all wavenumbers. The admittance values across the entrance plane of hard walled ducts of various lengths and geometries are computed and compared with certain "classical" (e.g., Weiner-Hopf) values. The internal wave structure is also investigated for straight hard walled ducts and compared with results obtained from other theories. The radiated sound fields from ducts of different geometries are then compared for both unlined and lined configurations. It is found that changes in the duct geometry result in significant changes in the radiated sound field. Thus, it is concluded that the sound suppression by liners predicted from the study of straight ducts may not be applicable to more complicated geometries such as inlet configurations.

Introduction

The development of an analytical method for predicting the sound field radiated from axisymmetric, finite length ducts is of much practical interest in the area of aeroacoustics, especially for the determination of the sound radiated from a turbofan inlet, as having such a capability can eliminate most of the costly full scale testing presently required. In a majority of past investigations of the sound radiated from ducts, either the radiation problem has been completely ignored[1,2,3] or the duct acoustics and the radiation problem have been treated separately.[4,5,6] In these studies, the behavior of the waves inside the duct was determined by specifying some heuristic boundary condition (e.g., a reflection coefficient) at the duct entrance. In the latter references this solution was then used to determine the sound distribution at the entrance plane of the duct and this was used to predict the properties of the radiated sound field. In reality the sound fields inside and outside the duct are not separate entities (i.e., they are coupled) and, therefore, they cannot be properly treated separately. These "separate" treatments of the interior and exterior sound fields in the duct radiation problem undoubtedly introduce errors whose determination requires comparison with available exact solutions.

In this paper the duct sound radiation problem is investigated by utilizing an integral solution[7,8] that considers the combination of the interior and exterior sound fields to be a single entity, thus eliminating the errors associated with many of the previously used approaches. Comparison of the solutions obtained using this method with exact solutions[9] and with those of related investigations should shed some light upon the applicability of the analytical approaches utilized in these other investigations.

The solution approach utilized in this study consists of the numerical solution of a special integral representation of the solutions of the Helmholtz equation for an exterior (i.e., to a given body) domain. The applicability and accuracy of this solution approach have been demonstrated for two dimensional[10,11], three dimensional[8,12], and axisymmetric[9,13] geometries in earlier investigations conducted under this program where it has been shown that the developed approach yields unique solutions at all wavenumbers.

Solution Procedure

The basis of this method is set forth in great detail in Ref. 14 and therefore will not be repeated here. In related studies conducted under this AFOSR program the applicability of this approach to the solution of acoustics problems involving two dimensional, three dimensional, and axisymmetric geometries has been demonstrated. Since the analytical developments and results of these studies have been published elsewhere[7,8,9], they also will not be repeated here. Instead, some of the advantages of this solution approach will be presented. First, as stated earlier, this method treats the duct radiation problem consisting of the sound generation, sound propagation and reflection, and the sound radiation to the outside as a whole without separating it into its component parts as has been done in related investigations. Second, the method can readily handle the infinite domains encountered in radiation problems. This is accomplished by employing a fundamental solution G(P,Q) which satisfies the Sommerfield radiation conditions in the integral equation. In the present study the free space Green's function has been used:

$$G(P,Q) = \frac{e^{ikr(P,Q)}}{r(P,Q)} \qquad (1)$$

where, as shown in Fig. 1, Q is a point on the surface of the body S, P is a point in the exterior domain, r(P,Q) is the distance between these points, and k is the wavenumber. The third advantage is that the computer program developed in a related investigation[9,13] is quite general and is applicable to a variety of acoustic radiation problems involving arbitrary geometries and variable boundary conditions. This computer program can be applied to different problems by merely changing the input data.

* This research was supported by AFOSR contract number F49620-77-C-0066; Lt. Col. Lowell Ormand, Grant Monitor.

** Assistant Research Engineer, Member AIAA.

† Scientist Associate; Present Address: Lockheed Georgia Company, Marietta, Georgia 30060; Member AIAA.

‡ Regents' Professor, Associate Fellow AIAA.

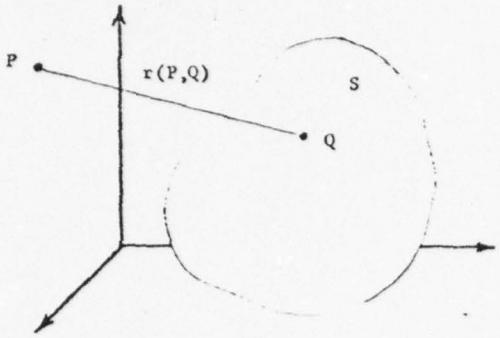

Fig. 1. General Geometry of the Radiation Problem.

It has been shown in Ref. 8 that unique solutions of the external acoustic radiation problem can be obtained at all wavenumbers by solving the following integral equation:

$$\int\int_S \left(\varphi(Q)\,\frac{\partial G(P,Q)}{\partial n_q} - G(P,Q)\,\frac{\partial \varphi(Q)}{\partial n_q}\right) dS_q + \alpha \int\int_S \left(\varphi(Q) - \varphi(P)\right) \frac{\partial^2 G(P,Q)}{\partial n_p \partial n_q}\, dS_q - \alpha\,\varphi(P) \int\int_S (\vec{n}_p \cdot \vec{n}_q)(ik)^2\, G(P,Q)\, dS_q - \alpha \int\int_S \frac{\partial \varphi(Q)}{\partial n_q} \cdot \frac{\partial G(P,Q)}{\partial n_p} dS_q = 2\pi\left(\varphi(P) + \alpha \frac{\partial \varphi(P)}{\partial n_p}\right) \tag{2}$$

where, as shown in Fig. 2, the point P has been moved to the surface of the body S, $\vec{n}$ represents an external normal from the body, $\frac{\partial}{\partial \vec{n}}$ represents a normal derivative $(\vec{\nabla}\cdot\vec{n})$, and α is a complex coupling constant.

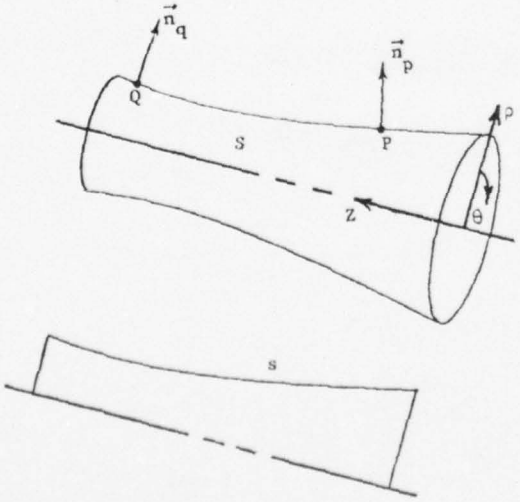

Fig. 2. General Axisymmetric Geometry and 2-D Projection.

It is shown in Ref. 9 that maximum accuracy is obtained when $\alpha = i/k$. In its present form, Eq. (2) contains no non-integrable singularities, a fact which considerably simplifies its numerical solution. Thus the solution of the entire duct radiation problem has been reduced, with the present formulation, to that of the solution of a surface integral over the body S.

The problem is further simplified in the present study by limiting attention to axisymmetric configurations. In this case Eq. (2) is further reduced to[9]

$$\int_o^{\ell} \phi(Q)\left\{K_1(P,Q) + K_2(P,Q)\right\} ds_q - \phi(P)\int_o^{\ell}\left\{F_1(P,Q) + F_2(P,Q)\right\} ds_q - \int_o^{\ell} V(Q)\left\{I_1(P,Q) + I_2(P,Q)\right\} ds_q = 2\pi\left\{\phi(P) + \alpha\, V(P)\right\} \tag{3}$$

where s is the distance along the 2-D projection of the body in the ρ-z plane (i.e., See Fig. 2), and the influence functions I_1 and I_2 are given by

$$I_1(P,Q) = 2\int_o^{\pi} G(P,Q)(\cos m\,\theta_q)\, d\theta_q$$
$$I_2(P,Q) = 2\alpha \int_o^{\pi} \frac{\partial G(P,Q)}{\partial n_p} (\cos m\,\theta_q)\, d\theta_q \tag{4}$$

the kernel functions K_1 and K_2 are

$$K_1(P,Q) = 2\int_o^{\pi} \frac{\partial G(P,Q)}{\partial n_q} (\cos m\,\theta_q)\, d\theta_q$$
$$K_2(P,Q) = 2\alpha \int_{o+}^{\pi} \frac{\partial^2 G(P,Q)}{\partial n_p \partial n_q} (\cos m\,\theta_q) d\theta_q \quad \theta_q \neq \theta_p \tag{5}$$

the forcing functions F_1 and F_2 are

$$F_1(P,Q) = 2\alpha \int_o^{\pi} G(P,Q)(ik)^2 (\vec{n}_p \cdot \vec{n}_q) d\theta_q \tag{6}$$
$$F_2(P,Q) = 2\alpha \int_o^{\pi} \frac{\partial^2 G(P,Q)}{\partial n_p \partial n_q}\, d\theta_q \quad \theta_q \neq \theta_p$$

and

$$\frac{\partial \varphi}{\partial n} = V \cos m\,\theta$$
$$\phi = \frac{\varphi}{\cos m\,\theta} \tag{7}$$

following the notation of Ref. 15. In the above notation m is the tangential mode and θ_p has been taken as zero (i.e., $\cos m\,\theta_p = 1$).

Introducing axisymmetry further simplifies the solution of Eq. (2) to the evaluation of line integrals on the 2-D projections of the body S in the ρ - Z plane as shown in Fig. 2. Also, the formulation is valid for all tangential modes; however, each mode must be solved for separately.

The required solution is obtained by solving Eq. (3) for the surface distribution of the acoustic potential ϕ or the normal acoustic velocity V, whichever is unknown. Also, solutions can be obtained for ϕ by using an effective admittance, defined as $Y = V/\phi = \partial\varphi/\partial n/\varphi$, as a boundary condition over any part of the surface of the body (e.g., replace V by ϕY in Eq. (3) at the points where Y is known on the body.).

Once the surface distributions of the acoustic potential and the normal acoustic velocity are known on the surface of the body, the radiated sound field can be determined using the following integral representations[14] for φ and $\frac{\partial\varphi}{\partial n}$ in the field:

$$\int\int_S (\varphi(Q) \frac{\partial G(P,Q)}{\partial n_q} - G(P,Q) \frac{\partial\varphi(Q)}{\partial n_q}) dS_q = 4\pi\varphi(P) \tag{8}$$

and

$$\int\int_S (\varphi(Q) \frac{\partial^2 G(P,Q)}{\partial n_p \partial n_q} - \frac{\partial G(P,Q)}{\partial n_p} \frac{\partial\varphi(Q)}{\partial n_q}) dS_q = 4\pi \frac{\partial\varphi(P)}{\partial n_p} \tag{9}$$

where the point P is now located in the space surrounding the body (i.e., See Fig. 1) so that the kernel functions are no longer singular. For axisymmetric bodies, Eqs. (8) and (9) reduce to:

$$\int_o^\ell (\phi(Q) K_1(P,Q) - I_1(P,Q) V(Q)) ds_q = 4\pi \phi(P) \tag{10}$$

and

$$\int_o^\ell (\phi(Q) K_2(P,Q) - I_2(P,Q) V(Q)) ds_q = 4\pi V(P) \tag{11}$$

Results

In the present investigation, the integral solution technique has been utilized to study the dependence of the radiated sound field and the acoustic characteristics of the duct upon the duct geometry and the acoustic properties of the duct wall. This investigation has been carried out with the objective of evaluating the dependence of the sound field radiated from a jet engine inlet on the inlet characteristics, and to evaluate the validity of the analytical approaches and assumptions utilized in related investigations. First, the effect of the length of the duct on the admittance values at the entrance plane of the duct was investigated. The purpose of this study was not only to show the effect of changing the L/a (i.e., length/radius) of the duct but also to show that the admittance is not a constant across the entrance plane. This is significant as many investigations of similar and related problems assume the existence of a constant "reflection coefficient" at this plane. Therefore, the effect of the radiated sound field on the duct acoustics cannot be properly accounted for. Second, the effect of the internal geometry of the duct on the radiated sound field was investigated. This was done to show that changes in the internal geometry of the duct result in large changes in the admittance values at the duct entrance and, therefore, in large changes in the radiated sound field; a fact which is often ignored in related studies. Third, the internal wave structure in the duct was investigated to show that this integral solution technique can predict both the internal and external sound fields. In this connection it should be pointed out again that this solution technique automatically accounts for the coupling effects between the internal and external sound fields. Fourth, the radiated sound fields for two, dimensionally similar, acoustically lined duct configurations (i.e., a straight duct and an engine inlet) are compared to show that optimum admittance values for liners, determined from the study of their effectiveness in a straight duct, do not necessarilly carry over to the more complicated inlet configurations.

In this study, the surface distributions of the unknowns of the problem (i.e., the acoustic potential and/or the normal acoustic velocity) are obtained from the numerical solution of Eq. (3). Since the unknown functions $\phi(Q)$ or $V(Q)$ appear in the integrands, it is necessary to solve a square matrix; thus, the required computing time increases roughly as the square of the number of points taken on the surface of the body S. In a typical run on the Georgia Tech CDC Cyber 70/74 computer, 140 seconds of computing time were required to solve for the surface values of either ϕ or V at 53 points on the body.

To obtain values for ϕ and V in the far field, Eqs. (10) and (11) are solved by simple numerical integration. The time required for this computation is roughly proportional to the number of points in the field and the number of points on the body. In a typical run, 70 seconds of computing time was required to calculate both ϕ and V at 57 points in the field with 53 points on the body.

To determine the dependence of the admittance at the duct entrance plane on the duct length, these admittance values were computed for hard walled straight ducts having different L/a values, as shown in Fig. 3.

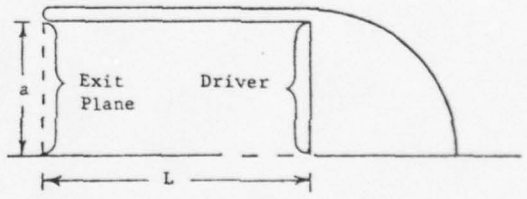

Fig. 3. Geometry Used for Straight Duct Computations.

In this case, driving consisted of a unit acoustic velocity (V = 1) across the driver face. The computed admittance values at the duct entrance plane are plotted for two non-dimensional wavenumbers (i.e., ka = 1 and 3) in Figure 4. Also noted for comparison are the "classical" values for flanged[16] and unflanged[17] pipes. These results indicate that even for plane wave sound excitation the admittance at the duct entrance plane varies with the trans-

verse dimension but it does not depend upon the ducts length-to-radius ratio, at least for the investigated range of L/a and ka values.

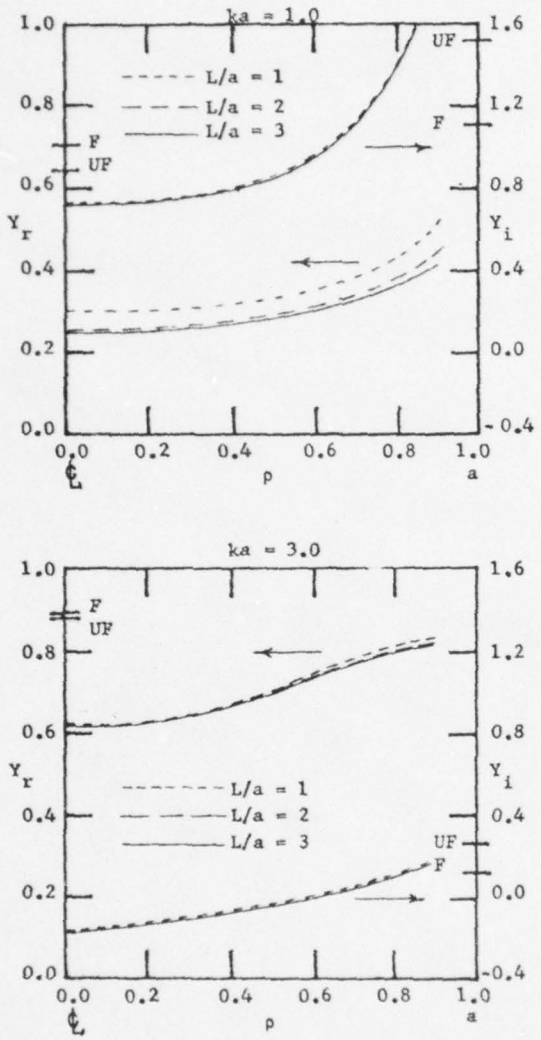

Fig. 4. Admittance at the Exit Plane of a Straight Duct with the Classical Values for Flanged and Unflanged Pipes.

To determine geometrical effects, the admittance at the entrance plane of a hard walled inlet configuration[18] (i.e., See Fig. 5.), with L/a = 2 was also calculated assuming the same type of source excitation for comparison. These results are plotted in Figure 6. When compared with the corresponding results for a straight duct of the same basic dimensions (See Fig. 4.) it is seen that the admittance values change significantly. This is but one indication of the importance of the need to properly account for the internal geometry of the duct when investigating duct radiation problems.

The internal wave structure was also investigated for two hard walled, straight ducts to determine its dependence upon the characteristics of

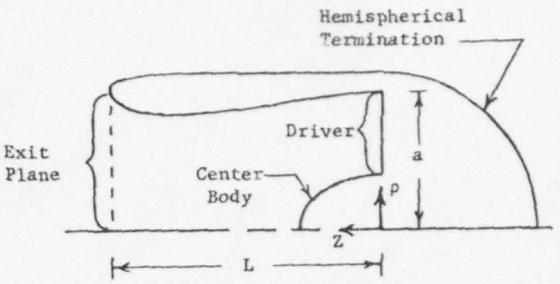

Fig. 5. Inlet Geometry (L/a = 2)

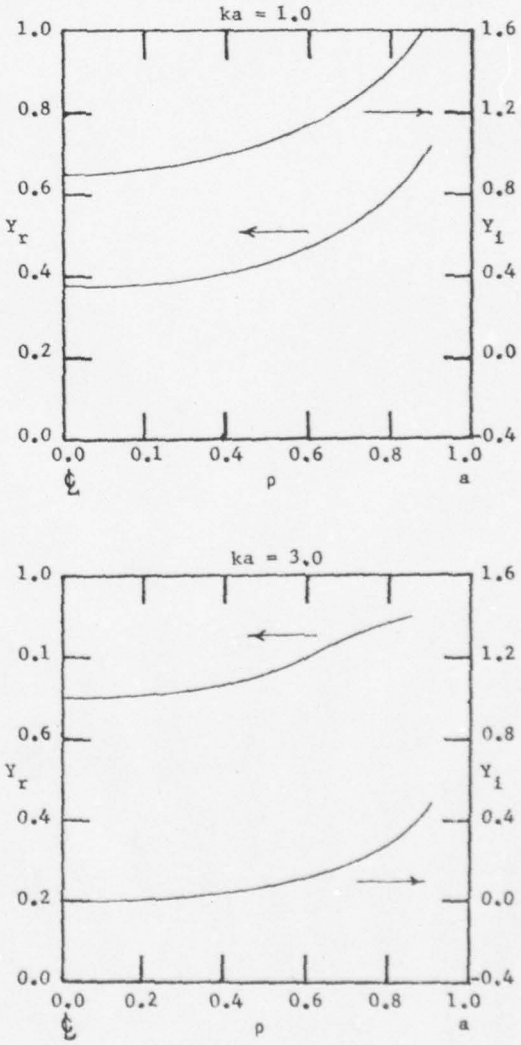

Fig. 6. Admittance at the Exit Plane of the Inlet (L/a = 2)

the sound source. The results are presented in Fig. for two different drivers, one having a constant unit normal acoustic velocity (i.e., V=1) and the other a cosine distribution (i.e., V= cos ($\pi\rho$) where $0 \leq \rho \leq 1$), at the sound source plane, for the case where ka = 1and m (the tangential mode number) equals zero. These results show that the difference between the sound sources quickly disappear with increasing distance from the source plane, as expected for low values of the non-dimensional wavenumber ka. The results for two additional cases are also presented;

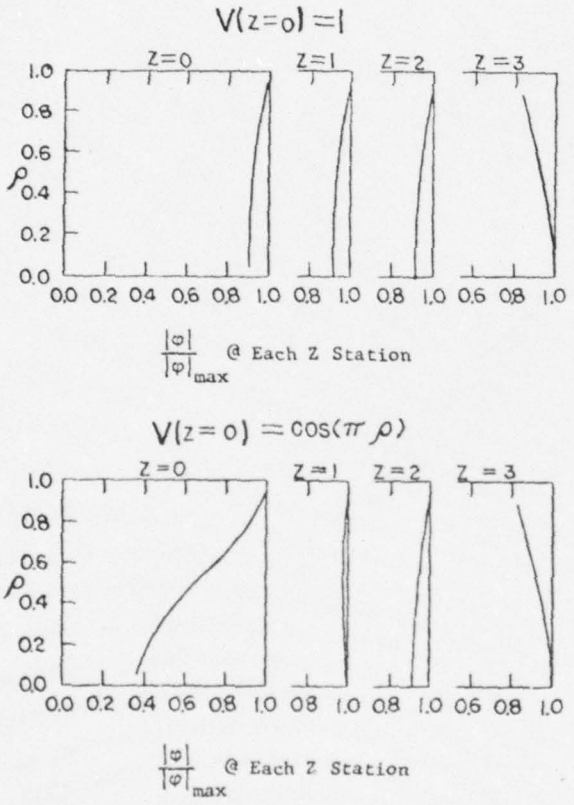

Fig. 7. Radial Distributions of the Acoustic Potential in a Hard Walled Straight Duct (L/a = 3, ka = 1, m = 0)

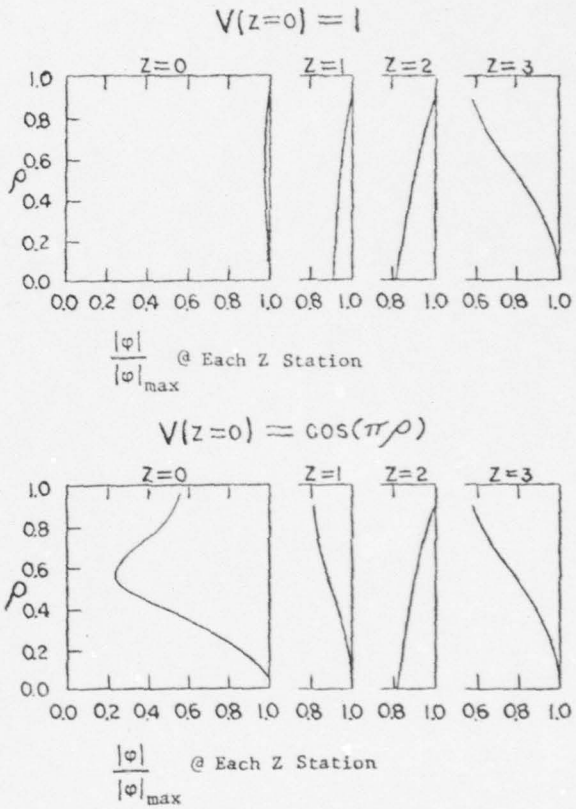

Fig. 8. Radial Distribution of the Acoustic Potential in a Hard Walled Straight Duct (L/a = 3, ka = 3, m = 0)

in Fig. 8 the same two sound sound sources are used for the higher wavenumber of ka = 2 while in Fig. 9 a sound source with a normal acoustic velocity distribution of V = sin ($\rho\pi$) and a tangential mode number m = 1 is used. All of these results indicate, in agreement with basic acoustics, that the finer details of the sound source are "washed out" within a length on the order of ka from the sound source plane.

Finally, the radiated sound fields from both a straight duct and an inlet configuration were computed and compared for both lined and unlined walls. The values used for the wall admittances and the wavenumbers were chosen to be the same as those used by Zorumski in Ref. 19 so that comparisons could be made. Two different liners were run; a constant admittance liner and a segmented liner. In the case of the straight duct the results do not show the same difference in the radiated sound pressure level between the segmented and constant admittance liners (See Fig. 10.) as did Zorumski (See Fig. 11.).

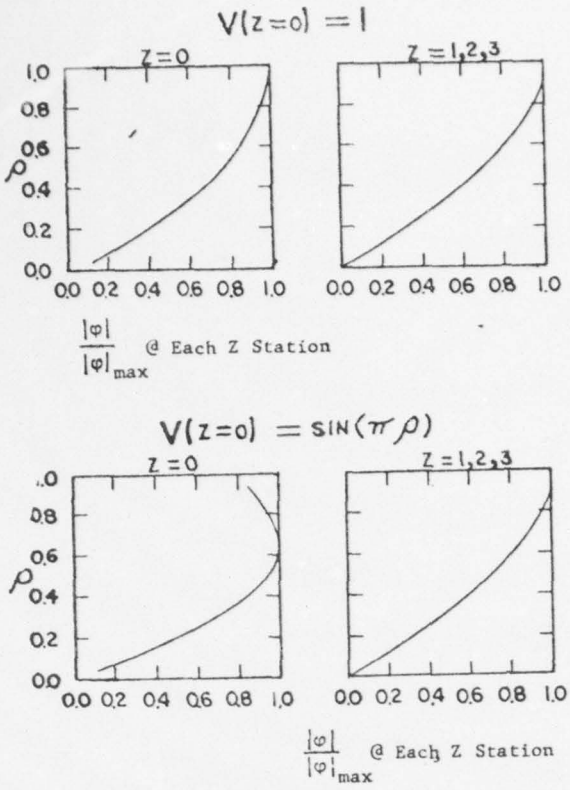

Fig. 9. Radial Distribution of the Acoustic Potential in a Hard Walled Straight Duct (L/a = 3, ka = 1, m = 1)

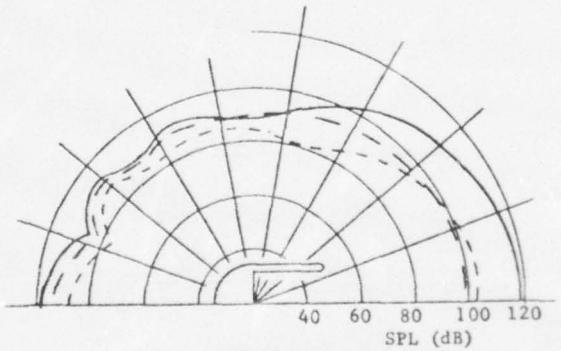

Fig. 10. Far Field (50a) Radiation From A Straight Duct (L/a = 2).

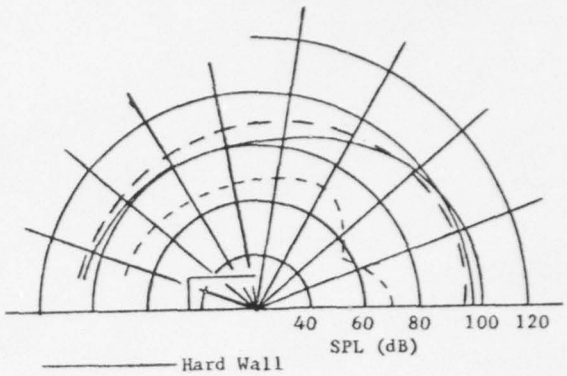

Fig. 11. Far Field Radiation From A Straight Duct as Per Ref. 19 (L/a = 2).

To investigate the effect of geometry, the inlet configuration shown in Fig. 5 was run with the same two liners at the same non-dimensional wavenumbers. The opposite trends to those predicted by Zorumski were noted (See Fig. 12.); that is, that the segmented liner is superior to the constant admittance liner in reducing the radiated sound pressure levels. Thus, it is concluded that geometrical details can significantly affect the characteristics of the sound power radiated from dimensionally similar ducts (i.e., ducts having the same L/a ratios.).

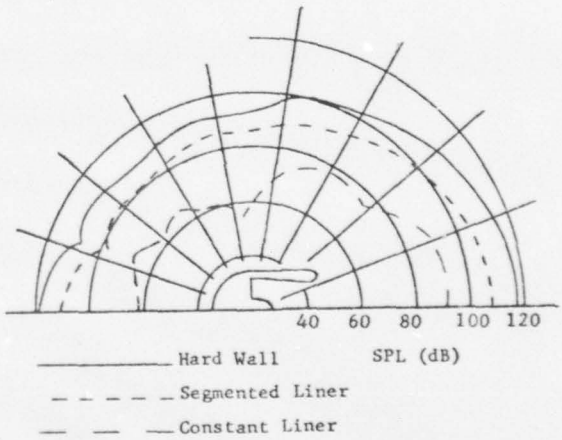

Fig. 12. Far Field (50a) Radiation From An Inlet (L/a = 2).

References

1.) Nayfeh, A. H., Kaiser, J. E., and Telinois, D. P., "Acoustics of Aircraft Engine-Duct Systems," AIAA Journal, Vol. 13, No. 2, pp. 130-153. February 1975.

2.) Tyler, J. M. and Sofrin, T. G., "Axial Flow Compressor Noise Studies," SAE Transactions, Vol. 70, pp. 309-332, 1962.

3.) Baumeister, K. J., "Finite-Difference Theory for Sound Propagation in a Lined Duct with Uniform Flow Using the Wave Envelope Concept," NASA Technical Paper 1001, Lewis Research Center, Cleveland, Ohio, August 1977.

4.) Plumblee, H. E., Dean, P. D., Wynne, G. A., and Burrin, R. H., "Sound Propagation in and Radiation from Acoustically Lined Flow Ducts: A Comparison of Experiment and Theory," NASA Contractor Report, NASA CR-2306, October 1973.

5.) Lansing, D. L. and Zorumski, W. E., "Effects of Wall Admittance Changes on Duct Transmission and Radiation of Sound," Journal of Sound and Vibration, Vol. 27, No. 1, pp. 85-100, 1973.

6.) Laan, J. N., "Sound Transmission in and Radiation from Hard-Walled Annular Ducts Related to Fan Engine Inlets," National Aerospace Laboratory NLR The Netherlands, NLR TR 75144 U, November 1975.

7.) Meyer, W. L., Bell, W. A. and Zinn, B. T., "Predicting the Acoustics of Arbitrarily Shaped Bodies Using an Integral Approach," AIAA Journal, Vol. 15, No. 6, pp. 813-820, June 1977.

8.) Meyer, W. L., Bell, W. A., Stallybrass, M. P., and Zinn, B. T., "Boundary Integral Solutions of Three Dimensional Acoustic Radiation Problems", Journal of Sound and Vibration, Vol. 59, No. 2, pp. 245-262, 1978.

9.) Meyer, W. L., Bell, W. A., Stallybrass, M. P., and Zinn, B. T., "Prediction of the Sound Field Radiated From Axisymmetric Surfaces," Accepted for publication in The Journal of the Acoustical Society of America.

10.) Bell, W. A., Meyer, W. L., and Zinn, B. T., "Prediction of the Acoustics of Solid Propellant Rocket Combustors by Integral Techniques," Proceedings of the 12th JANNAF Combustion Meeting, Newport, Rhode Island, August 11, 1975, CPIA Publication 273, Vol. II, pp. 19-34, December 1975.

11.) Bell, W. A., Meyer, W. L., and Zinn, B. T., "An Integral Approach for Determining the Resonant Frequencies and Natural Modes of Arbitrarily Shaped Ducts," Proceedings of the 3rd Interagency Symposium on University Research in Transportation Noise, Salt Lake City, Utah, November 12-14, 1975.

12.) Meyer, W. L., Bell, W. A. and Zinn, B. T., "Integral Solution of Three Dimensional Acoustic Radiation Problems," presented at the International Symposium on Innovative Numerical Analysis in Applied Engineering Science, Versailles, France, May 23-27, 1977.

13.) Meyer, W. L., Bell, W. A., and Zinn, B. T., "Prediction of the Sound Field Radiated from Axisymmetric Surfaces," AIAA Paper No. 78-195, presented at the AIAA 16th Aerospace Sciences Meeting, Huntsville, Alabama, January 16-18, 1978.

14.) Burton, A. J., "The Solution of Helmholtz' Equation in Exterior Domains using Integral Equations", NPL Report NAC 30, National Physical Laboratory, Teddington, Middlesex, January 1973.

15.) Chertock, G., "Sound Radiation from Vibrating Surfaces," Journal of the Acoustical Society of America, Vol. 36, No. 7, pp. 1305-1313, July 1964.

16.) Morse, P. M., and Ingard, K. U., Theoretical Acoustics, McGraw-Hill, New York, 1969, Chapter 9.

17.) Levine, H. and Schwinger, J., "On the Radiation of Sound from an Unflanged Circular Pipe", Physics Review, Vol. 73, No. 4, pp. 383-406, February 1948.

18.) Miller, B. A., Dastoli, B. J., and Wesoky, H. L., "Effect of Entry-Lip Design on Aerodynamics and Acoustics of High-Throat-Mach-Number Inlets for the Quiet, Clean, Short-Haul Experimental Engine", NASA TM X-3222. Lewis Research Center, Cleveland, Ohio, May 1975.

19.) Zorumski, W. E., "Acoustic Theory of Axisymmetric Multisectioned Ducts", NASA TR R-419, Langley Research Center, Hampton, Virginia, May 1974.

Appendix D

Determination of the Admittance of the Liner

Nomenclature

A	orifice area
c	speed of sound
d	orifice diameter
f	frequency
f_o	resonant frequency of the resonator
k	wave number
L	backing depth
ℓ_{EFF}	effective orifice length
n	normal
p	acoustic pressure
t	orifice length
V	cavity volume
v	acoustic velocity
Y	specific admittance of liner
y	effective admittance of liner
Z	specific impedance of liner
α	absorption coefficient
σ	open area ratio of the liner
$\bar{\sigma}$	open area ratio of a resonator
$\bar{\rho}$	density
$\bar{\mu}$	coefficient of viscosity
π	3.1415926
φ	acoustic potential
θ	specific resistance ratio
χ	specific reactance ratio

The liner, which was employed in the preliminary testing for this AFOSR contract, was originally developed for another program. Since it consists of a matix of Helmholtz resonators it is highly tuned; that is, it has a rather sharp absorption peak. As discussed in Section II, the liner was designed for use above the 1T cut-off frequency and thus shows little absorption below this frequency where most of the runs for this program will be made. Thus the liner must be retuned so that it becomes effective in the frequency range where most of the testing will be done. In this appendix basic liner theory is reviewed and a relatively simple redesign of the liner is proposed to make it more effective in the frequency range of interest in this research program.

For input into the computer program certain values must be known. First, the sound pressure level at the "driver plane" must be known. Experimentally this corresponds to the nozzle-liner plane and can be directly measured. The other value which must be known is the effective admittance of the liner defined as

$$y = \frac{\partial \varphi}{\partial n} \Big/ \varphi \qquad \text{(D-1)}$$

where φ is the acoustic potential and $\frac{\partial \varphi}{\partial n}$ is the normal acoustic velocity defined with an outward facing normal.

In Reference 1 equations are given to calculate the specific acoustic impedance of an array of helmholtz resonators, that is

$$Z = \theta - i\,\chi \qquad \text{(D-2)}$$

where the specific resistance ratio θ and the specific reactance ratio χ are defined as

$$\theta = \frac{4}{\sigma \bar{\rho} \bar{c}} (\pi \bar{\mu} \bar{\rho} f)^{1/2} (1 + {}^{t}/_{d})$$

$$\chi = \frac{2\pi f_o \ell_{EFF}}{\bar{c}\sigma} \left(\frac{f}{f_o} - \frac{f_o}{f}\right) \qquad \text{(D-3)}$$

For the definitions of the variables used here see Figure D-1. It will be noted here that these definitions assume an inward facing normal. The resonant frequency of the resonator is defined as

$$f_o = \frac{\bar{c}}{2\pi} \sqrt{\frac{A}{V\ell_{EFF}}} = \frac{\bar{c}}{2\pi} \sqrt{\frac{\bar{\sigma}}{L\sigma_{EFF}}} \qquad \text{(D-4)}$$

and the effective orifice length is found to be

$$\ell_{EFF} = t + 0.85\, d \left(1 - 0.7\sqrt{\bar{\sigma}}\right) \qquad \text{(D-5)}$$

The specific acoustic admittance is defined as

$$Y = \frac{1}{Z} = {}^{v}/_{p} \qquad \text{(D-6)}$$

and since the acoustic potential and the acoustic pressue are related by

$$p = i\, \bar{\rho}\, \bar{c}\, k\, \varphi \qquad \text{(D-7)}$$

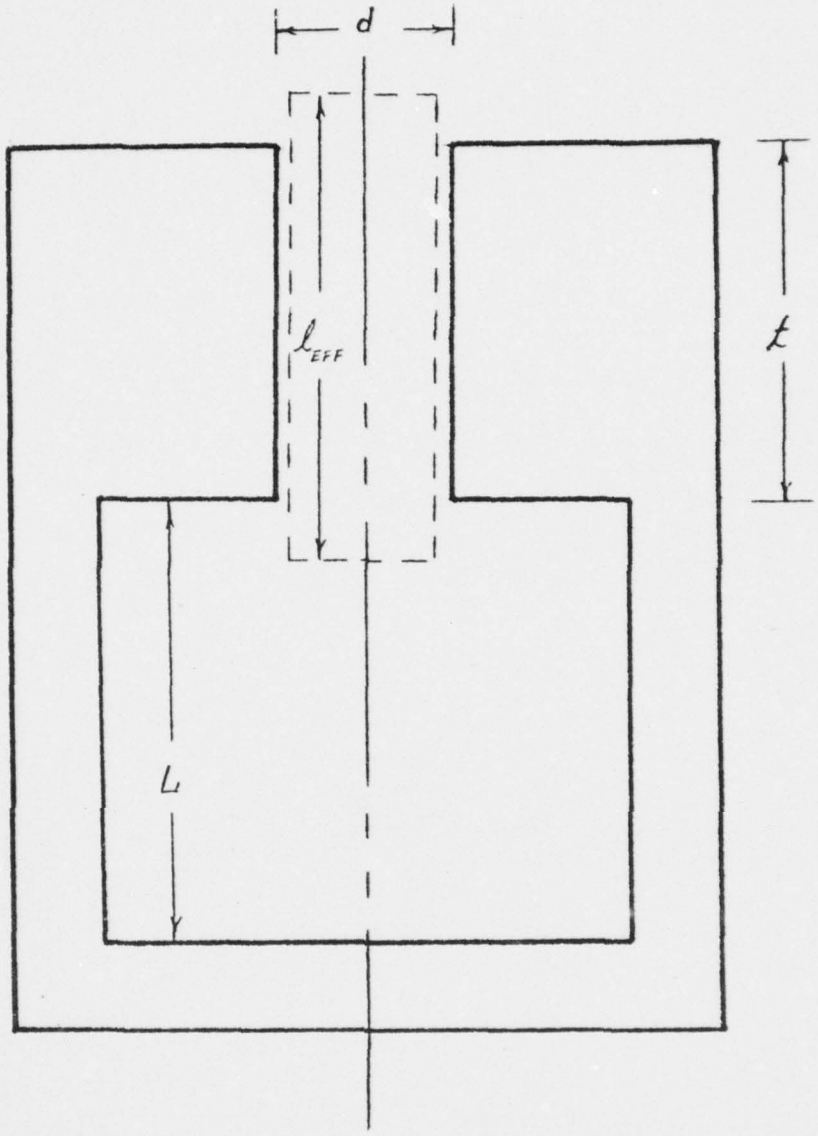

Figure D-1. Helmholtz Resonator

the effective admittance is found to be

$$y = -i\bar{\rho}\bar{c}\, k\, Y = -i\bar{\rho}\bar{c}\, k\, \frac{\theta+i\chi}{(\theta^2+\chi^2)} \qquad \text{(D-8)}$$

where the minus sign is due to the switch from inward to outward facing normal for the acoustic velocity.

The liner is most effective in damping acoustic waves at its resonant frequency which for our case is ~ 740 Hz. This is above the 1T mode of the duct which is ~ 695 Hz and thus the full effectiveness of this liner is never achieved. A plot of the absorption coefficient of the liner, α, vs. frequency is presented for the present liner configuration in Figure D-2. Here the absorption coefficient is defined as

$$\alpha = \frac{4\theta}{(\theta+1)^2+\chi^2} \qquad \text{(D-9)}$$

There are two paths that may be taken to obtain test results at maximum liner efficiency. The first method is to purposely drive a 1T wave by using two drivers driving 180° out of phase. This will create a transverse acoustic wave structure in the tube and the results can then be compared by using a mode number of 1 (instead of zero) in the computer programs. The other alternative is to redesign the liner such that its resonant frequency is reduced below the 1T mode cut-off frequency. This can be accomplished by increasing the backing distance, L. By increasing L from 0.5" to 0.775" the resonant frequency of the liner drops to ~685 Hz, below the 1T mode. If the diameter of the backing cavity is also increased from 1.0" to 1.25" the

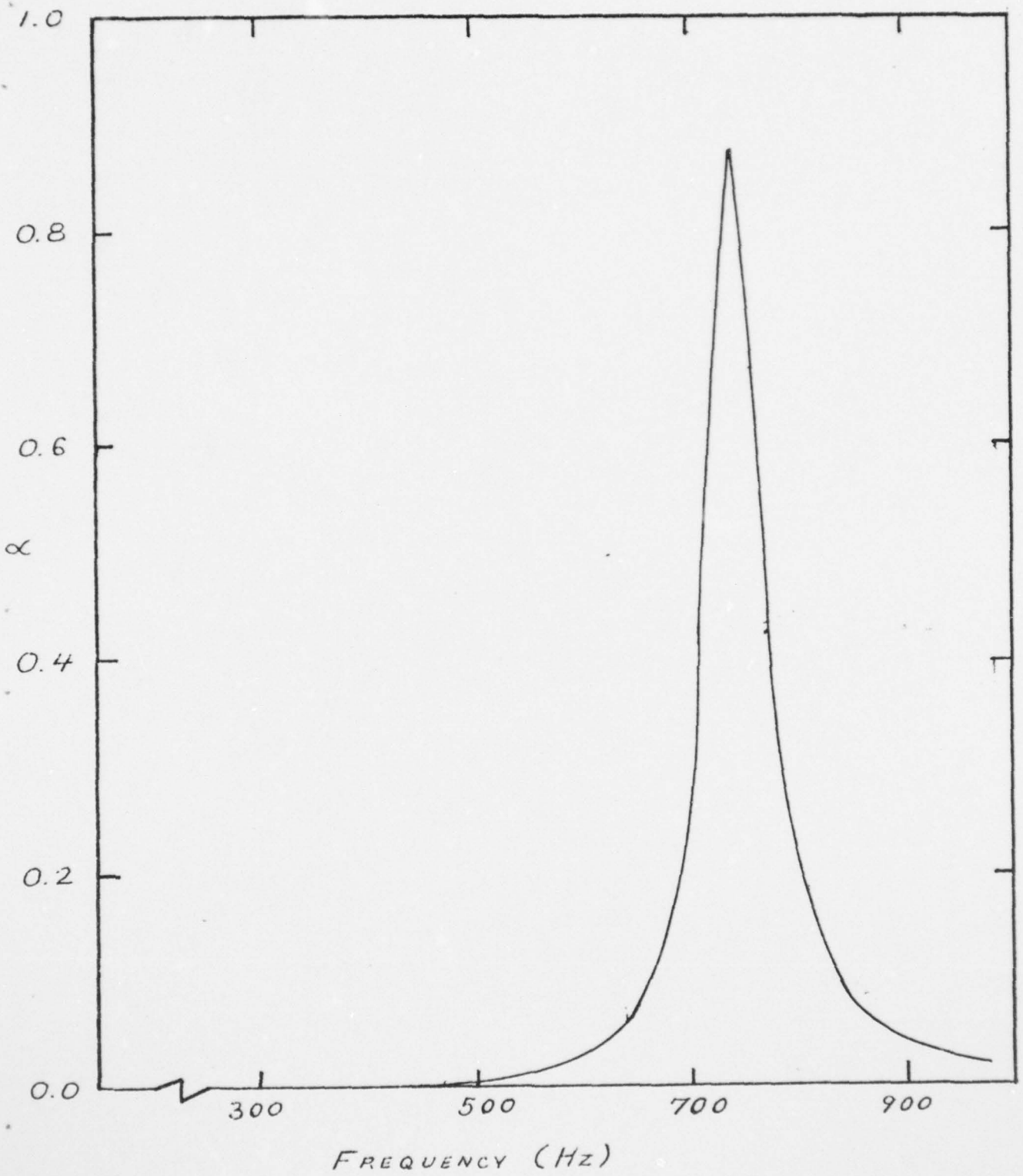

Figure D-2. Absorption Coefficient vs. Frequency For the Present Liner Configuration.

resonant frequency of the liner can be further reduced to ~550 Hz. Thus, by simply drilling out the backing cavity the tuning frequency of the liner can be altered enough so that its absorption peak is well below the 1T cut-off frequency; that is, in the range of frequencies that will normally be used for testing in this research program (i.e., 300-650 Hz).

References

1. Garrison, G. D., "A Study of the Suppression of Combustion Oscillations with Mechanical Damping Devices," Phase II Summary Report, Pratt & Whitney Aircraft Co., PWA FR-1922, July 15, 1966.

Appendix E

Technical Note to be submitted for publication to the AIAA Journal

(Draft copy)

"Sound Radiation from Ducts: A Comparison of Admittance Values"

Technical Note

Sound Radiation From Ducts: A Comparison of Admittance Values*

W. L. Meyer** Assistant Research Engineer

W. A. Bell† Research Engineer

B. T. Zinn‡ Regents' Professor

School of Aerospace Engineering

Georgia Institute of Technology

Atlanta, Ga. 30032

---

* This research was supported by AFOSR contract number F49620-77-C-0066; Lt. Col. Lowell Ormand, Grant Monitor.

** Assistant Research Engineer, Member AIAA.

† Scientist Associate; Present Address: Lockheed Georgia Company, Marietta, Georgia 30060; Member AIAA.

‡ Regents' Professor, Associate Fellow AIAA.

When considering the radiation from an open duct it is found that some of the energy is radiated and some reflected (with a phase shift) back down the duct. It is common to associate an effective admittance (impedance or reflection coefficient) at the exit plane with this phenomonon. In this note three methods for obtaining an effective admittance are compared.

The first method follows the analyses of Helmholtz and Rayleigh in which the end of the duct is approximated by a piston radiating into a half space from an infinite baffle. In this analysis the classical integral representation of the solutions of the Helmholtz equation is solved with certain approximations. Results for this configuration (commonly known as a flanged pipe) using this method are presented in Reference 1.

The second method consists of the solution of a Weiner-Hopf type integral equation. In this analysis the duct is assumed to be semi-infinite in length and infinitely thin. Results for this type of analysis are presented in Reference 2. This configuration is commonly known as the unflanged pipe.

It is interesting to note that these two configurations represent the logical limits of this type of problem in that the first can be viewed as an infinitely thick duct while the second is infinitely thin. Neither of these configurations can account for the case of a duct of finite length, however.

The third method employs a special cylindrically symmetric integral representation of the exterior solutions of the Helmholtz equation.[3,4,5] Using this method it is possible to calculate the acoustic pressure and velocity anywhere in the external field - including the inside of the duct itself. From these values inside the duct an effective admittance can be calculated using a simple standing wave analysis like that used in an

AD-A069 787 GEORGIA INST OF TECH ATLANTA SCHOOL OF AEROSPACE ENG--ETC F/G 20/1
NOISE SUPPRESSION IN JET INLETS.(U)
FEB 79 B T ZINN, W I MEYER, W A BELL F49620-77-C-0066
UNCLASSIFIED AFOSR-LTR-79-0614 NL

2 OF 2
AD
A069787

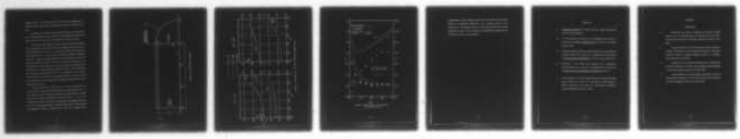

END
DATE
FILMED
7-79
DDC

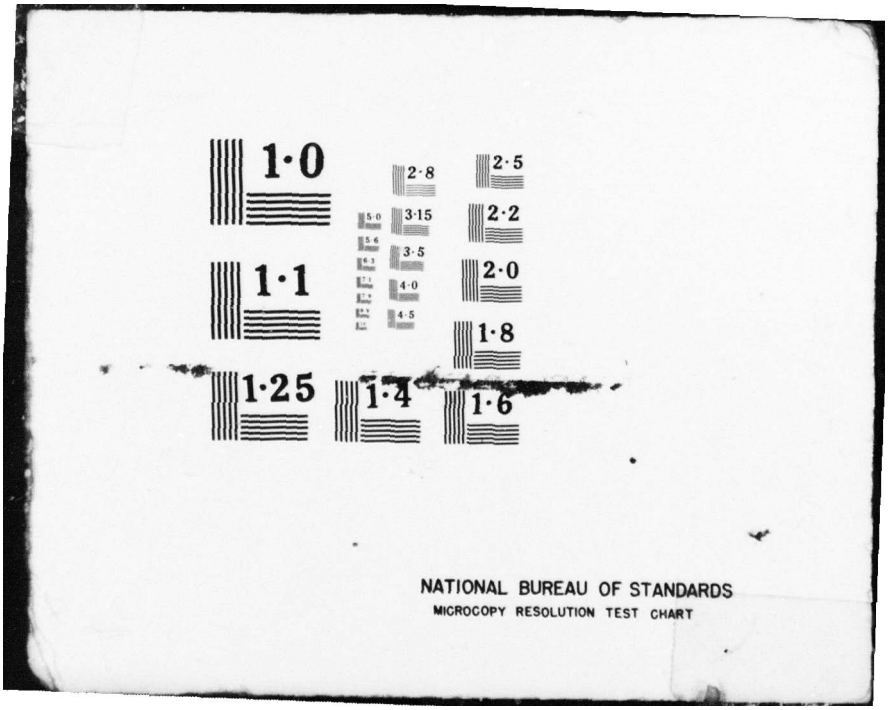
1·0
1·1
1·25
1·4
1·6
1·8
2·0
2·2
2·5
2·8
3·15
3·5
4·0
4·5
5·0
NATIONAL BUREAU OF STANDARDS
MICROCOPY RESOLUTION TEST CHART

impedance tube. All that is required for this method is knowledge of two complex acoustic quantities (i.e., amplitude and phase) at two points in the duct.

The geometric restrictions on the integral technique are that the duct (or any radiating body) must be a finite (i.e. no infinitely thin walls) closed body. A sketch of the duct used in this analysis is presented in Figure 1.

To determine if the length of the duct makes a significant difference in the admittance values at the duct entrance computer analyses of ducts of varying lengths were run (i.e. L/a = 1,2,3) at two different non-dimensional wave numbers (i.e. ka = 1 and 3). Since the method is capable of calculating the actual radially varying admittance across the exit plane of the duct, these are presented in Figure 2. The driver consisted of specifying a unit normal acoustic velocity while on the rest of the body the admittance was specified as zero. As can be seen the length of the duct L has little effect on the admittance, defined as the ratio of the component of the acoustic velocity normal to the surface to the acoustic pressure. Also noted for the sake of comparison are the values for the flanged and unflanged pipe at the appropriate values of ka.

Computer analyses of a duct with L/a = 3 were then done with the same boundary conditions specified as above for various values of ka. For each case the acoustic potential and velocity were calculated at 11 equally spaced points along the centerline of the duct from Z = 1 to Z = 2. A standing wave analysis was then done employing a Least-Square method to solve the overdetermined system of equations. The results of these analyses are presented in Figure 3 along with the values for a flanged and an

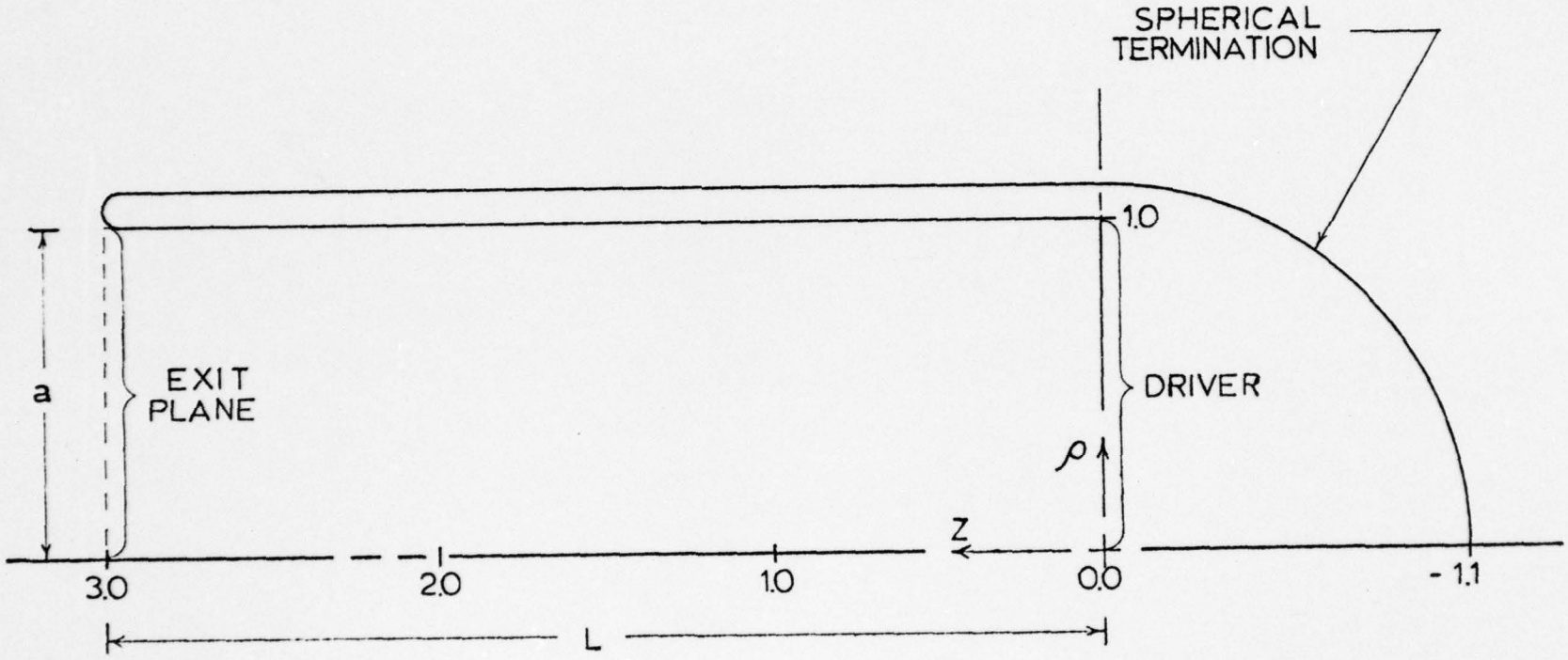

Figure 1. Straight Duct Geometry.

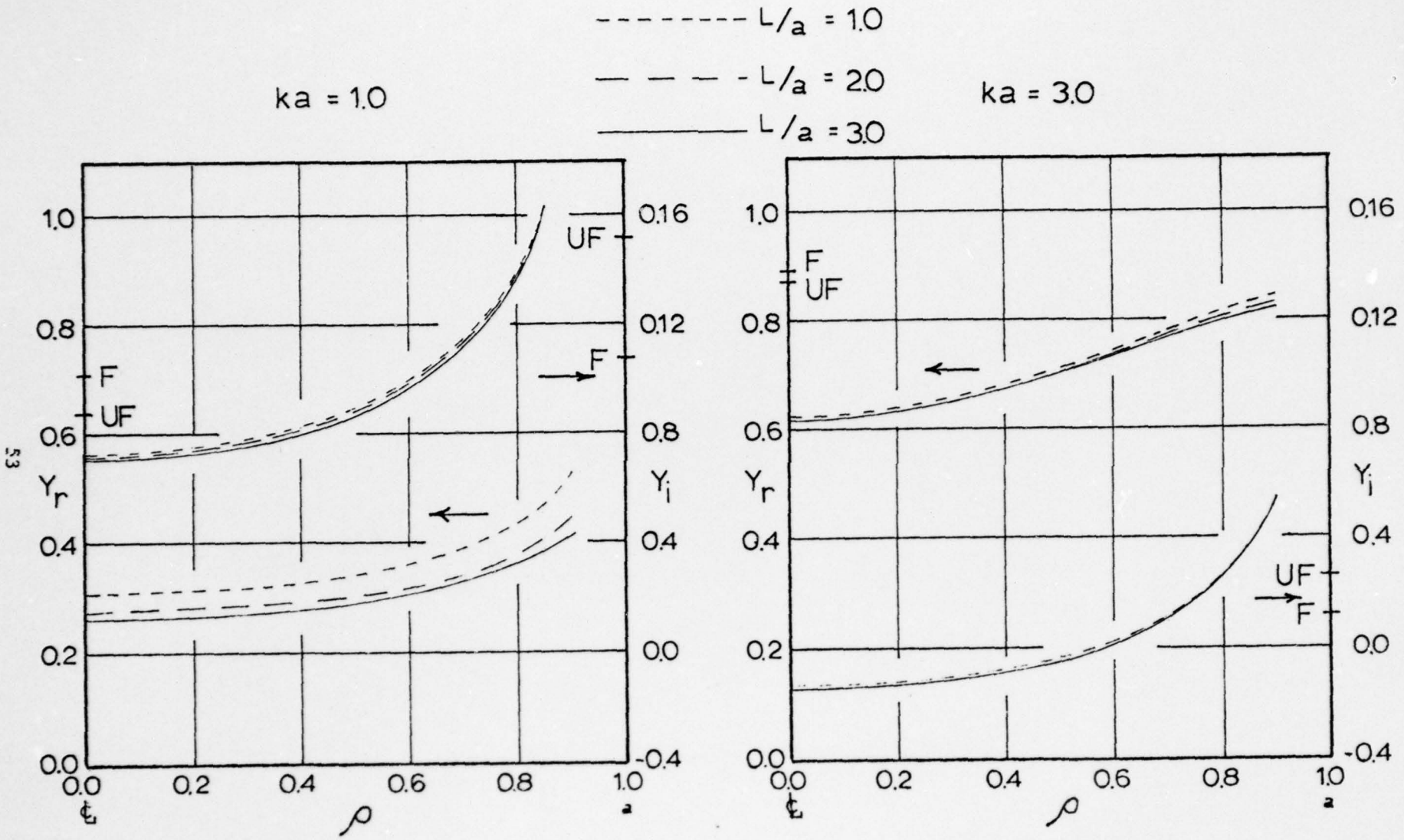

Figure 2. Admittance at the Exit Plane of Straight Ducts.

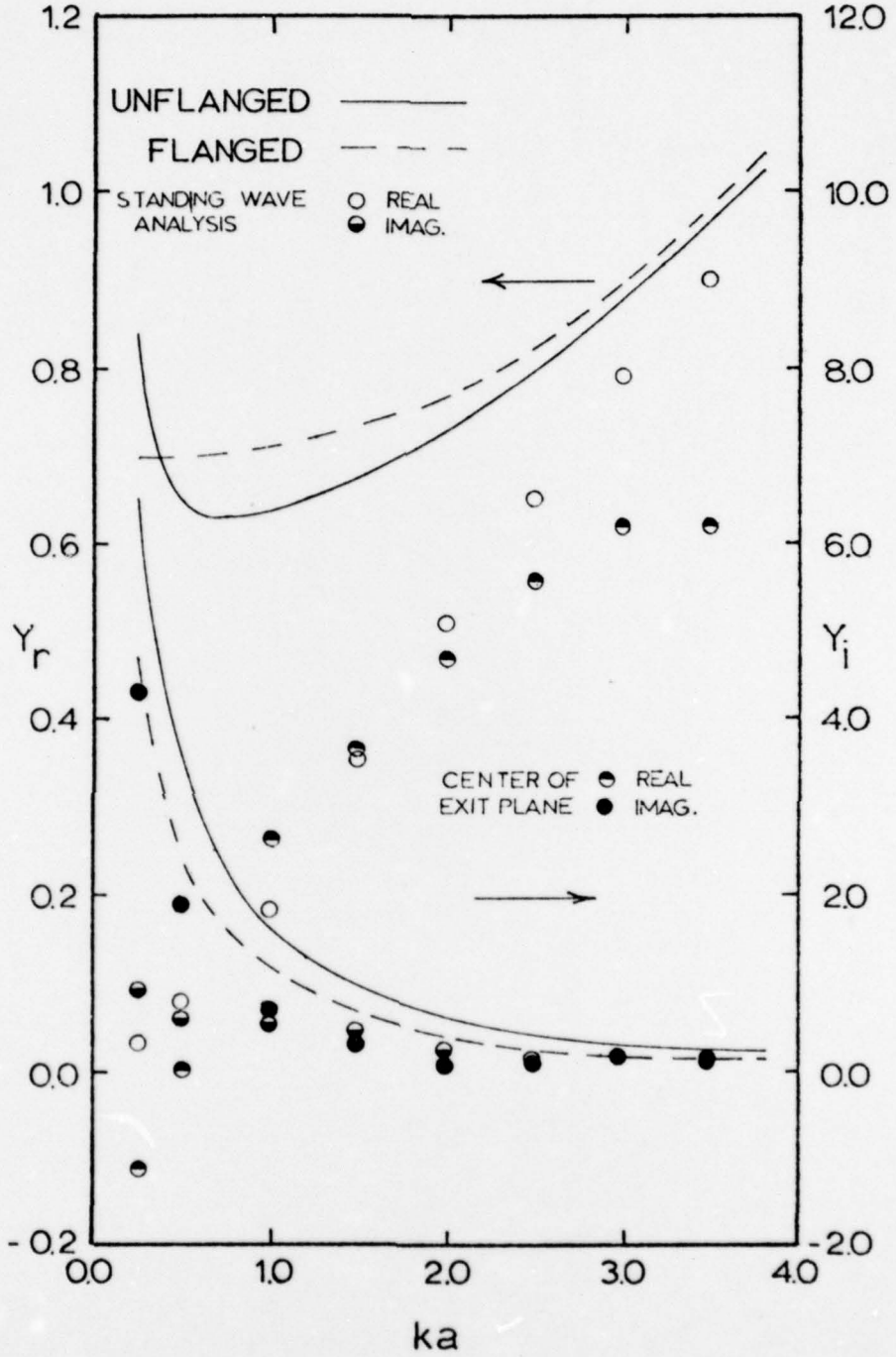

Figure 3. Admittance at the Open End of a Straight Duct.

unflanged pipe. Similar analyses were done off the centerline of the duct; however, no significant differences in the computed values for the admittance at the entrance plane of the duct were found. Also noted for comparison in Figure 3 are the values of the admittance calculated on the centerline of the duct at the exit plane.

References

1.) Theoretical Acoustics, P. M. Morse and K.U. Ingard, McGraw-Hill, New York, 1969, Chapter 9.

2.) "On the Radiation of Sound from an Unflanged Circular Pipe," H. Levine and J. Schwinger, Physics Review, Vol. 73, No. 4, pp. 383-406, February 1948.

3.) "Boundary Integral Solutions of Three Dimensional Acoustic Radiation Problems," Meyer, W. L., Bell, W. A., Stallybrass, M. P. and Zinn, B. T., Journal of Sound and Vibration, Vol. 59, No. 2, pp. 245-262, 1978.

4.) "Prediction of the Sound Field Radiated From Axisymmetric Surfaces," Meyer, W. L., Bell, W. A., Stallybrass, M. P., and Zinn, B. T.,Journal of the Acoustical Society of America, March 1979.

5.) "Sound Radiation from Finite Length Axisymmetric Ducts and Engine Inlets," Meyer, W. L., Bell, W. A., and Zinn,B. T., AIAA Paper No. 79-0675, presented at the AIAA 5th Aeroacoustics Conference, Seattle, Washington, March 12-14, 1979.

Appendix F

Presentations

A. "Predicting the Acoustic Properties of Arbitrarily Shaped Bodies by Use of an Integral Approach," Presented at the 3rd AIAA Aeroacoustics Conference at Palo Alto, California, July 20-23, 1976. (Zinn)

B. "Integral Solutions of Three Dimensional Acoustic Radiation Problems," Presented at the International Symposium on Innovative Numerical Analysis in Applied Engineering Science at Versailles, France, May 23-27, 1977 (Zinn)

C. "Prediction of the Sound Field Radiated from Axisymmetric Surfaces," Presented at the AIAA 16th Aerospace Sciences Meeting at Huntsville, Alabama, January 16-18, 1978. (Bell)

D. "Sound Radiation from Finite Length Axisymmetric Ducts and Engine Inlets," Presented at the 5th AIAA Aeroacoustics Conference at Seattle, Washington, March 12-14, 1979. (Zinn)